TU Kaiserslautern

Fachbereich Mathematik

MODELING AND DESIGN OPTIMIZATION OF TEXTILE-LIKE MATERIALS VIA HOMOGENIZATION AND ONE-DIMENSIONAL MODELS OF ELASTICITY

Vladimir Shiryaev

1. Gutachter: Prof. Dr. Grigory Panasenko
2. Gutachter: Prof. Dr. Axel Klar

Datum der Disputation: 27. Februar 2015

D 386

Vladimir Shiryaev

Abteilung Systemanalyse, Prognose und Regelung

Fraunhofer Institut für Techno- und Wirtschaftsmathematik (ITWM)

Fraunhofer-Platz 1, 67663 Kaiserslautern, Deutschland

shiryaev@itwm.fraunhofer.de

http://www.imtw.fhg.de

Acknowledgments

Abstract

This work consists of two parts.

The first part deals with optimization of large structures of linear elastic material with contact modeled by Robin-type boundary conditions. The structures model textile-like materials and possess certain periodicity or quasiperiodicity properties. The homogenization method is used to represent the structures by homogeneous elastic bodies and is essential for formulation of the effective properties optimization problems. Existing results for problems with Robin-type boundary conditions for thermal conductivity are extended to the case of elasticity. Some results, e.g. Korn's inequality, are absent in works on conductivity and are novel. It is also proven that the convergence to the homogenized solution is uniform with respect to geometrical parameters. Optimization problems are formulated for the homogenized model only, but the homogenized properties depend on the geometrical parameters. Poisson's ratio and effective stress profiles are optimized. In both problems a beam approximation is used to reduce the cell problems to algebraic equations and obtain derivatives of the effective properties symbolically. For the stress profile optimization problems, the adjoint approach is exploited for the PDE-constrained optimization problem resulting from the homogenization. The application of the homogenization approach with beam models to the problem of optimization of effective properties is new.

In the second part we consider a new model for simulation of textiles with frictional contact between fibers and no bending resistance. In the model, 1D hyperelasticity and the Capstan equation are combined. Its connection with conventional hyperelasticity and Coulomb friction models is shown. Then, the model is formulated as a problem with the rate-independent dissipation, and proofs of the problem's proper convexity and continuity are provided. The part ends with an numerical algorithm and numerical experiments. For one of them, a comparison of the results to real measurements is provided.

Contents

Chapter 1

Optimization of textile-like materials via homogenization and beam approximations

1.1 Introduction

This chapter presents an approach to the microstructure optimization problems of large structures possessing periodicity or quasiperiodicity properties. These structures consist of linear elastic material but are not homogeneous. They can be represented by repetitions of cells or meshes, not necessarily the same but of certain predefined structure. The cells considered in this work are beam structures, whereby some of the beams can be in contact with each other. Contact is modeled by the Robin boundary conditions, (see [6] and [24] for regularization and linearization of the quasistatic frictional model leading to the Robin boundary conditions). The goal of the work is to find a microstructure with desired properties of the homogenized material.

As the properties subject to optimization, minimal shrinkage and closeness of the effective stress profile under prescribed loading to some given function are considered. Such criteria are of interest in medical textile industry, for example for compressive stockings and bandages. With the help of the homogenization method, the effective stress profiles and the shrinkage can be expressed in a clear mathematical way. Minimization of the shrinkage properties corresponds to optimization of the effective Poisson's ratio, which in

turn reduces to optimization of an algebraic function of the effective elasticity tensor of the homogenized structure. The stress profile optimization is formulated as a PDE-constrained optimization problem.

There is a vast literature available on shape optimization via the homogenization method. See, e.g. [2, 4, 15, 42]. In these works, homogenization is used primarily as a relaxation technique for the design space of the optimization problem stated for the initial non-homogenized problem. The book [2] provides an in-depth analysis and a comprehensive introduction to the homogenization with generalizations to the non-periodic case and a rich summarization of the works on the topics existing at the time.

The approach of our work differs from the existing approaches in the role of the homogenization: for us the homogenization is an essential part of the statement of the optimization problem itself, not the relaxation technique.

The homogenization of models with frictional contact on the contact interfaces is studied in [12]. It turns out that for the Tresca friction model it is in general impossible to separate the scales. However, the model with Robin-type conditions can be used for regularization of quasistatic contact problems, see [6] and [24]. For such problems, the homogenization result with scale separation is available in [23].

For the cell problems, beam models are used as a solution approximation technique to reduce the three-dimensional elasticity with Robin-type conditions to an algebraic system of equations. In this case the derivatives of the cell problems' solutions, which are necessary for the classical gradient-based optimization, can be computed exactly by means of automatic symbolic differentiation. Homogenization of beam or rod systems without contact is considered in works [5, 36, 50, 51]. Results related to the reduction to beam models for Robin-type boundary conditions are available in [6]. The extension of the results of [6] are used to formulate algebraic systems for the cell problems.

The papers [50] and [51] are of particular theoretical interest. The authors develop the idea of representation of thin elastic structures by measures and formulate the convergence results of the homogenization using the convergence of these measures. Along with the size of the periodicity cell, the second parameter corresponding to the thickness of beams in the network is introduced and the limits of the solutions are investigated with respect to both parameters. Three cases of the relation between the parameters are studied, and the results are in agreement with the earlier work [37], where the complete asymptotic expansion method is used.

Optimization problems in the framework of [50] and [51] are considered in the article [25]. The optimization problem is stated for the initial non-homogenized problem, and then the limit with respect to the period of the structure is taken. The standard questions of convergence of the objective functional and the minimizers arise, and they are investigated in the work. It is shown that the solution of the homogenized optimization problem can be used as a suboptimal control for the original problem.

In our work we do not investigate the question of convergence of the objective functionals and their minimizers with respect to the limit taken by the period of the structure or thickness of beams. The optimization problem is formulated for the homogenized model only, which is quite natural for our example application. Namely, we consider the effective Poisson's ratio and the effective stress profile optimization problems. Both deal with the effective properties, not some quantities available in the original model. A statement of our optimization problems for the original model would require some non-trivial artificial constructs.

PDE-constrained optimization is a well developed field nowadays. The adjoint approach used in this work is similar to that of [2]. The general approach is described in [22, 27].

After this introduction, a set of geometries considered in this thesis is described. Then a general description of the 3D direct problem in Section 1.3 and the basic results of existence and uniqueness of the solutions are provided.

Before the homogenization results are formulated, the issue that the geometry from Section 1.1 is repeatable in connected manner only in two in-plane directions is addressed, but three-dimensional homogenization results are used. This problem arises from the geometrical fact that any geometry modeling a knot or any interlacing of yarns is essentially three-dimensional, but the limiting structure — a fabric, is essentially two-dimensional.

A similar setting was considered in Chapter 3 of [36], where the limiting behavior of the solutions of conductivity and elasticity problems are considered for a 3-dimensional domain shrinking to a plate. Some additional symmetry assumptions are required for out-of-plane bending equations and in-plane membrane equations to separate, since for a plate with a non-symmetric structure the in-plane moduli are coupled with the bending constants. Strictly speaking it is hard to differentiate the in-plane and out-of-plane moduli. That is why we will define the in-plane moduli of the textile via some extension of the textile to a 3D composite. Consider a 3D composite material consisting of an infinite periodic set of identical parallel plates "immersed" into some soft matrix, filling all space out of the

plates except for some small empty spaces (holes) around the contact interfaces between the fibres. The Young's modulus of the matrix is supposed to be of the order of a small in comparison to the fibers' Young's modulus parameter δ. It can be seen that the solution of the elasticity problem set in one plate with the Neumann condition on the lateral boundary is close to the solution of the elasticity problem set in a 3D composite material (see the fictitious domain approximation, Section 1.3.3). The homogenized moduli $A_{ijkl}^{\mathrm{hom}}(\delta)$ of this 3D composite can be defined according to the standard homogenization theory (see, for example, [5, 36]), modified with respect to the Robin-type interface conditions in Section 1.3.5 (for the conductivity setting this is done in [23]).

Let us define the in-plane moduli of the plate as the limit as $\delta \to 0$ of the above homogenized moduli with the subscripts 1 and 2 only, multiplied by the in-plane period of the cell of the knitting pattern of the textile-like material ε_0 (see Section 1.5.1 for details):

$$A_{ijkl}^{\mathrm{inp}} = \varepsilon_0 \lim_{\delta \to 0} A_{ijkl}^{\mathrm{hom}}(\delta), \quad i,j,k,l \in \{1,2\}.$$

According to the fictitious domain theory for periodic cell problems ([5, 36]) we obtain the algorithm for the calculation of the in-plane moduli $\boldsymbol{A}^{\mathrm{inp}} = \left(A_{ijkl}^{\mathrm{inp}} \right)$, $1 \leq i,j,k,l \leq 2$ described in Section 1.3.5.

The homogenization topic is discussed in Section 1.3.4, where the scaled version of Korn's inequality with respect to the period of the structure is provided. Such result is crucial for the justification of the homogenization. For problems with Robin-type jump conditions at the interfaces this result is new. Similar results for a different type of problem are presented in the state-of-the art work [11], and we use the similar technique for the proof. In Section 1.3.5 the homogenization results of [23] are extended to elasticity problems using the statements of the previous sections. This homogenization result is new. In Sections 1.3–1.3.5 the thickness parameter μ and geometry parameter $\boldsymbol{g}$ are discarded, because they don't play any role in the homogenization and overload the notation. Further the geometrical parameter μ is mentioned only in Section 1.6, where a question of relation between μ and ε is dealt with briefly. In the rest of the work it does not play any important role and is omitted. The geometrical parameter appears again in Section 1.4, where it is shown that all the solutions and homogenized properties used in this part depend continuously on the geometry described in Section 1.2. The continuity results are proved with the help of techniques from [13]. In Section 1.4.2 it is proved that the 2-scale convergence of

the homogenization is uniform with respect to the geometry. The corresponding extension of the Arzela-Ascoli theorem is provided. This result is new, but the constructions in the proof are the same as those used in the context of small domain perturbations from [33].

The optimization problems and their solution strategies are described in Section 1.5. The mainstream adjoint state technique is used for the stress profile optimization problem. At the level of cell problems, elastic beam models help to reduce the computational burden while computing the homogenized tensor and its derivatives. This is described in Section 1.6. Finally, our numerical examples are presented in Section 1.8.

1.2 Description of the geometry

1.2.1 One-dimensional geometry

Consider two non-parallel planes π_1 and π_2. Assume that the origin O belongs to the intersection line $l = \pi_1 \cap \pi_2$ and the coordinate axis Oz is aligned with l. Let the angle between the planes be $\beta < \pi$ and the plane Oxz evenly divide this angle. Let the axis Oy be such that the system $Oxyz$ is right-oriented. Introduce point $B = (0, 0, h)^T$ and two rays $r_{11} \in \pi_1$ and $r_{12} \in \pi_1$ with the origin at B, and $r_{21} \in \pi_2$ and $r_{22} \in \pi_2$ with the origin at O. Denote the direction vector of r_{ij} by $\boldsymbol{d}_{ij}$. Let

$$
\boldsymbol{d}_{11} = \begin{pmatrix} \sin(\alpha/2)\cos(\beta/2) \\ -\sin(\alpha/2)\sin(\beta/2) \\ -\cos(\alpha/2) \end{pmatrix}, \quad \boldsymbol{d}_{12} = \begin{pmatrix} -\sin(\alpha/2)\sin(\beta/2) \\ \sin(\alpha/2)\sin(\beta/2) \\ -\cos(\alpha/2) \end{pmatrix},
$$

$$
\boldsymbol{d}_{21} = \begin{pmatrix} \sin(\alpha/2)\cos(\beta/2) \\ \sin(\alpha/2)\sin(\beta/2) \\ \cos(\alpha/2) \end{pmatrix}, \quad \boldsymbol{d}_{22} = \begin{pmatrix} -\sin(\alpha/2)\cos(\beta/2) \\ -\sin(\alpha/2)\sin(\beta/2) \\ \cos(\alpha/2) \end{pmatrix}, \quad \alpha \in (0; \pi).
$$

Observe that axis Oz is the bisecting line for angles $r_{11}Br_{12}$ and $r_{21}Or_{22}$. Both angles have magnitude α and belong to π_1 and π_2, respectively. The distance between r_{11} and r_{21}, and between r_{12} and r_{22} can be computed explicitly:

$$
\mathrm{dist}\,(r_{11}, r_{21}) = \mathrm{dist}\,(r_{12}, r_{22}) = 2h\,|\sin(\alpha/2)\sin(\beta/2)|\,\frac{(\sin^2(\alpha/2)\sin^2(\beta/2) + \cos^2(\alpha/2))^{\frac{1}{2}}}{1 + \cos^2(\alpha/2) - \sin^2(\alpha/2)\cos(\beta)}.
$$

It is clear from this expression that one can always choose h in such a way that

$$\text{dist}\,(r_{11}, r_{21}) = \text{dist}\,(r_{12}, r_{22}) = 4\mu(1 - \zeta), \quad \zeta \in (0; 0.01). \tag{1.1}$$

Such choice ensures that semi-infinite cylinders of radii 2μ with axes r_{11} and r_{21} intersect, and that the intersection has a non-empty interior.

Denote the point of r_{11} closest to r_{21} by P_{11}. Define P_{12}, P_{21}, P_{22} in the similar way for r_{12}, r_{21}, and r_{22}. Further, for $i \in \{1, 2\}$ and $j \in \{1, 2\}$ introduce points $J_{ij} = P_{ij} + 4\mu d_{ij}$. Define the sets of segments $\Gamma_0^\mu = \{BP_{11}, P_{11}J_{11}, BP_{12}, P_{12}J_{12}, OP_{21}, P_{21}J_{21}, OP_{22}, P_{22}J_{22}\}$ and $\Gamma_0^{\mu c} = \Gamma_0^\mu \cup \{P_{11}P_{21}, P_{12}P_{22}\}$. Geometrical transformations of Γ_0^μ will form the set of axes of the cylinders, whose union forms the textile-like domain. At the same time, the same transformations of $\Gamma_0^{\mu c}$ contain additional segments, which correspond to the contact interfaces between (almost) cylindrical parts of the textile-like domain.

Define $\Gamma_K^\mu(g_x, g_y)$ and $\Gamma_K^{\mu c}(g_x, g_y)$ as the images of Γ_0^μ and $\Gamma_0^{\mu c}$ under the following transformation N:

1. rotation around axis Oy by the angle $\gamma + \pi/2$,

2. swap of the second and the third coordinates,

3. translation by $(g_x, g_y, 0)$ for $g_x \in [0.4; 0.8]$ and $g_y \in [0.4; 0.8]$.

For a point $x \in \mathbb{R}^3$ the matrix of the mapping N can be written down as follows:

$$N(x) = \begin{pmatrix} g_x \\ g_y \\ 0 \end{pmatrix} + \begin{pmatrix} \sin(\gamma) & 0 & -\cos(\gamma) \\ \cos(\gamma) & 0 & \sin(\gamma) \\ 0 & 1 & 0 \end{pmatrix} x.$$

Introduce notation $P'_{ij} = N(P_{ij})$, $J'_{ij} = N(J_{ij})$ for $i \in \{1, 2\}$ and $j \in \{1, 2\}$, $O' = N(O)$ and $B' = N(B)$. For the following parameter values

$$\alpha = \frac{2}{3}\pi, \quad \beta = \frac{1}{3}\pi, \quad \gamma = \arctan\left(\frac{2}{3}\right), \quad 0.4 \le g_x \le 0.8, \quad 0.4 \le g_y \le 0.8,$$

$\Gamma_K^\mu(g_x, g_y)$ and $\Gamma_K^{\mu c}(g_x, g_y)$ have their x and y coordinates in the interval $(0; 1)$, and the points closest to sets $\{x = 0\}$, $\{x = 1\}$, $\{y = 0\}$, $\{y = 1\}$ are J'_{22}, J'_{11}, J'_{21}, J'_{12}, respectively. Introduce $\Gamma_{\#K}^\mu(g_x, g_y) = \Gamma_K^\mu(g_x, g_y) \cup \{B_{22}J'_{22}, B_{21}J'_{21}, B_{12}J'_{12}, B_{11}J'_{11}\}$ and $\Gamma_{\#K}^{\mu c}(g_x, g_y) =$
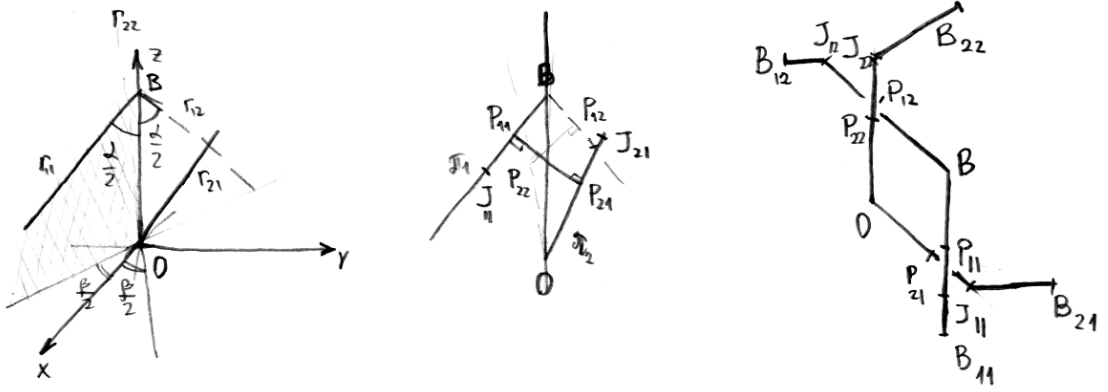
Figure 1.1: A set similar to $\Gamma^{\mu}_{\#K}(g_x, g_y)$.

$\Gamma^{\mu}_{\#K}(g_x, g_y) \cup \{P'_{11}P'_{21}, P'_{12}P'_{22}\}$, where

$$B_{11} = \begin{pmatrix} 1 \\ [J'_{11}]_2 \\ [J'_{11}]_3 \end{pmatrix}, \quad B_{12} = \begin{pmatrix} 0.5 \\ 1 \\ [J'_{12}]_3 \end{pmatrix}, \quad B_{21} = \begin{pmatrix} 0.5 \\ 0 \\ [J'_{21}]_3 \end{pmatrix}, \quad B_{22} = \begin{pmatrix} 0 \\ [J'_{22}]_2 \\ [J'_{22}]_3 \end{pmatrix}.$$

Here the i-th component of a vector (or a point) a is denoted by $[a]_i$. The choice of points B_{ij} guarantees that $\Gamma^{\mu}_{\#K}(g_x, g_y)$ and $\Gamma^{\mu c}_{\#K}(g_x, g_y)$ touch the boundary of the set $\{x \in [0; 1]\} \times \{y \in [0; 1]\}$. An example of what $\Gamma^{\mu}_{\#K}(g_x, g_y)$ looks like is shown in Figure 1.1. Note that the coordinates of B_{21} and B_{12} do not depend on the geometry shift parameters (g_x, g_y).

Let $\Gamma^{R\mu}_{\#K}(g_x, g_y)$ be the reflection of $\Gamma^{\mu}_{\#K}(g_x, g_y)$ with respect to the plane $x = 1$. Let $\Gamma^{U\mu}_{\#K}(g_x, g_y)$ be the image of $\Gamma^{\mu}_{\#K}(g_x, g_y)$ under superposition of the following two reflections: the first with respect to the set $x = 1/2$ and the second with respect to the plane $y = 1$. Let $\Gamma^{UR\mu}_{\#K}(g_x, g_y)$ be the reflection of $\Gamma^{U\mu}_{\#K}(g_x, g_y)$ with respect to the plane $x = 1$. Define $\Gamma^{R\mu c}_{\#K}(g_x, g_y)$, $\Gamma^{U\mu c}_{\#K}(g_x, g_y)$, and $\Gamma^{UR\mu c}_{\#K}(g_x, g_y)$ analogously as the images of $\Gamma^{\mu c}$. Define

$$\Gamma^{\mu}_Y(g_x, g_y) = S_{1/2}\left(\Gamma^{\mu}_{\#K}(g_x, g_y) \cup \Gamma^{R\mu}_{\#K}(g_x, g_y) \cup \Gamma^{U\mu}_{\#K}(g_x, g_y) \cup \Gamma^{UR\mu}_{\#K}(g_x, g_y)\right),$$

$$\Gamma^{\mu c}_Y(g_x, g_y) = S_{1/2}\left(\Gamma^{\mu c}_{\#K}(g_x, g_y) \cup \Gamma^{R\mu c}_{\#K}(g_x, g_y) \cup \Gamma^{U\mu c}_{\#K}(g_x, g_y) \cup \Gamma^{UR\mu c}_{\#K}(g_x, g_y)\right),$$

where $S_{1/2}$ is the uniform scaling operator with the scaling coefficient $1/2$. Observe that

$\Gamma_Y^\mu(g_x, g_y)$ and $\Gamma_Y^{\mu c}(g_x, g_y)$ are subsets of set $\{x \in [0;1]\} \times \{y \in [0;1]\}$ and that set

$$\Gamma_\infty^\mu(g_x, g_y) = \bigcup_{k_x \in \mathbb{Z}, k_y \in \mathbb{Z}} T_{k_x, k_y}\left(\Gamma_Y^\mu(g_x, g_y)\right),$$

where T_{k_x, k_y} is a translation operator by k_x along axis Ox and by k_y along axis Oy, is infinite and periodic in x and y set. Note that set

$$\Gamma_\infty^{\mu c}(g_x, g_y) = \bigcup_{k_x \in \mathbb{Z}, k_y \in \mathbb{Z}} T_{k_x, k_y}\left(\Gamma_Y^{\mu c}(g_x, g_y)\right)$$

is infinite, connected, and periodic in x and y.

Observe that due to the independence of coordinates of B_{12} and B_{21} on (g_x, g_y), $\Gamma_{\#K}^\mu(g_{1x}, g_{1y})$ can be connected to the translation $\Gamma_{\#K}^\mu(g_{2x}, g_{2y})$ in the vertical direction even if $g_{1x} \neq g_{2x}$ and $g_{1y} \neq g_{2y}$. For a sequence of geometrical parameters $\{g_x^k, g_y^k\}$, $k \in \mathbb{Z}$, define

$$\Gamma_\infty^\mu(\{g_x^k, g_y^k\}) = \bigcup_{k \in \mathbb{Z}} T_{0,k}\left(\bigcup_{m \in \mathbb{Z}} T_{m,0}\left(\Gamma_Y^\mu(g_x^k, g_y^k)\right)\right), \tag{1.2}$$

$$\Gamma_\infty^{\mu c}(\{g_x^k, g_y^k\}) = \bigcup_{k \in \mathbb{Z}} T_{0,k}\left(\bigcup_{m \in \mathbb{Z}} T_{m,0}\left(\Gamma_Y^{\mu c}(g_x^k, g_y^k)\right)\right). \tag{1.3}$$

Note that set $\Gamma_\infty^{\mu c}(\{g_x^k, g_y^k\})$ is connected and infinite, but not necessarily periodic.

Assume that g_x and g_y are elements of $C(\mathbb{R}^2, \mathbb{R})$. Introduce a new parameter ε and define

$$\Gamma_\infty^{\varepsilon,\mu}(g_x, g_y) = S_\varepsilon\left(\Gamma_\infty^\mu\left[\{g_x(\varepsilon(k+1/2)), g_y(\varepsilon(k+1/2))\}_{k \in \mathbb{Z}}\right]\right),$$

$$\Gamma_\infty^{\varepsilon,\mu c}(g_x, g_y) = S_\varepsilon\left(\Gamma_\infty^{\mu c}\left[\{g_x(\varepsilon(k+1/2)), g_y(\varepsilon(k+1/2))\}_{k \in \mathbb{Z}}\right]\right).$$

These two sets represent scaled structures, for which the geometrical parameters are defined by two continuous functions. As usual in homogenization, parameter ε will be assumed to be small, and these definitions adjust the defining sequences from (1.2) and (1.3) accordingly.

Introduce the enclosing domain Ω^{3D}. Assume it has a piecewise-Lipschitz boundary and satisfies the cone condition [19]. In our work $\Omega^{3D} = \Omega \times (0; H_{3D})$, where Ω is a Lipschitz

two-dimensional domain. In our example application Ω will be a rectangle. The following two sets will be of interest in the sequel:

$$\Gamma^{\varepsilon,\mu}(g_x, g_y) = \Omega^{3D} \cap \Gamma^{\varepsilon,\mu}_\infty(g_x, g_y), \quad \Gamma^{\varepsilon,\mu c}(g_x, g_y) = \Omega^{3D} \cap \Gamma^{\varepsilon,\mu c}_\infty(g_x, g_y).$$

It will also be convenient to consider $\Gamma^{\varepsilon,\mu}$ as a weighted graph. Sometimes we will refer to the segments as to edges, and to segments' ends as to nodes. Denote the set of all segment ends by N and for each node $n \in N$, let $E(n)$ be the set of all segments incident to n.

1.2.2 Three-dimensional geometry

For all the sets mentioned in the previous section we define the corresponding three-dimensional preliminary geometries as Minkowski sums of one-dimensional geometries with open ball $\mathcal{B}^\mu$ of radius μ centered at zero. Due to the choice of geometrical parameters and (1.1), any such 3D geometry will have self-intersections. Each of these intersections is a lateral intersection of exactly two cylinders of the same radius and non-parallel non-intersecting axes. Our aim is to state a 3D elasticity problem with Robin-type conditions at the contact interfaces. Therefore, we have to first eliminate any self-intersections of the geometry and then define the contact interfaces accordingly.

Since the intersections are always lateral intersections of exactly two cylinders, it is enough to consider a general case of two intersecting cylinders of the same radii. Denote the cylinders by C_1 and C_2 and their axes by a_1 and a_2. Assume that C_1 and C_2 are closed. Let P_1 and P_2 be the closest points of a_1 to a_2 and a_2 to a_1 respectively. Consider plane π_{mid} parallel to a_1 and a_2 and equidistant from P_1 and P_2. Observe that $R = C_1 \cap C_2 \cap \pi_{\mathrm{mid}}$ is a parallelogram P_{mid}. Denote the closed half-space with respect to π_{mid} containing a_1 by V_1, and the half-space containing a_2 by V_2. Let $\mathcal{C}_1 = \mathrm{int}\,(C_1 \setminus (C_2 \cap V_2))$ and $\mathcal{C}_2 = \mathrm{int}\,(C_2 \setminus (C_1 \cap V_1))$. Define

$$S = \overline{\mathcal{C}_1} \cap \overline{\mathcal{C}_2}, \ \mathrm{int}\,(S) = \varnothing, \ \mathrm{meas}_{\mathrm{surf}}\,(S) \neq 0 \tag{1.4}$$

and note that

$$\mathcal{C}_1 \cap \mathcal{C}_2 = \varnothing. \tag{1.5}$$
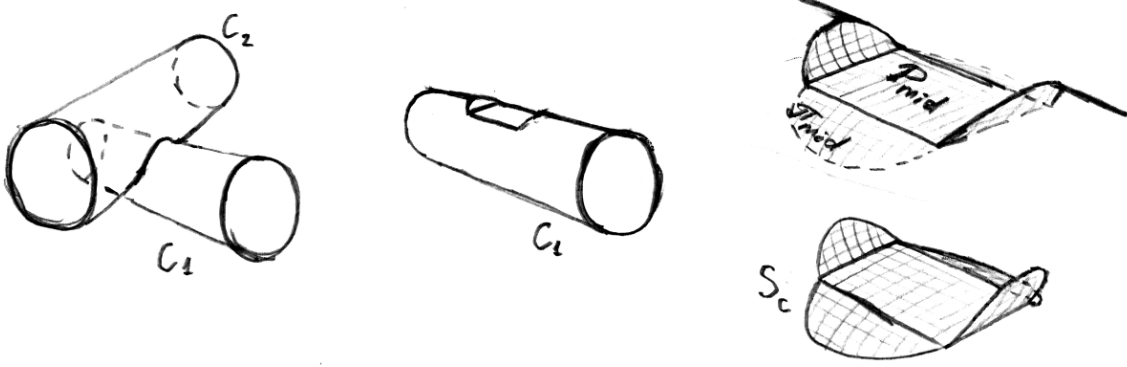
Figure 1.2: Sketch of a contact interface between two cylinders.

However, $P_{\mathrm{mid}} \subseteq S$. Observe that $S = (V_1 \cap \partial C_1 \cap C_2) \cup (V_2 \cap \partial C_2 \cap C_1) \cup P_{\mathrm{mid}}$. The sets mentioned are shown in Figure 1.2. For statements of elasticity problems instead of $C_1 \cup C_2$ we use C_1 and C_2, and S as the contact interface. Due to (1.4) and (1.5), the sets can be used as domains for elasticity problems with Robin conditions at S.

Consider set $\mathcal{O}_{\mathrm{inter}} = \Gamma_\infty^\mu(\{g_{x_k}, g_{y_k}\}) + \mathcal{B}^\mu$. At each translated component $\Gamma_Y^\mu(g_x^k, g_y^k)$ there are eight lateral intersections of cylindrical surfaces. Denote the modification of the set $\mathcal{O}_{\mathrm{inter}}^\mu(\{g_{x_k}, g_{y_k}\})$ according to the technique described above by $\mathcal{O}_\infty^\mu(\{g_{x_k}, g_{y_k}\})$ and the union of all its contact interfaces by $S_\infty^\mu(\{g_{x_k}, g_{y_k}\})$. For given continuous functions g_x and g_y, the set $\mathcal{O}_\infty^{\mu,\varepsilon}(g_x, g_y)$ is defined in a similar way, but with $\Gamma_\infty^{\varepsilon,\mu}(g_x, g_y)$ instead of $\Gamma_\infty^\mu(g_x, g_y)$ and $\mathcal{B}^{\mu\varepsilon}$ instead $\mathcal{B}^\mu$ in the Minkowski sum. The corresponding contact interface set is denoted by $S_\infty^{\mu,\varepsilon}(g_x, g_y)$.

Define a two-component continuous function $\widetilde{g} \in C(\mathbb{R}^2, \mathbb{R}) \times C(\mathbb{R}^2, \mathbb{R})$ and the following set:

$$\mathcal{O}_{\boldsymbol{g}}^{\mu,\varepsilon} = \Omega^{\mathrm{3D}} \cap \mathcal{O}_\infty^{\mu,\varepsilon}([\widetilde{\boldsymbol{g}}]_1, [\widetilde{\boldsymbol{g}}]_2).$$

Define $S_{\boldsymbol{g}}^{\mu,\varepsilon}$ as a union of all contact interfaces in $\mathcal{O}_{\boldsymbol{g}}^{\mu,\varepsilon}$. Further in the optimization problems, only the restriction of $\widetilde{g}$ onto Ω will be important. Further in this section we denote this restriction as follows: $\boldsymbol{g} \in C(\Omega, \mathbb{R}) \times C(\Omega, \mathbb{R})$.

Remark 1. In subsequent sections the symbol $\boldsymbol{g}$ is always used for the geometrical parameters. The underlying functional spaces will vary. For example, for the sections dealing with periodic case, the geometry is parametrized by two numbers. For quasi-periodic setting, parametrizations by Lipschitz and H^2 functions will be considered. Finally, in the

numerical examples the geometrical parameters will be either piecewise-affine functions or two real numbers. The corresponding function spaces will always be mentioned in the corresponding section.

In the sequel the set $\mathcal{O}_{\boldsymbol{g}}^{\mu,\varepsilon}$ will be considered as a union of cylinders with their axes obtained from the corresponding transformations of $\Gamma_\infty^\mu(\{g_{x_k}, g_{y_k}\})$. All the cylinders have circular cross-sections of radius μ everywhere except in the vicinity of the contact points. We ignore this issue when considering one-dimensional problems for the beams and treat their cross-sections as circular everywhere.

Denote the j-th connected component of $\mathcal{O}_{\boldsymbol{g}}^{\mu,\varepsilon}$ by $\mathcal{O}_{\boldsymbol{g},j}^{\mu,\varepsilon}$ for $j = 0, \ldots, m^\varepsilon$ (note that the number of these connected components does not depend on $\boldsymbol{g}$ and μ). Let $S_{\boldsymbol{g},j}^{\mu,\varepsilon} = S_{\boldsymbol{g}}^{\mu,\varepsilon} \cap \mathcal{O}_{\boldsymbol{g},j}^{\mu,\varepsilon}$. The 0-th component is assumed to have a special property: throughout this part it is assumed that for $\mathcal{O}_{\boldsymbol{g},0}^{\mu,\varepsilon}$ Dirichlet conditions are prescribed at some part of $\partial\mathcal{O}_{\boldsymbol{g},0}^{\mu,\varepsilon}$ with non-zero measure. By the construction procedure of the geometry, for any j there exists a sequence c_k^j, $k = 1, \ldots, K^j$ such that $c_1^j = 0$ and $c_{K^j}^j = j$ and for all integer $m > 1$, $m \leq K^j$, the components $\mathcal{O}_{\boldsymbol{g},j}^{\mu,\varepsilon}$ are connected by an interface of non-zero measure, i.e.

$$S_{\boldsymbol{g},i,j}^{\mu,\varepsilon} = \overline{\mathcal{O}_{\boldsymbol{g},i}^{\mu,\varepsilon}} \cap \overline{\mathcal{O}_{\boldsymbol{g},j}^{\mu,\varepsilon}}, \ \mathrm{meas}_{\mathrm{surf}}\, S_{\boldsymbol{g},i,j}^{\mu,\varepsilon} > 0.$$

Note that set

$$\mathcal{O}_{\boldsymbol{g},c}^{\mu,\varepsilon} = \mathrm{int}\,\overline{\mathcal{O}_{\boldsymbol{g}}^{\mu,\varepsilon}}$$

is a connected domain suitable for statement of an elasticity problem. The following relations are true: $\mathcal{O}_{\boldsymbol{g}}^{\mu,\varepsilon} \subset \mathcal{O}_{\boldsymbol{g},c}^{\mu,\varepsilon}$, $\mathcal{O}_{\boldsymbol{g}}^{\mu,\varepsilon} \cap S^{\mu,\varepsilon} = \varnothing$, $\mathcal{O}_{\boldsymbol{g}}^{\mu,\varepsilon} \cup \mathrm{rel\,int}\,(S^{\mu,\varepsilon}) = \mathcal{O}_{\boldsymbol{g},c}^{\mu,\varepsilon}$.

1.3 Description of periodic 3D direct problem

This section starts with a description of the periodic homogenization setting. Assume that $\widetilde{g}$ is periodic (and $\boldsymbol{g}$ is the restriction of a periodic function onto Ω). Since μ and $\boldsymbol{g}$ will not play any role in this section, they are omitted in the notation.

The domain $\mathcal{O}^\varepsilon$ is a union of connected open bounded Lipschitz domains $\mathcal{O}_i^\varepsilon$, $0 \leq i \leq M^\varepsilon$, each representing a single fiber. The contact interface S^ε between the fibers is known. The part $\partial\mathcal{O}_D^\varepsilon$ of the boundary $\partial\mathcal{O}^\varepsilon \cap \partial\Omega$ is fixed. The rest of $\partial\mathcal{O}^\varepsilon \setminus S^\varepsilon$, denoted by $\partial\mathcal{O}_N^\varepsilon$, is load-free.

Consider the following problem:

$$\begin{cases} -\nabla \cdot \left(\boldsymbol{A}^\varepsilon(\boldsymbol{x}) e(\boldsymbol{u}^\varepsilon(\boldsymbol{x})) \right) = \boldsymbol{f}^\varepsilon(\boldsymbol{x}) \text{ in } \mathcal{O}^\varepsilon, \\ \boldsymbol{u}^\varepsilon = 0 \text{ on } \partial\mathcal{O}^\varepsilon_D, \\ \boldsymbol{A}^\varepsilon e(\boldsymbol{u}^\varepsilon) \cdot \boldsymbol{n}(\boldsymbol{x}) = 0 \text{ on } \partial\mathcal{O}^\varepsilon_N, \\ \boldsymbol{A}^\varepsilon e(\boldsymbol{u}^\varepsilon) \cdot \boldsymbol{n}^\varepsilon_+ = \boldsymbol{A}^\varepsilon e(\boldsymbol{u}^\varepsilon) \cdot \boldsymbol{n}^\varepsilon_- \text{ on } S^\varepsilon, \\ \boldsymbol{A}^\varepsilon e(\boldsymbol{u}^\varepsilon) \cdot \boldsymbol{n}^\varepsilon_+ = \varepsilon^{-1} \boldsymbol{R}^\varepsilon \left[\boldsymbol{u}^\varepsilon \right] \text{ on } S^\varepsilon, \end{cases} \tag{1.6}$$

where $\boldsymbol{f}^\varepsilon$ is the volume force, $[\cdot]$ on S^ε denotes the jump of the vector on the opposite sides of the interface S^ε, $\boldsymbol{n}(\boldsymbol{x})$ is the normal vector to the interface. Matrix $\boldsymbol{R}^\varepsilon$ is the Robin condition matrix, it is assumed to be an element of $\mathcal{M}^+\left(S^\varepsilon\right)$. We say that matrix $\boldsymbol{R} \in \mathcal{M}^+\left(S^\varepsilon\right)$ if and only if

1. $\boldsymbol{R} \in L^\infty(S^\varepsilon, \mathbb{R}^{3\times 3})$,

2. $\boldsymbol{R}$ is symmetric and positive-definite.

In our case

$$\boldsymbol{R}^\varepsilon(\boldsymbol{x}) = r_n \boldsymbol{n}(\boldsymbol{x}) \otimes \boldsymbol{n}(\boldsymbol{x}) + r_t(I - \boldsymbol{n}(\boldsymbol{x}) \otimes \boldsymbol{n}(\boldsymbol{x})), \qquad r_n > 0, \ r_t > 0. \tag{1.7}$$

Tensor $\boldsymbol{A}^\varepsilon$ is the elasticity tensor, that is assumed to be an element of $\mathcal{T}^+\left(\mathcal{O}^\varepsilon\right)$. We say that tensor $\boldsymbol{T} \in \mathcal{T}^+\left(\mathcal{O}^\varepsilon\right)$ if and only if

1. $\boldsymbol{T} \in L^\infty(\mathcal{O}^\varepsilon, \mathbb{R}^{3\times 3\times 3\times 3})$,

2. $\boldsymbol{T}$ satisfies symmetry and coercivity conditions

$$[\boldsymbol{T}]_{ijkl} = [\boldsymbol{T}]_{klij} = [\boldsymbol{T}]_{jikl} = [\boldsymbol{T}]_{ijlk}, \ 1 \le i,j,k,l \le 3,$$
$$\exists \Lambda, \lambda \colon \Lambda \ge \lambda > 0, \ \Lambda \left| \boldsymbol{M} \right|^2 \ge \boldsymbol{T}\boldsymbol{M} : \boldsymbol{M} \ge \lambda \left| \boldsymbol{M} \right|^2 \ \forall \boldsymbol{M} \in \mathcal{M}^{\mathrm{sym}_3}, \tag{1.8}$$

where $\mathcal{M}^{\mathrm{sym}_3}$ is the space of symmetric 3×3 matrices. We additionally require that the boundaries $\partial\mathcal{O}^\varepsilon_i$ are piecewise Lipschitz and each $\mathcal{O}^\varepsilon_i$ satisfies the cone condition (see [19]).

Remark 2. In this work Sobolev spaces on non-connected open sets and trace spaces on non-connected boundaries are considered. These non-connected sets and boundaries are always finite unions of non-intersecting domains and boundaries in the classical sense (i.e. open connected sets). This is different from the standard theory, but is natural for our

problem (see also Section 3 in [23]). The extension of the inner product of H^1 onto unions of domains with interfaces can be done in at least two different ways, which are both logical: the first approach is to extend it with integrals of the traces on the interfaces (as it is done in [23]), the other is to take the sum of the standard H^1 inner products over the connected subdomains.

The second approach implies that for non-intersecting connected open sets $\mathcal{O}_i$, $1 \leq i \leq M$ and $\mathcal{O} = \bigcup_{i=1}^{M} \mathcal{O}_i$,

$$H_e^1(\mathcal{O}) = \bigcap_{i=1}^{M} H^1(\mathcal{O}_i),$$

and for any $\boldsymbol{u}, \boldsymbol{v} \in H_e^1(\mathcal{O})$ we extend the inner product as follows:

$$\langle \boldsymbol{u}, \boldsymbol{v} \rangle_{H_e^1(\mathcal{O})} = \langle \boldsymbol{u}, \boldsymbol{v} \rangle_{H_e^1\left(\bigcup_{i=1}^{M} \mathcal{O}\right)} = \sum_{i=1}^{M} \langle \boldsymbol{u}, \boldsymbol{v} \rangle_{H^1(\mathcal{O}_i)},$$

with the norm defined accordingly.

For $H^{1/2}$ the same construct is used, namely, for non-intersecting connected open sets $\mathcal{O}_i$, $1 \leq i \leq M$ and connected open sets Γ_j, $1 \leq j \leq K$, such that for any $j \colon 1 \leq j \leq K$, there exists $i \colon 1 \leq i \leq M$ such that $\Gamma_j \subseteq \partial \mathcal{O}_i$, we define $\Gamma = \bigcup_{j=1}^{K} \Gamma_j$ and

$$H_e^{1/2}(\Gamma) = \bigcap_{j=1}^{K} H^{1/2}(\Gamma_j),$$

where the holdall set is all functions defined on $\partial \mathcal{O}$. The norm is defined as follows: for any $\boldsymbol{u} \in H^{1/2}(\Gamma)$,

$$\|\boldsymbol{u}\|_{H_e^{1/2}(\Gamma)} = \sum_{j=1}^{K} \|\boldsymbol{u}\|_{H^{1/2}(\Gamma_j)}.$$

All fundamental properties of standard H^1 and $H^{1/2}$ spaces hold for H_e^1 and $H_e^{1/2}$.

Introduce the space of functions $H_e^1(\mathcal{O}^\varepsilon, \partial \mathcal{O}_D^\varepsilon)$ as follows:

$$H_e^1(\mathcal{O}^\varepsilon, \partial \mathcal{O}_D^\varepsilon) = \left\{ \boldsymbol{u} \in H_e^1(\mathcal{O}^\varepsilon) \colon \boldsymbol{u} = 0 \text{ at } \partial \mathcal{O}_D^\varepsilon \right\}.$$

The weak formulation of problem (1.6) reads: find $\boldsymbol{u}^\varepsilon \in H_e^1\left(\mathcal{O}^\varepsilon, \partial\mathcal{O}_D^\varepsilon\right)$ such that

$$\int_{\mathcal{O}^\varepsilon} \boldsymbol{A}^\varepsilon e(\boldsymbol{u}^\varepsilon) : e(\boldsymbol{v}) \, d\boldsymbol{x} + \frac{1}{\varepsilon} \int_{S^\varepsilon} \langle \boldsymbol{R}^\varepsilon \left[\boldsymbol{u}^\varepsilon\right], \left[\boldsymbol{v}\right] \rangle \, d\boldsymbol{s} = \boldsymbol{l}^\varepsilon(\boldsymbol{v}),$$

$$\boldsymbol{l}^\varepsilon(\boldsymbol{v}) = \int_{\mathcal{O}^\varepsilon} \langle \boldsymbol{f}^\varepsilon, \boldsymbol{v} \rangle \, d\boldsymbol{x}, \tag{1.9}$$

where $\boldsymbol{f}^\varepsilon \in L^2(\mathcal{O}^\varepsilon)$, for all $\boldsymbol{v} \in H_e^1(\mathcal{O}^\varepsilon, \partial\mathcal{O}_D^\varepsilon)$. The notation $\langle \boldsymbol{a}, \boldsymbol{b} \rangle$ denotes the scalar product of two vectors $\boldsymbol{a}$ and $\boldsymbol{b}$ from $\mathbb{R}^3$. To ensure uniqueness of the solution it is assumed that for some i the set $\partial\mathcal{O}_D^\varepsilon \cap \mathcal{O}_i^\varepsilon$ has a non-zero surface measure.

1.3.1   Auxiliary elasticity results

In this section auxiliary results used to prove the existence and uniqueness of the problems arising in homogenization are provided.

1.3.2   Korn's inequalities for connected chains of domains

The existence of the solution of the main problem (1.9) and cell problems introduced later is based on the following general

Theorem 1. *Let Ω_i, $i = 1, \ldots, M$ be bounded Lipschitz domains such that $\Omega_i \cap \Omega_j = \varnothing$, $\overline{\Omega}_i \cap \overline{\Omega}_j = \Gamma_{ij}$, $\Omega = \bigcup_{i=1}^M \Omega_i$, $\Gamma = \bigcup_{i,j=1}^M \Gamma_{ij}$. Let $\mathfrak{R}$ be the space of rigid displacements. Let V be a closed subspace of vector-valued functions in $\bigcap_{j=1}^M H^1(\Omega_j)$. Let $\widetilde{V} = \{\boldsymbol{v} \in V : [\boldsymbol{v}] = 0 \text{ on } \Gamma\}$. Assume that $\widetilde{V} \cap \mathfrak{R} = \{0\}$. Then every $\boldsymbol{v} \in V$ satisfies*

$$\sum_{j=1}^M \|\boldsymbol{v}\|_{H^1(\Omega_i)}^2 \le C\mathcal{E}(\boldsymbol{v}), \text{ where } \mathcal{E}(\boldsymbol{v}) = \int_\Omega (e(\boldsymbol{v}))^2 \, dx + \int_\Gamma [\boldsymbol{v}]^2 \, ds. \tag{1.10}$$

Proof. The theorem is proved from the contrary: assume that there exists a sequence of vectors $\{\boldsymbol{v}^m\} \in V$ such that

$$\sum_{j=1}^M \|\boldsymbol{v}^m\|_{H^1(\Omega_j)} = 1, \ \mathcal{E}(\boldsymbol{v}^m) \to 0 \text{ as } m \to \infty. \tag{1.11}$$

By the compactness of the imbedding $H_e^1(\Omega) \hookrightarrow L^2(\Omega)$, there exists a subsequence $m_l \to \infty$ such that for some $\boldsymbol{v} \in L^2(\Omega)$ we have $\boldsymbol{v}^{m_l} \to \boldsymbol{v}$ in $L^2(\Omega)$. According to the second Korn's

inequality, for every Ω_j we have

$$\left\|\boldsymbol{v}^{m+p} - \boldsymbol{v}^m\right\|_{H^1(\Omega_j)}^2 \le C \left(\left\|\boldsymbol{v}^{m+p} - \boldsymbol{v}^m\right\|_{L^2(\Omega_j)}^2 + \int_{\Omega_j} \left(e(\boldsymbol{v}^{m+p} - \boldsymbol{v}^m)_{ik}\right)^2 dx \right) \le$$

$$\le C \left(\left\|\boldsymbol{v}^{m+p} - \boldsymbol{v}^m\right\|_{L^2(\Omega_j)}^2 + \mathcal{E}(\boldsymbol{v}^{m+p} - \boldsymbol{v}^m) \right).$$

The first term in this expression tends to zero because $\boldsymbol{v}^{m_l} \to \boldsymbol{v}$ in $L^2(\Omega)$, and the second term tends to zero by the assumption (1.11). It follows that $\boldsymbol{v}^{m_l} \to \boldsymbol{v}$ in $H_e^1(\Omega)$. Since V is a closed subspace of $\bigcap_{j=1}^M H^1(\Omega_j)$, we conclude that

$$\boldsymbol{v} \in V, \quad \sum_{j=1}^M \|\boldsymbol{v}\|_{H^1(\Omega_j)}^2 = 1, \quad \mathcal{E}(\boldsymbol{v}) = 0.$$

The latter equality implies that $\boldsymbol{v} \in \widetilde{V}$ and that $e(\boldsymbol{v}) = 0$ in Ω_j, $j = 1, \ldots, M$. Then by the same argument as in Theorem 2.5 in [34], $\boldsymbol{v} \in \mathfrak{R}$. Therefore, $\boldsymbol{v} \in \mathfrak{R}$, $\boldsymbol{v} \in \widetilde{V}$, and $\sum_{j=1}^M \|\boldsymbol{v}\|_{H^1(\Omega_j)} = 1$. But this contradicts the condition $\widetilde{V} \cap \mathfrak{R} = \{0\}$. The theorem is proved. $\qquad \square$

1.3.3 Extension to fictitious domain

This section opens with the following general result similar to the extension-type theorems, but in our case it will also be used for homogenization purposes. The solutions of elasticity problems with Robin conditions on yarns (sets G_1^i defined below) are extended to a connected periodical three-dimensional domain by partially filling the void space (set G_2 defined below) with a soft material. The purpose of such extension is to obtain a set which can be repeated in the out-of-plane direction, so that three-dimensional homogenization results can be used for the geometries which converge to a plane geometry. This allows us not only to prove Korn's inequalities using standard techniques for perforated domains, but also to use three-dimensional homogenization for the problem, where the limiting geometry is plane and has a zero thickness.

Note that for geometries with certain symmetry conditions, the homogenization procedure without such extension is possible, see Chapter 3 of [36]. Although a very important question of convergence with respect to both the stiffness of the soft matrix material and the period of the structure arises, we do not study this question in this work. After the

justification of the three-dimensional homogenization for the material with the soft matrix, the in-plane homogenized properties $\boldsymbol{A}^{\mathrm{inp}}$ are obtained according to

$$A_{ijkl}^{\mathrm{inp}} = \varepsilon_0 \lim_{\delta \to 0} A_{ijkl}^{\mathrm{hom}}(\delta), \quad i,j,k,l \in \{1,2\}.$$

See Section 1.5.1 for more details on this relation. After this section, we imply everywhere the functions extended according to the results of this section without using δ in the notation.

Let $G = (0; L_1) \times (0; L_2) \times (0; h)$, let G_1 be a union of open non-intersecting domains G_1^i, $1 \le i \le M$, such that $G_1 \subseteq (0; L_1) \times (0; L_2) \times (\alpha; \beta)$, $0 < \alpha < \beta < h$ and that sets $\Gamma_0 = \partial G_1 \cap \{x_1 = 0\}$ and $\Gamma_1 = \partial G_1 \cap \{x_1 = L_1\}$ are non-empty and have a positive Lebesgue measure. We assume that ∂G_1 is a Lipschitzian boundary. Let

$$\partial G_N = (0; L_1) \times \{x_2 = 0\} \times (0; h) \cup (0; L_1) \times \{x_2 = L_2\} \times (0; h).$$

Sets

$$S_1^{ij} = \partial G_1^i \cap \partial G_1^j, \ 1 \le i \le M, \ 1 \le j \le M, \ i \neq j,$$
$$S_1 = \bigcup_{\substack{i \neq j \\ i=1, j=1}}^{i=M, j=M} \partial G_1^i \cap \partial G_1^j$$

represent the contact interfaces between the connected components of G_1. Let $\partial G_1^N = \partial G_1 \setminus (\Gamma_0 \cup \Gamma_1 \cup S_1)$. We assume that S_1 has a positive Lebesgue measure and that $\overline{G_1}$ is a connected Lipschitz set.

Consider the following problem

$$\begin{cases} -\nabla \cdot (\boldsymbol{A}^1 e(\boldsymbol{u})) = \boldsymbol{f} \ \text{in } G_1, \\ \boldsymbol{u} = 0 \ \text{on } \Gamma_0 \cup \Gamma_1, \\ \boldsymbol{A}^1 e(\boldsymbol{u}) \cdot \boldsymbol{n} = 0 \ \text{on } \partial G_1^N, \\ \boldsymbol{A}^1 e(\boldsymbol{u}) \cdot \boldsymbol{n}_+ = \boldsymbol{A}^1 e(\boldsymbol{u}) \cdot \boldsymbol{n}_- \ \text{on } S_1, \\ \boldsymbol{A}^1 e(\boldsymbol{u}) \cdot \boldsymbol{n}_+ = \boldsymbol{R}^1 [\boldsymbol{u}] \ \text{on } S_1, \end{cases} \qquad (1.12)$$

where $\boldsymbol{f} \in L^2(G_1)$, $\boldsymbol{A}^1 \in \mathcal{T}^+(G_1)$, $\boldsymbol{R}^1 \in \mathcal{M}^+(S_1)$.
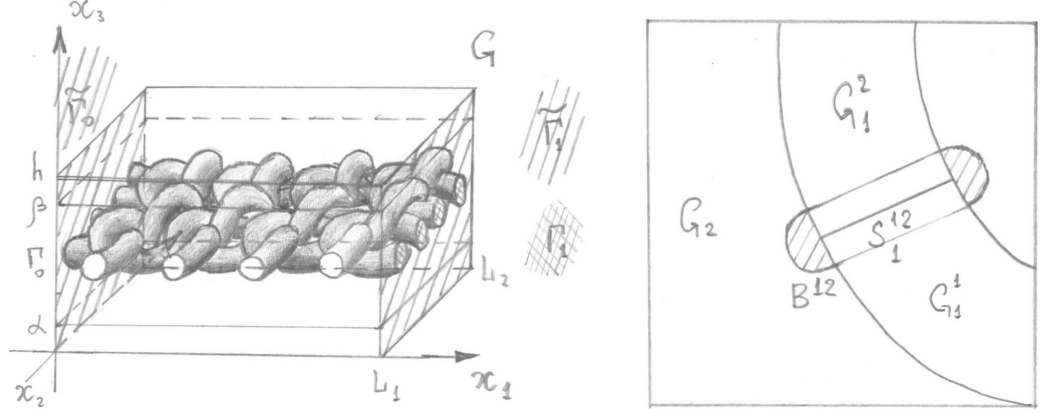
Figure 1.3: The textile layer in 3D (on the left) and an element of the geometry used for the extension.

Let ζ be some small positive number and define

$$\widehat{r} = \min\left(\zeta \min_{\substack{i,j:\, i\neq j,\\ S_1^{ij}\neq\varnothing}} \text{diam}\left(S_1^{ij}\right),\, \min_{\substack{(i_1,j_1)\neq(i_2,j_2)\\ S_1^{i_1 j_1}\neq\varnothing,\, S_1^{i_2 j_2}\neq\varnothing}} \text{dist}\left(S_1^{i_1 j_1}, S_1^{i_2 j_2}\right),\, \min_{\substack{i,j:\, S_1^{ij}\neq\varnothing}} \text{dist}\left(S_1^{ij}, \partial G\right)\right),$$

i.e. such a number that sets $B^{ij} = S_1^{ij} + \mathcal{B}^{\widehat{r}}$, $1 \le i \le M$, $1 \le j \le M$ intersect neither each other, nor ∂G, and that $\widehat{r}$ is small with respect to the size of S_1^{ij} themselves. Let $B = \bigcup_{i,j:\, i\neq j} B^{ij}$. Define $G_2 = \text{int}\,(G \setminus G_1 \setminus B)$. A schematic illustration for the geometries is provided in Figure 1.3.

From the definition of $\widehat{r}$ it follows that G_2 is a connected set. Additionally, it is assumed that its boundary is Lipschitz (the set subtraction of B from a Lipschitz domain is in general not Lipschitz), so that the standard elasticity problem on G_2 can be stated. The boundary of G_2 can be represented, up to some smooth curves, as the following union:

$$\partial G_2 = \partial G_N \cup \widetilde{\Gamma}_0 \cup \widetilde{\Gamma}_1 \cup \partial G_{12} \cup \partial G_2^B,$$

where $\partial G_{12} = \partial G_1 \cap \partial G_2$ and $\partial G_2^B = (G \setminus G_1) \cap \partial B$.

Extend the parameters of the problem (1.12) on G_2 as follows:

$$\boldsymbol{F}(\boldsymbol{x}) = \begin{cases} \boldsymbol{f}(\boldsymbol{x}), & \boldsymbol{x} \in G_1, \\ 0, & \boldsymbol{x} \in G_2, \end{cases} \quad \boldsymbol{A}^\delta(\boldsymbol{x}) = \begin{cases} \boldsymbol{A}^1(\boldsymbol{x}), & \boldsymbol{x} \in G_1, \\ \delta \boldsymbol{A}^2(\boldsymbol{x}), & \boldsymbol{x} \in G_2, \end{cases}$$

where $\boldsymbol{A}^2 \in \mathcal{T}^+(G)$ and $\delta > 0$. Consider the following fictitious domain problem:

$$\begin{cases} -\nabla \cdot (\boldsymbol{A}^\delta e(\boldsymbol{u}^\delta)) = \boldsymbol{F}, \text{ in } \operatorname{int}\left(\overline{G_1} \cup \overline{G_2}\right), \\ \boldsymbol{u}^\delta = 0 \text{ on } \widetilde{\Gamma}_0 \cup \widetilde{\Gamma}_1, \\ \boldsymbol{A}^\delta e(\boldsymbol{u}^\delta) \cdot \boldsymbol{n} = 0 \text{ on } \partial G_2^N \cup \partial G_2^B, \\ \boldsymbol{A}^\delta e(\boldsymbol{u}^\delta) \cdot \boldsymbol{n}_+ = \boldsymbol{A}^\delta e(\boldsymbol{u}^\delta) \cdot \boldsymbol{n}_- \text{ on } S_1, \\ \boldsymbol{A}^\delta e(\boldsymbol{u}^\delta) \cdot \boldsymbol{n}_+ = \boldsymbol{R}^1 \left[\boldsymbol{u}^\delta\right] \text{ on } S_1, \boldsymbol{u}^\delta \text{ is periodic w.r.t. } x_3 \text{ with the period } h, \end{cases} \tag{1.13}$$

where $\widetilde{\Gamma}_0 = \{x_1 = 0\} \times (0; L_2) \times (0; h)$, $\widetilde{\Gamma}_1 = \{x_1 = L_1\} \times (0; L_2) \times (0; h)$. The corresponding variational formulation for (1.12) is: find $\boldsymbol{u} \in H^1(G_1, \Gamma_0 \cup \Gamma_1)$ such that $\forall \boldsymbol{v} \in H^1(G_1, \Gamma_0 \cup \Gamma_1)$,

$$\int_{G_1} \boldsymbol{A}^1 e(\boldsymbol{u}) : e(\boldsymbol{v}) \, d\boldsymbol{x} + \int_{S_1} \left\langle \boldsymbol{R}^1\left[\boldsymbol{u}\right], [\boldsymbol{v}] \right\rangle ds = \int_{G_1} \langle \boldsymbol{f}, \boldsymbol{v} \rangle \, d\boldsymbol{x}. \tag{1.14}$$

For (1.13) it is: find $\boldsymbol{u}^\delta \in H^1_{e\#3}\left(G_1 \cup G_2, \widetilde{\Gamma}_0 \cup \widetilde{\Gamma}_1\right)$ such that $\forall\, \boldsymbol{v} \in H^1_{e\#3}\left(G_1 \cup G_2, \widetilde{\Gamma}_0 \cup \widetilde{\Gamma}_1\right)$

$$\int_{G_1 \cup G_2} \boldsymbol{A}^\delta e(\boldsymbol{u}^\delta) : e(\boldsymbol{v}) \, \boldsymbol{x} + \int_{S_1} \left\langle \boldsymbol{R}^\delta \left[\boldsymbol{u}^\delta\right], [\boldsymbol{v}] \right\rangle ds = \int_{G_1 \cup G_2} \langle \boldsymbol{F}, \boldsymbol{v} \rangle \, d\boldsymbol{x}, \tag{1.15}$$

where $H^1_{e\#3}\left(G_1 \cup G_2, \widetilde{\Gamma}_0 \cup \widetilde{\Gamma}_1\right)$ is the closure in the H^1-norm of the set of functions from $C^\infty\left(G_1, \widetilde{\Gamma}_0 \cup \widetilde{\Gamma}_1\right) \cap C^\infty\left(G_2, \widetilde{\Gamma}_0 \cup \widetilde{\Gamma}_1\right)$, periodic with respect to x_3 with the period h. In other words, the Sobolev space of functions, periodic in the third direction and satisfying the Dirichlet conditions at the x_1-sides.

Observe that problem (1.15) can be interpreted as problem (1.14), where the void space is partially filled with some "weak" material. Further we will also refer to fhis material as "soft matrix" material. It is crucial that by the repetition of $\overline{G_1} \cup \overline{G_2}$ with respect to the third axis one arrives at a periodic connected set.

It turns out that for δ sufficiently small, the solution of the extended problem approximates the solution of the original problem in G_1.

Theorem 2. *There exists a unique solution $\boldsymbol{u}$ to problem* (1.14) *and there exists a unique solution $\boldsymbol{u}^\delta$ to problem* (1.15)*. For the difference $\boldsymbol{u} - \boldsymbol{u}^\delta$ an estimate holds:*

$$\left\| \boldsymbol{u} - \boldsymbol{u}^\delta \right\|_{H_e^1(G_1)} \leq C\delta, \tag{1.16}$$

where C is a constant independent of δ.

Proof. Existence and uniqueness follow immediately from Corollary (2), because problems (1.14) and (1.15) are of the type 1.9.

Consider an auxiliary problem

$$\begin{cases} -\nabla \cdot (\boldsymbol{A}^2 e(\boldsymbol{u}_a)) = 0 \text{ in } G_2, \\ \boldsymbol{u}_a = 0 \text{ on } (\widetilde{\Gamma}_0 \setminus \Gamma_0) \cap (\widetilde{\Gamma}_1 \setminus \Gamma_1), \\ \boldsymbol{u}_a = \boldsymbol{u} \text{ on } \partial G_{12}, \\ \boldsymbol{A}^2 e(\boldsymbol{u}_a) \cdot \boldsymbol{n} = 0 \text{ on } \partial G_2^N \cup \partial G_2^B, \\ \boldsymbol{u}_a \text{ is periodic w.r.t. } x_3 \text{ with period } h. \end{cases}$$

The uniqueness and the existence of the solution to this problem are standard. By the standard a priori estimate, the following holds:

$$\|\boldsymbol{u}_a\|_{H^1(G_2)} \leq C_1 \|\boldsymbol{u}\|_{H_e^{1/2}(\partial G_{12})}. \tag{1.17}$$

Consider the function $\widetilde{\boldsymbol{u}} \in H_{e\#3}^1(G_1 \cup G_2, \widetilde{\Gamma}_0 \cup \widetilde{\Gamma}_1)$,

$$\widetilde{\boldsymbol{u}} = \begin{cases} \boldsymbol{u}(\boldsymbol{x}), & \boldsymbol{x} \in G_1, \\ \boldsymbol{u}_a(\boldsymbol{x}), & \boldsymbol{x} \in G_2. \end{cases} \tag{1.18}$$

Consider $\boldsymbol{w} = \boldsymbol{u}^\delta - \widetilde{\boldsymbol{u}} \in H_{e\#3}^1(G_1 \cup G_2, \widetilde{\Gamma}_0 \cup \widetilde{\Gamma}_1)$. Equations (1.14) and (1.15) yield

$$\int_{G_1 \cup G_2} \boldsymbol{A}^\delta e(\boldsymbol{w}) \,:\, e(\boldsymbol{v}) \, d\boldsymbol{x} + \int_{S_1} \left\langle \boldsymbol{R}^1 [\boldsymbol{w}], [\boldsymbol{v}] \right\rangle \, d\boldsymbol{s} = -\delta \int_{G_2} \boldsymbol{A}^2 e(\boldsymbol{u}_a) \,:\, e(\boldsymbol{v}) \, d\boldsymbol{x} \tag{1.19}$$

for any $\boldsymbol{v} \in H_{e\#3}^1(G_1 \cup G_2, \widetilde{\Gamma}_0 \cup \widetilde{\Gamma}_1)$. By the boundedness of $\boldsymbol{A}^2$ and (1.17),

$$\left| \delta \int_{G_2} \boldsymbol{A}^2 e(\boldsymbol{u}_a) : e(\boldsymbol{v}) \, d\boldsymbol{x} \right| \leq \delta C_2 \|\boldsymbol{u}_a\|_{H^1(G_2)} \|\boldsymbol{v}\|_{H^1(G_2)} \leq \delta C_1 C_2 \|\boldsymbol{u}\|_{H_e^{1/2}(\partial G_1^N)} \|\boldsymbol{v}\|_{H^1(G_2)}.$$

Let us choose $v = w$ in G. We get from (1.19) and the last estimate

$$\int_{G_1 \cup G_2} \boldsymbol{A}^\delta e(\boldsymbol{w}) : e(\boldsymbol{w}) \, d\boldsymbol{x} + \int_{S_2} \left\langle \boldsymbol{R}^1 \left[\boldsymbol{w}\right], \left[\boldsymbol{w}\right] \right\rangle \, d\boldsymbol{s} \leq \delta C_1 C_2 \left\| \boldsymbol{u} \right\|_{H_e^{1/2}(\partial G_{12})} \left\| \boldsymbol{w} \right\|_{H^1(G_2)}.$$

Note that $\boldsymbol{w}$ satisfies homogeneous boundary and periodicity conditions everywhere at the boundary of the problem (we mean $\widetilde{\Gamma}_0$, $\widetilde{\Gamma}_1$, ∂G^N and the sides $(0; L_1) \times (0; L_2) \times \{x_3 = 0\}$ and $(0; L_1) \times (0; L_2) \times \{x_3 = h\}$, not the interfaces). This allows us to apply the trace theorem with respect to G_1, G_2 and ∂G_{12} to estimate $\left\| \boldsymbol{w} \right\|_{G_2}$ by $\left\| \boldsymbol{w} \right\|_{G_1}$:

$$\left\| \boldsymbol{w} \right\|_{H^1(G_2)} \leq C_0 \left\| \boldsymbol{w} \right\|_{H_e^{1/2}(\partial G_{12})} \leq C_0 C_1 \left\| \boldsymbol{w} \right\|_{H_e^{1/2}(\partial G_1^N)} \leq C_0 C_1 C_3 \left\| \boldsymbol{w} \right\|_{H_e^1(G_1)}.$$

Finally,

$$\int_{G_1} \boldsymbol{A}^1 e(\boldsymbol{w}) : e(\boldsymbol{w}) \, d\boldsymbol{x} \leq \int_{G_1 \cup G_2} \boldsymbol{A}^\delta e(\boldsymbol{w}) : e(\boldsymbol{w}) \, d\boldsymbol{x} + \int_{S_1} \left\langle \boldsymbol{R}^1 \left[\boldsymbol{w}\right], \left[\boldsymbol{w}\right] \right\rangle \, d\boldsymbol{s} \leq$$
$$\leq \delta C_0 C_1^2 C_2 C_3 \left\| \boldsymbol{u} \right\|_{H_e^{1/2}(\partial G_{12})} \left\| \boldsymbol{w} \right\|_{H_e^1(G_1)}.$$

Applying Korn's inequality, we get

$$C_4 \left\| \boldsymbol{w} \right\|_{H_e^1(G_1)}^2 \leq \delta C_0 C_1^2 C_2 C_3 \left\| \boldsymbol{u} \right\|_{H_e^{1/2}(\partial G_1^N)} \left\| \boldsymbol{w} \right\|_{H_e^1(G_1)}.$$

The assertion of the theorem follows. $\square$

1.3.4 ε-scaled Korn's inequality

In this section we deal with the solutions extended using the soft matrix mentioned in the previous section. Korn's inequalities obtained in this section use the soft matrix material as a connected perforated domain used in [11, 34] to obtain Korn's inequalities with constants not depending on ε.

For homogenization purposes one needs the estimate of the type (1.10) for ε-scaled domains with the constant in the inequality not depending on ε. In this section the corresponding result is formulated.

Let Ω_m, $m = 1, \ldots, q$ be 1-periodic sets in $\mathbb{R}^3$ such that

1. $\Gamma_{mn} = \partial \Omega_m \cap \partial \Omega_n$ are piecewise-smooth Lipschitz surfaces $(m \neq n)$; $\Gamma_{mn} \subset B^{mn}$, where B^{mn} are open connected sets in $\mathbb{R}^3$ such that for any $l = 1, \ldots, q$ set
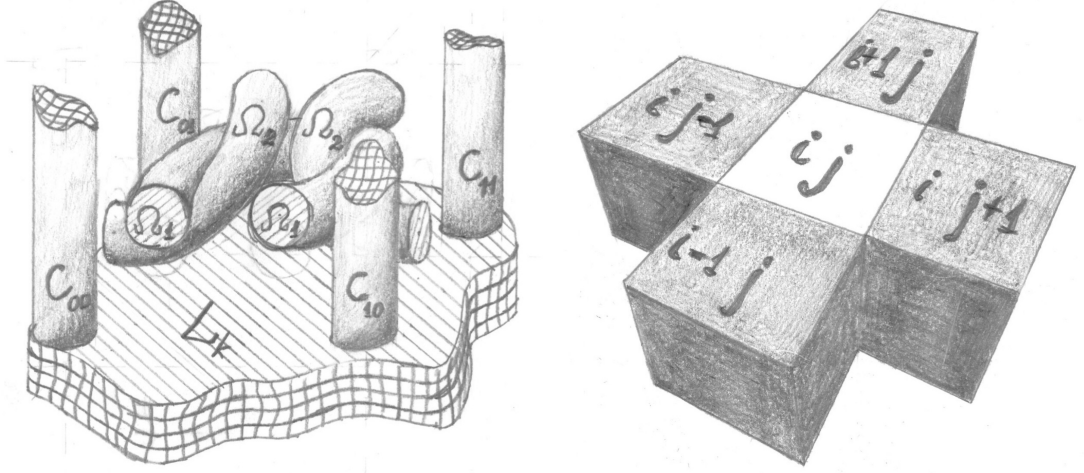
(a) The cylinders, the layer and parts of the sets Ω_1 and Ω_2 representing fibers.

(b) extension from the white cubes to the black cubes

Figure 1.4: Sets used in the extension lemma

int $\left(\left(\mathbb{R}^3 \setminus (\overline{B} \cup \overline{\Omega})\right) \cup \overline{\Omega_l}\right)$ is a 1-periodic domain with Lipschitz boundary, $B = \bigcup_{m,n=1}^q B^{mn}$, $\Omega = \bigcup_{m=1}^q \Omega_m$;

2. for any $l = 1, \ldots, q$, int $\left(\left(Q \setminus (\overline{B} \cup \overline{\Omega})\right) \cup \left(Q \cap \overline{\Omega_l}\right)\right)$ is a domain with Lipschitz boundary, $Q = (0;1)^3$;

3. $\mathbb{R}^3 \setminus (\overline{B} \cup \overline{\Omega})$ contains $\left(\bigcup_{i,j=-\infty}^{+\infty} C_{ij}\right) \cup \left(\bigcup_{k=-\infty}^{+\infty} L_k\right)$, where C_{ij} are cylinders $\left\{\boldsymbol{x} \in \mathbb{R}^3 \colon (x_1 - i)^2 + (x_2 - j)^2 < r^2\right\}$ with some positive r, L_k are layers $\left\{\boldsymbol{x} \in \mathbb{R}^3 \colon |x_3 - k| < r\right\}$.

Lemma 1. *Let I, J, K be positive integers. For any $l \in \{1, \ldots, q\}$ there exists an extension of a vector-valued function $\boldsymbol{u} \in H^1\left(\mathrm{int}\left(\left(Q_{IJK} \setminus (\overline{B} \cup \overline{\Omega})\right) \cup \left(\overline{\Omega_k} \cap Q_{IJK}\right)\right)\right)$ to $\widetilde{\boldsymbol{u}} \in H^1\left(\left(Q_{IJK} \setminus \overline{B}\right) \cup \left(\Omega_k \cap Q_{IJK}\right)\right)$ and to $\widetilde{\widetilde{\boldsymbol{u}}} \in H^1(Q_{IJK})$ such that*

$$\left\|\nabla \widetilde{\widetilde{\boldsymbol{u}}}\right\|_{L^2(Q_{IJK})}^2 \leq C_1 \left\|\nabla \widetilde{\boldsymbol{u}}\right\|_{L^2\left(Q_{IJK} \setminus \overline{B} \cup (\Omega \cup Q_{IJK})\right)}^2 \leq C_2 \left\|\nabla \boldsymbol{u}\right\|_{L^2\left(\mathrm{int}\left(\left(Q_{IJK} \setminus (\overline{B} \cup \overline{\Omega})\right) \cup \left(\overline{\Omega_l} \cap Q_{IJK}\right)\right)\right)}^2,$$

$$\left\|e\left(\widetilde{\widetilde{\boldsymbol{u}}}\right)\right\|_{L^2(Q_{IJK})}^2 \leq C_1 \left\|e(\widetilde{\boldsymbol{u}})\right\|_{L^2\left(\left(Q_{IJK} \setminus \overline{B}\right) \cup (\Omega \cap Q_{IJK})\right)}^2 \leq$$
$$\leq C_2 \left\|e(\boldsymbol{u})\right\|_{L^2\left(\mathrm{int}\left(\left(Q_{IJK} \setminus (\overline{B} \cup \overline{\Omega})\right) \cup \left(\overline{\Omega_l} \cap Q_{IJK}\right)\right)\right)}^2,$$

where $Q = (0; I) \times (0; J) \times (0; K)$, C_1 and C_2 are independent of $\boldsymbol{u}$, I, J, K.

Remark 3. Sets Ω_i correspond to threads, Γ_{mn} correspond to the contact interfaces between the threads, $Q \setminus (\overline{B} \cup \overline{\Omega})$ corresponds to a set occupied with the soft matrix material in a single unit cube. Finally, set $Q_{IJK} \setminus (\overline{B} \cup \overline{\Omega})$ is a connected perforated domain filled with the soft material. Lemma 1 means that it is possible to extended displacement fields from the set occupied with the soft material to the whole volume with the corresponding bilateral estimates on the H^1-norms of the functions. The constants in the estimates do not depend on I, J, K, i.e. the relation of the size of the domain to the size of its single periodicity cell does not affect the constants in the bilateral estimates of the norms. Later in Proposition 1 this fact will be expoited to prove Korn's inequality with the constant independent of ε.

Proof. The extension is constructed first in the layer $(\mathbb{R}^2 \times (0; 1)) \cap Q_{IJK}$ (in the layers $\mathbb{R}^2 \times (k; k+1)$ it is done in the same way). We proceed in 2 steps: we call "black" cubes $q_{i\,j} = (i; i+1) \times (j; j+1) \times (0; 1)$ with even $i + j$, and "white" all other cubes with odd $i + j$. At the first step we construct an extension from $\operatorname{int}\left((q_{i\,j} \setminus (\overline{B} \cup \overline{\Omega}))\right) \cup (\overline{\Omega_l} \cap q_{i\,j})$ to $\left((q_{i\,j} \setminus \overline{B}) \cup (\Omega \cap q_{i\,j})\right)$ and then to $q_{i\,j}$ for even $i + j$ as in Lemma 4.1 from [34]. At the second step we construct the extension from

$$\operatorname{int}\left((q_{i\,j} \setminus (\overline{B} \cup \overline{\Omega})) \cup (\overline{\Omega_l} \cap q_{i\,j})\right) \cup \left((q_{i-1\,j} \cup q_{i+1\,j} \cup q_{i\,j-1} \cup q_{i\,j+1}) \setminus \overline{B} \cup \right.$$
$$\left. \cup\, (q_{i-1\,j} \cup q_{i+1\,j} \cup q_{i\,j-1} \cup q_{i\,j+1}) \cap \Omega\right)$$

to $(q_{i\,j} \cup q_{i-1\,j} \cup q_{i+1\,j} \cup q_{i\,j-1} \cup q_{i\,j+1}) \setminus \overline{B} \cup (q_{i\,j} \cup q_{i-1\,j} \cup q_{i+1\,j} \cup q_{i\,j-1} \cup q_{i\,j+1}) \cup \Omega$ and then to $q_{i\,j} \cup q_{i-1\,j} \cup q_{i+1\,j} \cup q_{i\,j-1} \cup q_{i\,j+1}$ for odd $i + j$; if i (j) equals 0 or I (J), then the cubes $q_{i-1\,j}, q_{i+1\,j}, q_{i\,j-1}, q_{i\,j+1}$ with the values of subscripts out of $[0; I]$ (or $[0; J]$) are omitted. $\qquad \square$

For any set $\mathcal{F}$ denote by $\mathcal{F}^\varepsilon$ its contraction $\mathcal{F}^\varepsilon = \left\{ \boldsymbol{x} \in \mathbb{R}^3 \colon \dfrac{\boldsymbol{x}}{\varepsilon} \in \mathcal{F} \right\}$. Consider the space $\widetilde{H}_0^1$ of vector-valued functions $\boldsymbol{u}$ defined in $(Q \setminus \overline{B^\varepsilon}) \cup (Q \cap \Omega^\varepsilon)$ vanishing for $x_1 = 0$ and such that for any $l \in \{1, \ldots q\}$, $\boldsymbol{u} \in H^1\left((Q \setminus \overline{B^\varepsilon}) \cup (Q \cap \Omega_l^\varepsilon)\right)$.

Proposition 1. *There exist $C_3, C_4 \geq 0$ independent of ε, such that $\forall\, \boldsymbol{u} \in \widetilde{H}_0^1$,*

$$\|\boldsymbol{u}\|^2_{L^2\left((Q \setminus \overline{B^\varepsilon}) \cup (Q \cap \Omega^\varepsilon)\right)} \leq C_3 \|\nabla \boldsymbol{u}\|^2_{L^2\left((Q \setminus \overline{B^\varepsilon}) \cup (Q \cap \overline{\Omega^\varepsilon})\right)} \leq C_4 \|e(\boldsymbol{u})\|^2_{L^2\left((Q \setminus \overline{B^\varepsilon}) \cup (Q \cap \Omega^\varepsilon)\right)} . \quad (1.20)$$

Here ε is sufficiently small.

Proof. Make the change of variables $\boldsymbol{y} = \boldsymbol{x}/\varepsilon$ and apply extension Lemma 1 from $H^1\left((Q_{1/\varepsilon} \setminus \overline{B}) \cup (Q_{1/\varepsilon} \cap \Omega_l)\right)$ to $H^1\left(Q_{1/\varepsilon}\right)$, where $Q_{1/\varepsilon} = (0, 1/\varepsilon)^3$. Then we immediately obtain the estimates of the proposition by contraction. □

1.3.5 Homogenization of 3D direct problem

This section opens with important corollaries from statements of Section 1.3.1. Then the homogenized problem is described and then the analog of Theorem 6.1 and Theorem 7.1 from [23], which characterize the convergence of the solutions of the ε-problems to the solution of the homogenized problem, is stated and proved. After these two corollaries, all estimates and all problems in this section imply that the fictitious domain technique described in Section 1.3.3 is applied. In other words, we fix some $\delta > 0$ and imply that all domains and elasticity problems are modified according to (1.13). For all sets from Section 1.3 with symbol "$\mathcal{O}$" in the notation, the corresponding connected modifications are denoted similarly with symbol "Ω" instead of "$\mathcal{O}$". At the same time there will be no δ in the notation for the elasticity tensor, i.e. we re-define $\boldsymbol{A}^\varepsilon$ and $\boldsymbol{f}^\varepsilon$ to be the corresponding extensions of $\boldsymbol{A}^\varepsilon$ and $\boldsymbol{f}^\varepsilon$ from Section 1.3 from $\mathcal{O}^\varepsilon$ onto Ω^ε.

Corollary 1. *Inequality* (1.10) *holds for any* $\boldsymbol{u} \in H_e^1\left(\mathcal{O}^\varepsilon, \partial\mathcal{O}_D^\varepsilon\right)$.

Proof. Take $H_e^1\left(\mathcal{O}^\varepsilon, \partial\mathcal{O}_D^\varepsilon\right)$ as V. Observe that in this case $\widetilde{V}$ coincides with $H^1(\Omega_c, \partial\Omega_D) \equiv H^1(\Omega_c) \cap \{\boldsymbol{u} \colon \boldsymbol{u} = 0 \text{ on } \partial\Omega_D\}$. Since $H^1(\Omega_c) \cap \mathfrak{R} = \{0\}$, Theorem 1 is applicable and the corollary is proved. For details on spaces $H^1(\Omega, \gamma)$ see [34]. □

Corollary 2. *Problem* (1.9) *has a unique solution for any* ε *and* $\boldsymbol{f}^\varepsilon \in L^2(\mathcal{O}^\varepsilon)$.

Proof. The proof is similar to classical proofs in mathematical elasticity except that Korn's inequality now has form (1.10) and the bilinear form on the left-hand side of (1.9) includes the boundary term. The coercivity and boundedness of the bilinear form follows from conditions (1.7) and (1.8). The equivalence of the induced norm to the norm of $H_e^1(\mathcal{O}^\varepsilon)$ is proved in Lemma 3.6 in [23]. Finally, the existence and uniqueness in $H_e^1(\mathcal{O}^\varepsilon)$ follow from Lax-Milgram theorem. □

Corollary 3. *There exists H^1-extension of $\widehat{\boldsymbol{u}}^\varepsilon$ of the solution $\boldsymbol{u}^\varepsilon$ of problem* (1.9) *to Ω^ε from $\mathcal{O}^\varepsilon$, such that*

$$\|\widehat{\boldsymbol{u}}^\varepsilon\|_{H^1(\Omega^\varepsilon)} \le C \|\boldsymbol{u}^\varepsilon\|_{H_e^1(\mathcal{O}^\varepsilon)},$$

where $C > 0$ depends only on $\mathcal{O}^\varepsilon$.

Proof. The statement follows directly from Theorem 2. □

For homogenization purposes, we need a straightforward modifications of Theorem (2) for some fixed δ to have a material connected along the direction of the axis x_3 and having a coercive elasticity tensor. The potentially important question of the limiting behaviour of solutions with respect to both $\delta \to 0$ and $\varepsilon \to 0$ is not studied in this work.

Proposition 2. *Let $\boldsymbol{u}^\varepsilon$ be the solution of problem* (1.9) *There exists $C_H > 0$ independent of ε such that*

$$\|\boldsymbol{u}^\varepsilon\|_{H^1(\Omega^\varepsilon)} \leq C_H \|\boldsymbol{f}^\varepsilon\|_{L^2(\Omega^\varepsilon)}.$$

Proof. The proposition follows directly from Proposition 1 and coercivity of the bilinear form of problem (1.9). □

Consider the following problem on the encompassing domain Ω^{3D}

$$\int_{\Omega^{3D}} \boldsymbol{A}^{\text{hom}} e(\boldsymbol{u}^0) : e(\boldsymbol{v}) \, d\boldsymbol{x} = \int_{\Omega^{3D}} \left\langle \boldsymbol{f}^{\text{hom}}, \boldsymbol{v} \right\rangle d\boldsymbol{x}, \quad \forall \boldsymbol{v} \in H^1(\Omega^{3D}, \partial\Omega_D^{3D}) \qquad (1.21)$$

for $\boldsymbol{u}^0 \in H^1(\Omega^{3D}, \partial\Omega_D^{3D})$. The corresponding strong form is

$$\begin{cases} -\nabla \cdot (\boldsymbol{A}^{\text{hom}} e(\boldsymbol{u}^0)) = \boldsymbol{f}^{\text{hom}} \text{ in } \Omega^{3D}, \\ \boldsymbol{u}^0 = 0 \text{ on } \partial\Omega_D^{3D}, \\ \boldsymbol{A}^{\text{hom}} e(\boldsymbol{u}^0)\boldsymbol{n}(\boldsymbol{x}) = 0 \text{ on } \partial\Omega_N^{3D}. \end{cases}$$

By Ω_Y denote the 1-scaled periodicity cell of Ω^ε, and let S_Y to be the contact interfaces between the connected components of Ω_Y. The homogenized tensor $\boldsymbol{A}^{\text{hom}}$ is defined by

$$\begin{aligned} A_{ijkl}^{\text{hom}} &= \int_{\Omega_Y} \boldsymbol{e}_{ij} : \boldsymbol{A}(e(\boldsymbol{w}_{kl}) + \boldsymbol{e}_{kl}) \, d\boldsymbol{y} = \\ &= \int_{\Omega_Y} \boldsymbol{A}(e(\boldsymbol{w}_{ij}) + \boldsymbol{e}_{ij}) : (e(\boldsymbol{w}_{kl}) + \boldsymbol{e}_{kl}) \, d\boldsymbol{y} + \int_{S_Y} \boldsymbol{R}\left[\boldsymbol{w}_{ij}\right]\left[\boldsymbol{w}_{kl}\right] d\boldsymbol{s}, \end{aligned} \qquad (1.22)$$

where

$$\boldsymbol{R}(\boldsymbol{x}) = r_n \boldsymbol{n}(\boldsymbol{x}) \otimes \boldsymbol{n}(\boldsymbol{x}) + r_t(I - \boldsymbol{n}(\boldsymbol{x}) \otimes \boldsymbol{n}(\boldsymbol{x})), \qquad r_n > 0, \ r_t > 0,$$

e_{ij} are the unit basis vectors in the space of deformation gradients. In three dimensions they are

$$
\boldsymbol{e}_{11} = \begin{pmatrix} 1 & 0 & 0 \\ 0 & 0 & 0 \\ 0 & 0 & 0 \end{pmatrix}, \quad \boldsymbol{e}_{12} = \boldsymbol{e}_{21} = \begin{pmatrix} 0 & 1/2 & 0 \\ 1/2 & 0 & 0 \\ 0 & 0 & 0 \end{pmatrix}, \quad \boldsymbol{e}_{13} = \boldsymbol{e}_{31} = \begin{pmatrix} 0 & 0 & 1/2 \\ 0 & 0 & 0 \\ 1/2 & 0 & 0 \end{pmatrix},
$$

$$
\boldsymbol{e}_{22} = \begin{pmatrix} 0 & 0 & 0 \\ 0 & 1 & 0 \\ 0 & 0 & 0 \end{pmatrix}, \quad \boldsymbol{e}_{23} = \boldsymbol{e}_{32} = \begin{pmatrix} 0 & 0 & 0 \\ 0 & 0 & 1/2 \\ 0 & 1/2 & 0 \end{pmatrix}, \quad \boldsymbol{e}_{33} = \begin{pmatrix} 0 & 0 & 0 \\ 0 & 0 & 0 \\ 0 & 0 & 1 \end{pmatrix}.
$$

The functions $\boldsymbol{w}_{ij} \in H^1_{\#}(\Omega_Y)$, $i, j = 1, \ldots, 3$ are the solutions of the following cell problems

$$
\int_{\Omega_Y} (e(\boldsymbol{w}_{ij}) + \boldsymbol{e}_{ij}) : \boldsymbol{A}e(\boldsymbol{v}) \, d\boldsymbol{x} + \int_{S_Y} \langle \boldsymbol{R}[\boldsymbol{w}_{ij}], [\boldsymbol{v}] \rangle \, d\boldsymbol{s} = 0 \quad \forall \boldsymbol{v} \in H^1_{\#}(\Omega_Y) \tag{1.23}
$$

the corresponding strong form is

$$
\begin{cases} -\nabla \cdot (\boldsymbol{A}(e(\boldsymbol{w}_{ij}) + \boldsymbol{e}_{ij})) = 0 \text{ in } \Omega_Y \\ \boldsymbol{A}(e(\boldsymbol{w}_{ij}) + \boldsymbol{e}_{ij}) \cdot \boldsymbol{n}_+ = \boldsymbol{A}(e(\boldsymbol{w}_{ij}) + \boldsymbol{e}_{ij}) \cdot \boldsymbol{n}_- \text{ on } S_Y, \\ \boldsymbol{A}(e(\boldsymbol{w}_{ij}) + \boldsymbol{e}_{ij}) \cdot \boldsymbol{n}_+ = \boldsymbol{R}[\boldsymbol{w}_{ij}] \text{ on } S_Y, \end{cases} \tag{1.24}
$$

where $H^1_{\#}(\Omega_Y)$ is the closure of Y-periodic functions from $C^\infty(\Omega_Y)$ in the norm of $H^1(\Omega_Y)$. Introduce a closed subspace of functions with zero average from $H^1_{\#}(\Omega_Y)$:

$$
H^1_{\#0}(\Omega_Y) = \left\{ \boldsymbol{u} \in H^1_{\#}(\Omega_Y) \colon \int_{\Omega_Y} \boldsymbol{u} \, d\boldsymbol{x} = 0 \right\}.
$$

Theorem 3. *There exists a unique solution of problem* (1.23) *for any* $i, j = 1, \ldots, 3$.

Proof. The idea of the proof is to apply Theorem 1 to obtain Korn's inequality for the problem (1.23). Then the theorem follows by the application of Lax-Milgram theorem.

Transform the left-hand side of (1.23) into a bilinear form with respect to the unknown function:

$$
\int_{\Omega_Y} (e(\boldsymbol{w}_{ij}) + \boldsymbol{e}_{ij}) : \boldsymbol{A}e(\boldsymbol{v}) \, d\boldsymbol{x} + \int_{S_Y} \langle \boldsymbol{R}[\boldsymbol{w}_{ij}], [\boldsymbol{v}] \rangle \, d\boldsymbol{s} = \int_{\Omega_Y} \boldsymbol{e}_{ij} : \boldsymbol{A}e(\boldsymbol{v}) \, d\boldsymbol{x} + a^{\#}(\boldsymbol{w}_{ij}, \boldsymbol{v}),
$$

$$
a^{\#}(\boldsymbol{w}_{ij}, \boldsymbol{v}) = \int_{\Omega_Y} e(\boldsymbol{w}_{ij}) : \boldsymbol{A}e(\boldsymbol{v}) \, d\boldsymbol{x} + \int_{S_Y} \langle \boldsymbol{R}[\boldsymbol{w}_{ij}], [\boldsymbol{v}] \rangle \, d\boldsymbol{s}.
$$

This bilinear form is coercive by conditions (1.7) and (1.8).

Observe that

$$\left\{ \boldsymbol{v} \colon \boldsymbol{v} \in H^1_\#(\Omega_Y), [\boldsymbol{v}] = 0 \text{ on } S_Y, \int_{\Omega_Y} \boldsymbol{v}\, d\boldsymbol{x} = 0 \right\} = H^1_{\#0}\left(\operatorname{int}\left(\overline{\Omega_Y}\right)\right),$$

here it is important that $\operatorname{int}\left(\overline{\Omega_Y}\right)$ is a connected open set which connects the opposite sides of Y. Therefore this space is a classical space of periodic functions with zero average. It is easy to see that $H^1_{\#0}\left(\operatorname{int}\left(\overline{\Omega_Y}\right)\right) \cap \mathfrak{R} = \{0\}$. We can use $H^1_{\#0}\left(\operatorname{int}\left(\overline{\Omega_Y}\right)\right)$ as $\widetilde{V}$ and $H^1_{\#0}$ as V in Theorem 1 to prove the Korn's inequality. The statement is proved. $\square$

In order to extend the results of [23] to elasticity, the Poincare inequality formulated in Lemma 3.3 and Proposition 3.4 therein have to be replaced with the corresponding Korn's inequality. It is provided by the following

Lemma 2. *There exists $C_P > 0$ independent of ε such that for any $\boldsymbol{u} \in H^1\left(\Omega^\varepsilon\right)$*

$$\|\boldsymbol{u}\|^2_{H^1(\Omega^\varepsilon)} \le C_P \left(\|e(\boldsymbol{u})\|^2_{H^1(\Omega^\varepsilon)} + \varepsilon^{-1} \|[\boldsymbol{u}]\|^2_{S^\varepsilon} \right). \tag{1.25}$$

Proof. The lemma follows from Proposition 1 by an addition of a non-negative term $\varepsilon^{-1} \|[\boldsymbol{u}]\|^2_{S^\varepsilon}$ to the right-hand side of the inequality. $\square$

Remark 4. It might look like it is not important, which term to add to the right-hand side of (1.20). In general case where the fictitious domain technique is not used, this power crucially affects the convergence with respect to ε. It follows from the scaling techniques used in papers [23, 11] that the choice of ε^{-1} as a power is the only case where the contact interface terms affect the properties of the homogenized medium without ruining the convergence of the solutions of ε-problems to the solution of the homogenized problem.

From now on, we deal with the fictitious domain modifications of problems (1.6) and (1.9):

$$\begin{cases} -\nabla \cdot \left(\boldsymbol{A}^\varepsilon(\boldsymbol{x}) e(\boldsymbol{u}^\varepsilon(\boldsymbol{x}))\right) = \boldsymbol{f}^\varepsilon(\boldsymbol{x}) \text{ in } \Omega^\varepsilon, \\ \boldsymbol{u}^\varepsilon = 0 \text{ on } \partial\Omega^\varepsilon_D, \\ \boldsymbol{A}^\varepsilon e(\boldsymbol{u}^\varepsilon) \cdot \boldsymbol{n}(\boldsymbol{x}) = 0 \text{ on } \partial\Omega^\varepsilon_N, \\ \boldsymbol{A}^\varepsilon e(\boldsymbol{u}^\varepsilon) \cdot \boldsymbol{n}^\varepsilon_+ = \boldsymbol{A}^\varepsilon e(\boldsymbol{u}^\varepsilon) \cdot \boldsymbol{n}^\varepsilon_- \text{ on } S^\varepsilon, \\ \boldsymbol{A}^\varepsilon e(\boldsymbol{u}^\varepsilon) \cdot \boldsymbol{n}^\varepsilon_+ = \varepsilon^{-1} \boldsymbol{R}^\varepsilon [\boldsymbol{u}^\varepsilon] \text{ on } S^\varepsilon \end{cases} \tag{1.26}$$

and its corresponding weak formulation: find $\boldsymbol{u}^\varepsilon \in H^1_e\left(\mathcal{O}^\varepsilon, \partial\mathcal{O}^\varepsilon_D\right)$ such that

$$\int_{\Omega^\varepsilon} \boldsymbol{A}^\varepsilon e(\boldsymbol{u}^\varepsilon) : e(\boldsymbol{v})\, d\boldsymbol{x} + \frac{1}{\varepsilon}\int_{S^\varepsilon} \langle \boldsymbol{R}^\varepsilon\left[\boldsymbol{u}^\varepsilon\right], [\boldsymbol{v}]\rangle\, d\boldsymbol{s} = \boldsymbol{l}^\varepsilon(\boldsymbol{v}),$$
$$\boldsymbol{l}^\varepsilon(\boldsymbol{v}) = \int_{\Omega^\varepsilon} \langle \boldsymbol{f}^\varepsilon, \boldsymbol{v}\rangle\, d\boldsymbol{x}, \tag{1.27}$$

Further, Theorem 4.1 of [23] in our setting is formulated as follows:

Theorem 4. *There exists $C_K > 0$ independent of ε such that for any solution $\boldsymbol{u}^\varepsilon$ of (1.27) the following inequality is true:*

$$\|e(\boldsymbol{u}^\varepsilon)\|^2_{H^1(\Omega^\varepsilon)} + \varepsilon^{-1}\|[\boldsymbol{u}^\varepsilon]\|^2_{L^2(S^\varepsilon)} \leq C_K \|\boldsymbol{f}^\varepsilon\|^2_{L^2(\Omega^\varepsilon)}. \tag{1.28}$$

Proof. The theorem is proved by the standard application of Cauchy-Schwarz inequality to weak formulation (1.27) for $\boldsymbol{v} = \boldsymbol{u}^\varepsilon$. □

Remark 5. In the homogenization theory for perforated domains it is common to divide the right-hand side of (1.22) by the volume of the material in the periodicty cell, see the expression for the homogenized tensor of Section 1.1 in Chapter II of [34]. We do not have this fraction in the expression for the homogenized tensor, but the corresponding multiplier appears in the limit of the right-hand side volume force. This causes no significant changes in proofs.

The main homogenization result used in this work is the modification of Theorem 6.1 and Theorem 7.1 from [23] for the case of elasticity:

Theorem 5. *Let $\boldsymbol{u}^\varepsilon \in H^1\left(\Omega^\varepsilon, \partial\Omega^\varepsilon_D\right)$ be a sequence of solutions of (1.27) and assume that*

$$\lim_{\varepsilon\to 0} \sup_{\substack{\boldsymbol{v}\in H^1(\Omega^\varepsilon, \partial\Omega^\varepsilon) \\ \|\boldsymbol{v}\|=1}} \int_{\Omega^\varepsilon} \left\langle \boldsymbol{f}^{\mathrm{hom}} - |\Omega_Y|\, \boldsymbol{f}^\varepsilon, \boldsymbol{v}\right\rangle\, d\boldsymbol{x} \to 0,$$

where $|\Omega_Y|$ is the volume of Ω_Y. Let $\boldsymbol{u}^0 \in H^1\left(\Omega^{\mathrm{3D}}, \Omega^{\mathrm{3D}}_D\right)$ be the solution of (1.21). Then

$$\boldsymbol{u}^\varepsilon \to \boldsymbol{u}^0 \text{ strongly in } L^2\left(\Omega^{\mathrm{3D}}\right),$$
$$\mathbf{1}_{\Omega^\varepsilon} \boldsymbol{A}^\varepsilon e(\boldsymbol{u}^\varepsilon) \to \boldsymbol{A}^{\mathrm{hom}} e(\boldsymbol{u}^0) \text{ weakly in } L^2\left(\Omega^{\mathrm{3D}}\right),$$
$$\left\|e(\boldsymbol{u}^\varepsilon) - e(\boldsymbol{u}^0) - e_y(\boldsymbol{c}^0)\right\|_{L^2(\Omega^\varepsilon)} \to 0,$$

where

$$\boldsymbol{c}^0(\boldsymbol{x},\boldsymbol{y}) = \sum_{i,j=1}^{3} e(\boldsymbol{u}^0(\boldsymbol{x}))_{ij}\boldsymbol{w}_{ij}(\boldsymbol{y}).$$

Proof. The proof repeats the proofs of Theorems 6.1 and 7.1, but with the Poincare inequality replaced with the Korn's inequality (1.25) and boundedness result (1.28). □

1.4   Continuity with respect to the geometry variations

In this section it is proven that the homogenized tensor, the solutions of the cell problems and the ε-problems are continuous with respect to geometrical parameters $\boldsymbol{g}$. All the quantities, i.e. the elasticity tensor, the Robin condition matrix, the right-hand side and the solutions of the elasticity problems become dependent on $\boldsymbol{g}$. Everywhere in this section it is assumed that $\boldsymbol{g} \in U_{\boldsymbol{g}}^2 \subset \mathbb{R}^2$, where $U_{\boldsymbol{g}}^2$ is some compact set.

Note that in this section functions defined on different domains have to be compared, and it is not possible to simply estimate the norm of the difference. Various approaches addressing this issue exist. For our purposes, it is enough to "transport" the functions onto some reference domain and then to work with the norm of the difference of the "transported" functions. This technique is called function space parametrization, see Section 2.2 of Chapter 10 in [13]. Namely, we define $\Omega_{\boldsymbol{g}_0}^\infty = \Omega_\infty^\mu(\boldsymbol{g}_0)$ to be the non-scaled infinite periodic reference domain (see Section 1.2.2 for the definition of $\Omega_\infty^\mu(\boldsymbol{g}_0)$) and for any $\boldsymbol{g} \in U_{\boldsymbol{g}}^2$ define the orientation-preserving diffeomorphism $\boldsymbol{T}_{\boldsymbol{g}}$ such that it transforms $\Omega_{\boldsymbol{g}_0}^\infty$ into $\Omega_{\boldsymbol{g}} = \Omega_\infty^\mu(\boldsymbol{g})$ together with the contact interfaces:

$$\boldsymbol{T}_{\boldsymbol{g}}\left(\Omega_\infty^\mu(\boldsymbol{g}_0)\right) = \Omega_\infty^\mu(\boldsymbol{g}), \quad \boldsymbol{T}_{\boldsymbol{g}}\left(S_\infty^\mu(\boldsymbol{g}_0)\right) = S_\infty^\mu(\boldsymbol{g}). \tag{1.29}$$

Under the action of this diffeomorphism, the integrals in weak formulations and expressions for the homogenized tensor change their form according to the standard formulas for various cases of integration by substitution. These formulas can be found in Section 4 of Chapter 9 in [13] and further in this section.

Remark 6. The notation for transformation of functions deserves clarification. For some point $\boldsymbol{x} \in \Omega_{\boldsymbol{g}_0}^\infty$ denote its image $\boldsymbol{T}_{\boldsymbol{g}}(\boldsymbol{x})$ by $\boldsymbol{y}$. Assume a three-dimensional field $\boldsymbol{u}_{\boldsymbol{g}}$ is defined on $\Omega_{\boldsymbol{g}}$. By the substitution of $\boldsymbol{T}_{\boldsymbol{g}}(\boldsymbol{x})$ in $\boldsymbol{u}_{\boldsymbol{g}}$, we arrive at a new function $\boldsymbol{u}_{\boldsymbol{g}}(\boldsymbol{T}_{\boldsymbol{g}}(\boldsymbol{x}))$ depending

on $\boldsymbol{x}$. Following [13], we denote this function by $\boldsymbol{u_g} \circ \boldsymbol{T_g}$. It is obvious that $\boldsymbol{u_g} \circ \boldsymbol{T_g} \circ \boldsymbol{T_g}^{-1} \equiv \boldsymbol{u_g}$. In the sequel we will actively use Jacobi matrices of $\boldsymbol{u_g}$ and $\boldsymbol{u_g} \circ \boldsymbol{T_g}$. For consistency with the classical notation, the Jacobians of the functions from elasticity will be denoted by the symbol ∇, for other quantities the symbol D will be used. Jacobians are always taken with respect to the argument of the last function in the superposition, i.e.

$$\nabla \boldsymbol{u_g} = \begin{pmatrix} \dfrac{\partial u_{\boldsymbol{g},1}(\boldsymbol{y})}{\partial y_1} & \dfrac{\partial u_{\boldsymbol{g},1}(\boldsymbol{y})}{\partial y_2} & \cdots & \dfrac{\partial u_{\boldsymbol{g},1}(\boldsymbol{y})}{\partial y_n} \\ \dfrac{\partial u_{\boldsymbol{g},2}(\boldsymbol{y})}{\partial y_1} & \dfrac{\partial u_{\boldsymbol{g},2}(\boldsymbol{y})}{\partial y_2} & \cdots & \dfrac{\partial u_{\boldsymbol{g},2}(\boldsymbol{y})}{\partial y_n} \\ \vdots & \vdots & \ddots & \vdots \\ \dfrac{\partial u_{\boldsymbol{g},n}(\boldsymbol{y})}{\partial y_1} & \dfrac{\partial u_{\boldsymbol{g},n}(\boldsymbol{y})}{\partial y_2} & \cdots & \dfrac{\partial u_{\boldsymbol{g},n}(\boldsymbol{y})}{\partial y_n} \end{pmatrix},$$

the derivative is taken with respect to the argument of $\boldsymbol{u_g}$, and

$$\nabla (\boldsymbol{u_g} \circ \boldsymbol{T_g}) = \begin{pmatrix} \dfrac{\partial u_{\boldsymbol{g},1}(\boldsymbol{T_g}(\boldsymbol{x}))}{\partial x_1} & \dfrac{\partial u_{\boldsymbol{g},1}(\boldsymbol{T_g}(\boldsymbol{x}))}{\partial x_2} & \cdots & \dfrac{\partial u_{\boldsymbol{g},1}(\boldsymbol{T_g}(\boldsymbol{x}))}{\partial x_n} \\ \dfrac{\partial u_{\boldsymbol{g},2}(\boldsymbol{T_g}(\boldsymbol{x}))}{\partial x_1} & \dfrac{\partial u_{\boldsymbol{g},2}(\boldsymbol{T_g}(\boldsymbol{x}))}{\partial x_2} & \cdots & \dfrac{\partial u_{\boldsymbol{g},2}(\boldsymbol{T_g}(\boldsymbol{x}))}{\partial x_n} \\ \vdots & \vdots & \ddots & \vdots \\ \dfrac{\partial u_{\boldsymbol{g},n}(\boldsymbol{T_g}(\boldsymbol{x}))}{\partial x_1} & \dfrac{\partial u_{\boldsymbol{g},n}(\boldsymbol{T_g}(\boldsymbol{x}))}{\partial x_2} & \cdots & \dfrac{\partial u_{\boldsymbol{g},n}(\boldsymbol{T_g}(\boldsymbol{x}))}{\partial x_n} \end{pmatrix},$$

the derivative is taken with respect to the argument of $\boldsymbol{T_g}$. The chain rule applies here and has the following form:

$$\nabla(\boldsymbol{u_g} \circ \boldsymbol{T_g})(\boldsymbol{x}) = \nabla \boldsymbol{u_g}(\boldsymbol{T_g}(\boldsymbol{x})) D \boldsymbol{T_g}(\boldsymbol{x}),$$

where "$\nabla \boldsymbol{u_g}(\boldsymbol{T_g}(\boldsymbol{x}))$" means the Jacobian $\nabla \boldsymbol{u_g}$ at the point $\boldsymbol{T_g}(\boldsymbol{x})$, not the chain derivative with respect to $\boldsymbol{x}$. The arguments' parentheses $(\boldsymbol{x})$ and $(\boldsymbol{T_g}(\boldsymbol{x}))$ will often be omitted.

Remark 7. The diffeomorphisms $\boldsymbol{T_g}$ can be defined explicitly using the velocity method, see Chapter 4 of [13]. These fields can be found for the geometric constructions of Section (1.2) explicitly. Since this material is very elementary and cumbersome, we omit it. In the sequel we assume that all the objects corresponding to our geometries set have the proper smoothness properties.

Assumption 1. *The family of diffeomorphisms $\boldsymbol{T_g}$ satisfies the following conditions:*

1. $\boldsymbol{T_{g_0}} = \boldsymbol{I}$,

2. $\forall \boldsymbol{g} \in U_{\boldsymbol{g}}^2$, $\boldsymbol{T_g} \in W^{1,\infty}(\Omega_{\boldsymbol{g_0}}^\infty)$,

3. $\forall \boldsymbol{g} \in U_{\boldsymbol{g}}^2$, $\boldsymbol{Q_g} = (\boldsymbol{T_g})^{-1} \in W^{1,\infty}(\Omega_{\boldsymbol{g_0}}^\infty)$,

4. $\forall \boldsymbol{g_1}, \boldsymbol{g_2} \in U_{\boldsymbol{g}}^2$, $\left\| \boldsymbol{T_{g_1}} - \boldsymbol{T_{g_2}} \right\|_{W^{1,\infty}} \to 0$, *as* $\boldsymbol{g_1} \to \boldsymbol{g_2}$,

5. $\boldsymbol{T_g}$ *is periodic with the same periodicity properties as* $\Omega_{\boldsymbol{g}}$.

1.4.1   Continuity of the homogenized tensor and homogenized displacements

In this section it is proved that the solutions of the cell problems (1.23) and the form (1.22) are continuous with respect to the geometrical parameters $\boldsymbol{g}$. As in the cell problems and in the expression for the homogenized tensor, here we deal with a single periodicity cell, not with the whole periodic domain. This is indicated by the use of $\Omega_{\boldsymbol{g},Y}$ and $S_{\boldsymbol{g},Y}$ as domains instead of $\Omega_{\boldsymbol{g}}$ and $S_{\boldsymbol{g}}$.

Recall the following elementary domain and integral transformation rules: for any diffeomorphism $\boldsymbol{T} \in W^{1,\infty}(\Omega_{\boldsymbol{g_0},Y})$, any volume field $\boldsymbol{f} \in L^1(\Omega_{\boldsymbol{g_0},Y})$, any surface field $\boldsymbol{k} \in L^1(S_{\boldsymbol{g_0},Y})$, and any differentiable volume field $\boldsymbol{h} \in W^{1,1}(\Omega_{\boldsymbol{g_0},Y})$,

- the volume integral transformation rule is:

$$\int_{\boldsymbol{T}(\Omega)} \boldsymbol{f}(\boldsymbol{y})\, d\boldsymbol{y} = \int_{\Omega} \boldsymbol{f} \circ \boldsymbol{T}(\boldsymbol{x}) \left| \det\left(D\boldsymbol{T}(\boldsymbol{x})\right) \right|\, d\boldsymbol{x}, \tag{1.30}$$

- the surface integral transformation rule is:

$$\int_{\boldsymbol{T}(\Gamma)} \boldsymbol{k}(\boldsymbol{s}_y)\, d\boldsymbol{s}_y = \int_{\Gamma} \boldsymbol{k} \circ \boldsymbol{T}(\boldsymbol{s}_x) \left| \mathrm{cof}\left(D\boldsymbol{T}(\boldsymbol{s}_x)\right) \boldsymbol{\nu} \right|\, d\boldsymbol{s}_x,$$

- the function's gradient and symmetrized gradient transformation rule is:

$$\nabla \boldsymbol{h} \circ \boldsymbol{T} = \nabla\left(\boldsymbol{h} \circ \boldsymbol{T}\right)\left(D\boldsymbol{T}\right)^{-1},$$

$$e(\boldsymbol{h}) \circ \boldsymbol{T} = \frac{1}{2}\left(\nabla\left(\boldsymbol{h} \circ \boldsymbol{T}\right)\left(D\boldsymbol{T}\right)^{-1} + \left(\nabla\left(\boldsymbol{h} \circ \boldsymbol{T}\right)\left(D\boldsymbol{T}\right)^{-1}\right)^T \right) = e_{\boldsymbol{T}}(\boldsymbol{h}) \circ \boldsymbol{T}, \tag{1.31}$$

where for any invertible $\boldsymbol{M} \in \mathbb{R}^{n \times n}$, $\mathrm{cof}\left(\boldsymbol{M}\right) \equiv \det\left(\boldsymbol{M}\right)\boldsymbol{M}^{-T}$, and $\boldsymbol{\nu}$ is the unit normal vector to the surface (due to the structure of the integrals, in this section it

is not important, whether it is an outward or inward unit normal vector). We will also use the notation $\boldsymbol{M}^{-T}$, meaning the transpose of the inverse for any invertible $\boldsymbol{M} \in \mathbb{R}^{n \times n}$.

Consider some $\boldsymbol{g} \in U_{\boldsymbol{g}}^2$ such that $\boldsymbol{g} \neq \boldsymbol{g}_0$. By the application of (1.30)–(1.31) it is possible to transform problems (1.23) and the entries of the homogenized tensor from $\Omega_{\boldsymbol{g},Y}$ to $\Omega_{\boldsymbol{g}_0,Y}$, whereby all fields $\boldsymbol{f}$ defined on $\Omega_{\boldsymbol{g},Y}$ correspond to the fields $\boldsymbol{f} \circ \boldsymbol{T_g}$ on $\Omega_{\boldsymbol{g}_0,Y}$:

$$
\int_{\Omega_{\boldsymbol{g},Y}} (e(\boldsymbol{w}_{ij}^{\boldsymbol{g}}(\boldsymbol{y})) + \boldsymbol{e}_{ij}) : \boldsymbol{A_g} \cdot e(\boldsymbol{v}(\boldsymbol{y}))\, d\boldsymbol{y} + \int_{S_{\boldsymbol{g},Y}} \left\langle \boldsymbol{R_g}(\boldsymbol{s_y}) \left[\boldsymbol{w}_{ij}^{\boldsymbol{g}}(\boldsymbol{s_y})\right], [\boldsymbol{v}(\boldsymbol{s_y})] \right\rangle d\boldsymbol{s_y} =
$$
$$
= \int_{\Omega_{\boldsymbol{g}_0,Y}} (e_{\boldsymbol{T_g}}(\boldsymbol{w}_{ij}^{\boldsymbol{g}} + \boldsymbol{q}_{ij}^{\boldsymbol{g}})) \circ \boldsymbol{T_g} : \boldsymbol{A_g} \circ \boldsymbol{T_g} \cdot e_{\boldsymbol{T_g}}(\boldsymbol{v}) \circ \boldsymbol{T_g} \left|\det\left(D\boldsymbol{T_g}\right)\right| d\boldsymbol{x} +
$$
$$
+ \int_{S_{\boldsymbol{g}_0,Y}} \left\langle \boldsymbol{R_g} \circ \boldsymbol{T_g} \left[\boldsymbol{w}_{ij}^{\boldsymbol{g}} \circ \boldsymbol{T_g}\right], [\boldsymbol{v} \circ \boldsymbol{T_g}] \right\rangle \left|\text{cof}\left(D\boldsymbol{T_g}(\boldsymbol{s_x})\right)\boldsymbol{\nu}\right| d\boldsymbol{s_x} = 0,
$$

$$(1.32)$$

for any $\boldsymbol{v} \in H_{\#}^1(\Omega_{\boldsymbol{g},Y})$, where $\boldsymbol{q}_{ij}^{\boldsymbol{g}} \in H^1(\Omega_{\boldsymbol{g}})$ is any function continuous with respect to $\boldsymbol{g}$ such that $e(\boldsymbol{q}_{ij}^{\boldsymbol{g}}) = \boldsymbol{e}_{ij}$, $i, j = 1, \ldots, 3$. Note that the definition of $H_{\#}^1$ for all values of $\boldsymbol{g}$ is the same. Moreover, due to the periodicity assumption on $\boldsymbol{T_g}$, $\boldsymbol{v} \in H_{\#}^1(\Omega_{\boldsymbol{g},Y})$ implies $\boldsymbol{v} \circ \boldsymbol{T_g} \in H_{\#}^1(\Omega_{\boldsymbol{g}_0,Y})$. For the integral for the homogenized coefficients one arrives at

$$
A_{\boldsymbol{g}\, ijkl}^{\text{hom}} = \int_{\Omega_{\boldsymbol{g},Y}} \boldsymbol{A_g}(\boldsymbol{y})(e(\boldsymbol{w}_{ij}^{\boldsymbol{g}}) + \boldsymbol{e}_{ij}) : (e(\boldsymbol{w}_{kl}^{\boldsymbol{g}}) + \boldsymbol{e}_{kl})\, d\boldsymbol{y} +
$$
$$
+ \int_{S_{\boldsymbol{g},Y}} \left\langle \boldsymbol{R_g}(\boldsymbol{s_y}) \left[\boldsymbol{w}_{ij}^{\boldsymbol{g}}(\boldsymbol{s_y})\right], [\boldsymbol{w}_{kl}^{\boldsymbol{g}}(\boldsymbol{s_y})] \right\rangle d\boldsymbol{s_y} =
$$
$$
= \int_{\Omega_{\boldsymbol{g}_0,Y}} \boldsymbol{A_g} \circ \boldsymbol{T_g} \cdot e_{\boldsymbol{T_g}}(\boldsymbol{w}_{ij}^{\boldsymbol{g}} + \boldsymbol{q}_{ij}^{\boldsymbol{g}}) : e_{\boldsymbol{T_g}}(\boldsymbol{w}_{kl}^{\boldsymbol{g}} + \boldsymbol{q}_{kl}^{\boldsymbol{g}}) \left|\det\left(D\boldsymbol{T_g}\right)\right| d\boldsymbol{x} +
$$
$$
+ \int_{S_{\boldsymbol{g}_0,Y}} \left\langle \boldsymbol{R_g} \circ \boldsymbol{T_g} \left[\boldsymbol{w}_{ij}^{\boldsymbol{g}} \circ \boldsymbol{T_g}\right], [\boldsymbol{w}_{kl}^{\boldsymbol{g}} \circ \boldsymbol{T_g}] \right\rangle \left|\text{cof}\left(\boldsymbol{T_g}\right)\boldsymbol{\nu}\right| d\boldsymbol{s_x}.
$$

$$(1.33)$$

The continuity of the homogenized tensor is proved in two steps: show the continuity of the solution of (1.32) with respect to $\boldsymbol{g}$, and then the continuity of the form (1.33) with respect to $\boldsymbol{w}_{ij}^{\boldsymbol{g}}$, which, in turn, depends continuously on $\boldsymbol{g}$.

Assumption 2. *The coefficients $\boldsymbol{A_g}, \boldsymbol{R_g}, \boldsymbol{f_g}$ are continuous with respect to $\boldsymbol{g}$ in the following*

sense:

$$\left\| \boldsymbol{A_g} \circ \boldsymbol{T_g} - \boldsymbol{A_{g_0}} \right\|_{L^\infty \left(\Omega_{g_0, Y} \right)} \to 0,$$

$$\left\| \boldsymbol{R_g} \circ \boldsymbol{T_g} - \boldsymbol{R_{g_0}} \right\|_{L^\infty \left(S_{g_0, Y} \right)} \to 0,$$

$$\left\| \boldsymbol{f_g} \circ \boldsymbol{T_g} - \boldsymbol{f_{g_0}} \right\|_{L^2 \left(\Omega_{g_0, Y} \right)} \to 0$$

as $\boldsymbol{g} \to \boldsymbol{g}_0$.

Assumption 3. *In the sequel we will need Theorem 1 formulated for domains depending on $\boldsymbol{g}$ with the constant C depending continuously on $\boldsymbol{g}$.*

Let $\Omega_i^{\boldsymbol{g}} = \boldsymbol{T_g}(\Omega_i)$, $i = 1, \ldots, M$, where Ω_i are the domains satisfying the conditions of Theorem 1. By analogy with the theorem, define $\Omega^{\boldsymbol{g}} = \boldsymbol{T_g}(\Omega)$, $\Gamma^{\boldsymbol{g}} = \boldsymbol{T_g}(\Gamma)$, $V^{\boldsymbol{g}}$, rigid displacements space $\mathfrak{R}$, and $\widetilde{V}^{\boldsymbol{g}} = \{ \boldsymbol{v} \in V^{\boldsymbol{g}} \colon [\boldsymbol{v}] = 0 \text{ on } \Gamma^{\boldsymbol{g}} \}$. Assume that $\widetilde{V}^{\boldsymbol{g}} \cap \mathfrak{R} = \varnothing$. Then by Theorem 1 every $\boldsymbol{v} \in V^{\boldsymbol{g}}$ satisfies the modified Korn's inequality

$$\sum_{j=1}^{M} \| \boldsymbol{v} \|_{H^1(\Omega_i^{\boldsymbol{g}})}^2 \leq C^{\boldsymbol{g}} \mathcal{E}^{\boldsymbol{g}}(\boldsymbol{v}), \text{ where } \mathcal{E}^{\boldsymbol{g}}(\boldsymbol{v}) = \int_{\Omega^{\boldsymbol{g}}} e^2(\boldsymbol{v}) \, dx + \int_{\Gamma^{\boldsymbol{g}}} [\boldsymbol{v}]^2 \, ds. \tag{1.34}$$

Additionally, we assume that $C^{\boldsymbol{g}} \in C\left(U_{\boldsymbol{g}}^2 \right)$.

Theorem 6. *Let $\boldsymbol{w}_{ij}^{\boldsymbol{g}}$ be the solution of (1.32) and the transformation diffeomorphisms satisfy conditions of Assumption 1. Then $\boldsymbol{w}_{ij}^{\boldsymbol{g}} \circ \boldsymbol{T_g} \in C(U_{\boldsymbol{g}}^2, H_{\#}^1 \left(\Omega_{g_0, Y} \right))$.*

Proof. In (1.32) transfer all known terms to the right-hand side. This yields the following problem:

$$\mathcal{A}_{\boldsymbol{g}}(\boldsymbol{w}_{ij}^{\boldsymbol{g}} \circ \boldsymbol{T_g}, \boldsymbol{v} \circ \boldsymbol{T_g}) + \mathcal{R}_{\boldsymbol{g}}(\boldsymbol{w}_{ij}^{\boldsymbol{g}}, \boldsymbol{v} \circ \boldsymbol{T_g}) = \mathfrak{f}_{ij}^{\boldsymbol{g}}(\boldsymbol{v} \circ \boldsymbol{T_g}), \quad \forall \boldsymbol{v} \in H_{\#}^1 \Omega_{\boldsymbol{g}, Y},$$

$$\mathcal{A}_{\boldsymbol{g}}(\boldsymbol{u}, \boldsymbol{v}) = \int_{\Omega_{g_0, Y}} \boldsymbol{A_g} \circ \boldsymbol{T_g} \cdot \frac{1}{2} \left(\nabla \boldsymbol{u} (D\boldsymbol{T_g})^{-1} + \left(\nabla \boldsymbol{u} (D\boldsymbol{T_g})^{-1} \right)^T \right) :$$

$$: \frac{1}{2} \left(\nabla \boldsymbol{v} (D\boldsymbol{T_g})^{-1} + \left(\nabla \boldsymbol{v} (D\boldsymbol{T_g})^{-1} \right)^T \right) |\det (D\boldsymbol{T_g})| \, d\boldsymbol{x},$$

$$\mathcal{R}_{\boldsymbol{g}}(\boldsymbol{u}, \boldsymbol{v}) = \int_{S_{g_0, Y}} \langle \boldsymbol{R_g} \circ \boldsymbol{T_g} [\boldsymbol{u}], [\boldsymbol{v}] \rangle |\text{cof} (D\boldsymbol{T_g}) \boldsymbol{\nu}| \, ds_{\boldsymbol{x}},$$

$$\mathfrak{f}_{ij}^{\boldsymbol{g}}(\boldsymbol{v}) = - \int_{\Omega_{g_0, Y}} \boldsymbol{A_g} \circ \boldsymbol{T_g} \cdot \frac{1}{2} \left(\nabla \left(\boldsymbol{q}_{ij}^{\boldsymbol{g}} \circ \boldsymbol{T_g} \right) (D\boldsymbol{T_g})^{-1} + \left(\nabla \left(\boldsymbol{q}_{ij}^{\boldsymbol{g}} \circ \boldsymbol{T_g} \right) (D\boldsymbol{T_g})^{-1} \right)^T \right) :$$

$$: \frac{1}{2} \left(\nabla \boldsymbol{v} (D\boldsymbol{T_g})^{-1} + \left(\nabla \boldsymbol{v} (D\boldsymbol{T_g})^{-1} \right)^T \right) |\det (D\boldsymbol{T_g})| \, d\boldsymbol{x}.$$

Consider $g_1 \to g_2$. It is straightforward to verify that Assumption 1 and Assumption 2 guarantee the following relations:

$$\sup_{\substack{v \in H^1(\Omega_{g_0,Y}), \\ \|v\|=1}} \left\| \left(\nabla v (DT_{g_2})^{-1} + \left(\nabla v (DT_{g_2})^{-1} \right)^T \right) - \left(\nabla v (DT_{g_1})^{-1} + \left(\nabla v (DT_{g_1})^{-1} \right)^T \right) \right\| \to 0.$$

$$\left\| A_{g_1} \circ T_{g_1} \left| \det(DT_{g_1}) \right| - A_{g_2} \circ T_{g_2} \left| \det(DT_{g_2}) \right| \right\|_{\mathcal{L}\left(S^+ \left(S^+ (\Omega_{g_0,Y}) \right), S^+ \left(S^+ (\Omega_{g_0,Y}) \right) \right)} \to 0,$$

$$\sup_{\nu: \|\nu\|=1} \left\| R_{g_1} \circ T_{g_1} \left| \mathrm{cof}(DT_{g_1}) \nu \right| - R_{g_2} \circ T_{g_2} \left| \mathrm{cof}(DT_{g_2}) \nu \right| \right\|_{\mathcal{L}\left(L^2(S_{g_0,Y}), L^2(S_{g_0,Y}) \right)} \to 0,$$

$$\left\| \left| \det(DT_{g_1}) \right| A_{g_1} \circ T_{g_1} \cdot e_{T_{g_1}} (q_{ij}^{g_1}) \circ T_{g_1} - \left| \det(DT_{g_2}) \right| A_{g_2} \circ T_{g_2} \cdot e_{T_{g_2}} (q_{ij}^{g_2}) \circ T_{g_2} \right\|_{S^+ (\Omega_{g_0,Y})} \to 0.$$

These, in turn, guarantee that the bilinear form $\mathcal{B}_g(u,v) = \mathcal{A}_g(u,v) + \mathcal{R}_g(u,v)$ is itself continuous with respect to g:

$$\sup_{\substack{u,v \in H^1(\Omega_{g_0,Y}), \\ \|u\|=\|v\|=1}} \left| (\mathcal{B}_{g_1} - \mathcal{B}_{g_2})(u,v) \right| \to 0 \text{ as } g_1 \to g_2. \tag{1.35}$$

Consider the coercivity constant $c_{\mathcal{B},g}$, defined as

$$c_{\mathcal{B},g} = \inf_{\substack{v \in H^1_{\#0}(\Omega_{g_0,Y}) \\ \|v\|=1}} \mathcal{B}_g(v,v).$$

Let us prove that this quantity is bounded from below by some positive number not depending on g. Observe that for any $u \in H^1_{\#0}(\Omega_{g,Y})$, $\mathcal{B}_g(u \circ T_g, u \circ T_g) \equiv \mathcal{E}^g(u)$, the Korn's inequality (1.34) is applicable (see the proof of Theorem 3). Together with uniform non-degeneracy of DT_g by Assumption 1, this delivers $c_{\mathcal{B},g} > 0$ for any fixed g. For any $v \in H^1_{\#0}(\Omega_{g_0,Y})$ one arrives at the same result by considering $u = v \circ T_g \in H^1_{\#0}(\Omega_{g,Y})$. We obtain that for any fixed g, $c_{\mathcal{B},g} > 0$.

Further, consider the uniform coercivity constant

$$c_{\mathrm{inf}} = \inf_{g \in U_g^2} c_{\mathcal{B},g} > 0.$$

By the Assumption 1 and Assumption 3, $c_{\mathcal{B},g}$ is continuous with respect to g. But due to the

compactness of $U_{\boldsymbol{g}}^2$, there exists $\boldsymbol{g}_{\mathrm{inf}} \in U_{\boldsymbol{g}}^2$ such that

$$c_{\mathrm{inf}} = c_{\mathcal{B},\boldsymbol{g}_{\mathrm{inf}}},$$

but the latter is positive. Thus, the uniform coercivity of $\mathcal{B}_{\boldsymbol{g}}$ is proven.

The boundedness of $\mathcal{B}_{\boldsymbol{g}}$ is proven in the similar way, but instead of Korn's inequality the trace theorem should be used.

Therefore, $\mathcal{B}_{\boldsymbol{g}}$ is uniformly coercive and bounded. Since functions $\boldsymbol{w}_{ij}^{\boldsymbol{g}}$ are the solutions of

$$\mathcal{B}_{\boldsymbol{g}}(\boldsymbol{w}_{ij}^{\boldsymbol{g}} \circ \boldsymbol{T}_{\boldsymbol{g}}, \boldsymbol{v}) = \mathfrak{f}_{ij}^{\boldsymbol{g}}(\boldsymbol{v}) \qquad \forall\, \boldsymbol{v} \in H^1(\Omega_{\boldsymbol{g}_0,Y}), \tag{1.36}$$

where $\mathfrak{f}_{ij}^{\boldsymbol{g}}$ are bounded by the same continuity-compactness argument, we conclude that $\boldsymbol{w}_{ij}^{\boldsymbol{g}} \circ \boldsymbol{T}_{\boldsymbol{g}}$ is a uniformly bounded family of functions. By Assumption 1 this implies that $\boldsymbol{w}_{ij}^{\boldsymbol{g}}$ is also a uniformly bounded family of functions.

Finally, let $\boldsymbol{w}_{ij}^{\boldsymbol{g}_1}$ and $\boldsymbol{w}_{ij}^{\boldsymbol{g}_2}$ be the solutions to (1.36) for $\boldsymbol{g} = \boldsymbol{g}_1$ and $\boldsymbol{g} = \boldsymbol{g}_2$, respectively. Subtract the corresponding transported weak formulations:

$$(\mathfrak{f}_{ij}^{\boldsymbol{g}_1} - \mathfrak{f}_{ij}^{\boldsymbol{g}_2})(\boldsymbol{v}) = \mathcal{B}_{\boldsymbol{g}_1}(\boldsymbol{w}_{ij}^{\boldsymbol{g}_1} \circ \boldsymbol{T}_{\boldsymbol{g}_1}, \boldsymbol{v}) - \mathcal{B}_{\boldsymbol{g}_2}(\boldsymbol{w}_{ij}^{\boldsymbol{g}_2} \circ \boldsymbol{T}_{\boldsymbol{g}_2}, \boldsymbol{v}) =$$
$$= \mathcal{B}_{\boldsymbol{g}_1}(\boldsymbol{w}_{ij}^{\boldsymbol{g}_1} \circ \boldsymbol{T}_{\boldsymbol{g}_1}, \boldsymbol{v}) - \mathcal{B}_{\boldsymbol{g}_2}(\boldsymbol{w}_{ij}^{\boldsymbol{g}_1} \circ \boldsymbol{T}_{\boldsymbol{g}_2}, \boldsymbol{v}) + \mathcal{B}_{\boldsymbol{g}_2}(\boldsymbol{w}_{ij}^{\boldsymbol{g}_1} \circ \boldsymbol{T}_{\boldsymbol{g}_1}, \boldsymbol{v}) - \mathcal{B}_{\boldsymbol{g}_2}(\boldsymbol{w}_{ij}^{\boldsymbol{g}_2} \circ \boldsymbol{T}_{\boldsymbol{g}_2}, \boldsymbol{v}) =$$
$$= (\mathcal{B}_{\boldsymbol{g}_1} - \mathcal{B}_{\boldsymbol{g}_2})(\boldsymbol{w}_{ij}^{\boldsymbol{g}_1} \circ \boldsymbol{T}_{\boldsymbol{g}_1}, \boldsymbol{v}) + \mathcal{B}_{\boldsymbol{g}_2}(\boldsymbol{w}_{ij}^{\boldsymbol{g}_1} \circ \boldsymbol{T}_{\boldsymbol{g}_1} - \boldsymbol{w}_{ij}^{\boldsymbol{g}_2} \circ \boldsymbol{T}_{\boldsymbol{g}_2}, \boldsymbol{v}) \qquad \forall\, \boldsymbol{v} \in H^1\left(\Omega_{\boldsymbol{g}_0,Y}\right).$$

In the latter estimate we can put $\boldsymbol{v} = \boldsymbol{w}_{ij}^{\boldsymbol{g}_1} \circ \boldsymbol{T}_{\boldsymbol{g}_1} - \boldsymbol{w}_{ij}^{\boldsymbol{g}_2} \circ \boldsymbol{T}_{\boldsymbol{g}_2}$ and obtain

$$c_{\mathrm{inf}} \left\| \boldsymbol{w}_{ij}^{\boldsymbol{g}_1} \circ \boldsymbol{T}_{\boldsymbol{g}_1} - \boldsymbol{w}_{ij}^{\boldsymbol{g}_2} \circ \boldsymbol{T}_{\boldsymbol{g}_2} \right\|_{H^1\left(\Omega_{\boldsymbol{g}_0,Y}\right)}^2 + (\mathcal{B}_{\boldsymbol{g}_1} - \mathcal{B}_{\boldsymbol{g}_2})(\boldsymbol{w}_{ij}^{\boldsymbol{g}_1} \circ \boldsymbol{T}_{\boldsymbol{g}_1}, \boldsymbol{w}_{ij}^{\boldsymbol{g}_1} \circ \boldsymbol{T}_{\boldsymbol{g}_1} - \boldsymbol{w}_{ij}^{\boldsymbol{g}_2} \circ \boldsymbol{T}_{\boldsymbol{g}_2}) \le$$
$$\le \mathcal{B}_{\boldsymbol{g}_2}(\boldsymbol{w}_{ij}^{\boldsymbol{g}_1} \circ \boldsymbol{T}_{\boldsymbol{g}_1} - \boldsymbol{w}_{ij}^{\boldsymbol{g}_2} \circ \boldsymbol{T}_{\boldsymbol{g}_2}, \boldsymbol{w}_{ij}^{\boldsymbol{g}_1} \circ \boldsymbol{T}_{\boldsymbol{g}_1} - \boldsymbol{w}_{ij}^{\boldsymbol{g}_2} \circ \boldsymbol{T}_{\boldsymbol{g}_2}) +$$
$$+ (\mathcal{B}_{\boldsymbol{g}_1} - \mathcal{B}_{\boldsymbol{g}_2})(\boldsymbol{w}_{ij}^{\boldsymbol{g}_1} \circ \boldsymbol{T}_{\boldsymbol{g}_1}, \boldsymbol{w}_{ij}^{\boldsymbol{g}_1} \circ \boldsymbol{T}_{\boldsymbol{g}_1} - \boldsymbol{w}_{ij}^{\boldsymbol{g}_2} \circ \boldsymbol{T}_{\boldsymbol{g}_2}) = (\mathfrak{f}_{ij}^{\boldsymbol{g}_1} - \mathfrak{f}_{ij}^{\boldsymbol{g}_2})(\boldsymbol{w}_{ij}^{\boldsymbol{g}_1} \circ \boldsymbol{T}_{\boldsymbol{g}_1} - \boldsymbol{w}_{ij}^{\boldsymbol{g}_2} \circ \boldsymbol{T}_{\boldsymbol{g}_2}).$$

As $\boldsymbol{g}_1 \to \boldsymbol{g}_2$, the term $(\mathcal{B}_{\boldsymbol{g}_1} - \mathcal{B}_{\boldsymbol{g}_2})(\boldsymbol{w}_{ij}^{\boldsymbol{g}_1} \circ \boldsymbol{T}_{\boldsymbol{g}_1}, \boldsymbol{w}_{ij}^{\boldsymbol{g}_1} \circ \boldsymbol{T}_{\boldsymbol{g}_1} - \boldsymbol{w}_{ij}^{\boldsymbol{g}_2} \circ \boldsymbol{T}_{\boldsymbol{g}_2})$ tends to zero by the continuity of $\mathcal{B}_{\boldsymbol{g}}$ (1.35) and the uniform boundedness of $\boldsymbol{w}_{ij}^{\boldsymbol{g}} \circ \boldsymbol{T}_{\boldsymbol{g}}$. The right-hand side $(\mathfrak{f}_{ij}^{\boldsymbol{g}_1} - \mathfrak{f}_{ij}^{\boldsymbol{g}_2})(\boldsymbol{w}_{ij}^{\boldsymbol{g}_1} \circ \boldsymbol{T}_{\boldsymbol{g}_1} - \boldsymbol{w}_{ij}^{\boldsymbol{g}_2} \circ \boldsymbol{T}_{\boldsymbol{g}_2})$ tends to zero due to the continuity of $\mathfrak{f}_{ij}^{\boldsymbol{g}}$.

Thus, by letting $\boldsymbol{g}_1 \to \boldsymbol{g}_2$ we arrive at the statement of the theorem. $\qquad\square$

Theorem 7. *Let the transformation diffeomorphisms satisfy conditions of Assumption 1. Then*

$\boldsymbol{A}_{\boldsymbol{g}}^{\mathrm{hom}} \in C(U_{\boldsymbol{g}}^2, \mathcal{T}^+)$ *is uniformly coercive and bounded, i.e.*

$$
\begin{aligned}
&\exists c_{\mathrm{inf}}^{\mathrm{hom}} \in \mathbb{R}, c_{\mathrm{inf}}^{\mathrm{hom}} > 0 \colon \forall \boldsymbol{g} \in U_{\boldsymbol{g}}^2, \ \boldsymbol{A}_{\boldsymbol{g}}^{\mathrm{hom}}\boldsymbol{m} : \boldsymbol{m} \geq c_{\mathrm{inf}}^{\mathrm{hom}}\boldsymbol{m} : \boldsymbol{m} \quad \forall \boldsymbol{m} \in \mathcal{S}^+, \\
&\exists C_{\mathrm{sup}}^{\mathrm{hom}} \in \mathbb{R}, C_{\mathrm{sup}}^{\mathrm{hom}} > 0 \colon \forall \boldsymbol{g} \in U_{\boldsymbol{g}}^2, \ \boldsymbol{A}_{\boldsymbol{g}}^{\mathrm{hom}}\boldsymbol{m} : \boldsymbol{m} \leq C_{\mathrm{sup}}^{\mathrm{hom}}\boldsymbol{m} : \boldsymbol{m} \quad \forall \boldsymbol{m} \in \mathcal{S}^+.
\end{aligned}
\tag{1.37}
$$

Proof. The continuity can be proven by the same argument as in the previous theorem by showing the continuity of the functions under the integral signs in (1.33).

The symmetry and positivity properties follow from the symmetry of the forms of (1.33) and from the standard homogenization results, which can be applied right after it is proven that the bilinear form of the cell problem is coercive and positive-definite.

The uniform coercivity and boundedness are proved by the continuity and compactness argument in the same way as in Theorem 6. □

Finally, consider $\boldsymbol{g}$-dependent form of problem (1.21):

$$
\boldsymbol{u}_{\boldsymbol{g}}^0 \in H^1\left(\Omega^{\mathrm{3D}}, \partial\Omega_D^{\mathrm{3D}}\right) \colon \int_{\Omega^{\mathrm{3D}}} \boldsymbol{A}_{\boldsymbol{g}}^{\mathrm{hom}}e(\boldsymbol{u}_{\boldsymbol{g}}^0) : e(\boldsymbol{v})\, d\boldsymbol{x} =
$$
$$
= \int_{\Omega^{\mathrm{3D}}} \left\langle \boldsymbol{f}_{\boldsymbol{g}}^{\mathrm{hom}}, \boldsymbol{v} \right\rangle d\boldsymbol{x} \quad \forall \boldsymbol{v} \in H^1\left(\Omega^{\mathrm{3D}}, \partial\Omega_D^{\mathrm{3D}}\right). \tag{1.38}
$$

Theorem 8. *Assume the conditions of Theorem 7 are true. Then the solution $\boldsymbol{u}_{\boldsymbol{g}}^0$ of problem 1.38 is continuous with respect to $\boldsymbol{g}$, i.e. $\boldsymbol{u}_{\boldsymbol{g}}^0 \in C\left(U_{\boldsymbol{g}}^2, H^1\left(\Omega^{\mathrm{3D}}, \partial\Omega_D^{\mathrm{3D}}\right)\right)$.*

Proof. Consider arbitrary $\boldsymbol{g}_1$ and $\boldsymbol{g}_2$ from $U_{\boldsymbol{g}}^2$. By subtraction of weak formulation (1.38) for $\boldsymbol{g} = \boldsymbol{g}_2$ from the one for $\boldsymbol{g} = \boldsymbol{g}_1$ and addition-subtraction of the term $\int_{\Omega^{\mathrm{3D}}} \boldsymbol{A}_{\boldsymbol{g}_2}^{\mathrm{hom}}e(\boldsymbol{u}_{\boldsymbol{g}_1}^0) : e(\boldsymbol{v})\, d\boldsymbol{x}$, one arrives at

$$
\int_{\Omega^{\mathrm{3D}}} \left(\boldsymbol{A}_{\boldsymbol{g}_1}^{\mathrm{hom}} - \boldsymbol{A}_{\boldsymbol{g}_2}^{\mathrm{hom}}\right) e(\boldsymbol{u}_{\boldsymbol{g}_1}^0) : e(\boldsymbol{v})\, d\boldsymbol{x} + \int_{\Omega^{\mathrm{3D}}} \boldsymbol{A}_{\boldsymbol{g}_2}^{\mathrm{hom}}e(\boldsymbol{u}_{\boldsymbol{g}_1}^0 - \boldsymbol{u}_{\boldsymbol{g}_2}^0) : e(\boldsymbol{v})\, d\boldsymbol{x} =
$$
$$
= \int_{\Omega^{\mathrm{3D}}} \left\langle \boldsymbol{f}_{\boldsymbol{g}_1}^{\mathrm{hom}} - \boldsymbol{f}_{\boldsymbol{g}_2}^{\mathrm{hom}}, \boldsymbol{v} \right\rangle d\boldsymbol{x}, \quad \forall \boldsymbol{v} \in H^1\left(\Omega^{\mathrm{3D}}, \partial\Omega_D^{\mathrm{3D}}\right).
$$

Put $\boldsymbol{v} = \boldsymbol{u}_{\boldsymbol{g}_1}^0 - \boldsymbol{u}_{\boldsymbol{g}_2}^0$ and use estimate 1.37 and standard Korn's inequality:

$$
c_{\mathrm{inf}}^{\mathrm{hom}} \left\| \boldsymbol{u}_{\boldsymbol{g}_1}^0 - \boldsymbol{u}_{\boldsymbol{g}_2}^0 \right\|_{H^1(\Omega^{\mathrm{3D}})}^2 \leq \int_{\Omega^{\mathrm{3D}}} \boldsymbol{A}_{\boldsymbol{g}_2}^{\mathrm{hom}}e(\boldsymbol{u}_{\boldsymbol{g}_1}^0 - \boldsymbol{u}_{\boldsymbol{g}_2}^0) : e(\boldsymbol{u}_{\boldsymbol{g}_1}^0 - \boldsymbol{u}_{\boldsymbol{g}_2}^0)\, d\boldsymbol{x} =
$$
$$
= \int_{\Omega^{\mathrm{3D}}} \left\langle \boldsymbol{f}_{\boldsymbol{g}_1}^{\mathrm{hom}} - \boldsymbol{f}_{\boldsymbol{g}_2}^{\mathrm{hom}}, \boldsymbol{u}_{\boldsymbol{g}_1}^0 - \boldsymbol{u}_{\boldsymbol{g}_2}^0 \right\rangle d\boldsymbol{x} - \int_{\Omega^{\mathrm{3D}}} (\boldsymbol{A}_{\boldsymbol{g}_1}^{\mathrm{hom}} - \boldsymbol{A}_{\boldsymbol{g}_2}^{\mathrm{hom}})e(\boldsymbol{u}_{\boldsymbol{g}_1}^0) : e(\boldsymbol{u}_{\boldsymbol{g}_1}^0 - \boldsymbol{u}_{\boldsymbol{g}_2}^0)\, d\boldsymbol{x}.
$$

The right-hand side can be estimated from above by

$$\left\| \boldsymbol{f}_{\boldsymbol{g}_1}^{\mathrm{hom}} - \boldsymbol{f}_{\boldsymbol{g}_2}^{\mathrm{hom}} \right\|_{H^{-1}\left(\Omega^{\mathrm{3D}}, \partial\Omega_D^{\mathrm{3D}}\right)} \left\| \boldsymbol{u}_{\boldsymbol{g}_1}^0 - \boldsymbol{u}_{\boldsymbol{g}_2}^0 \right\|_{H^1(\Omega^{\mathrm{3D}})} +$$
$$+ \left\| \boldsymbol{A}_{\boldsymbol{g}_1}^{\mathrm{hom}} - \boldsymbol{A}_{\boldsymbol{g}_2}^{\mathrm{hom}} \right\|_{L^\infty(\Omega^{\mathrm{3D}})} \left\| \boldsymbol{u}_{\boldsymbol{g}_1}^0 \right\|_{H^1(\Omega^{\mathrm{3D}})} \left\| \boldsymbol{u}_{\boldsymbol{g}_1}^0 - \boldsymbol{u}_{\boldsymbol{g}_2}^0 \right\|_{H^1(\Omega^{\mathrm{3D}})}.$$

Finally, we arrive at the inequality

$$c_{\mathrm{inf}}^{\mathrm{hom}} \left\| \boldsymbol{u}_{\boldsymbol{g}_1}^0 - \boldsymbol{u}_{\boldsymbol{g}_2}^0 \right\|_{H^1(\Omega^{\mathrm{3D}})} \leq \left\| \boldsymbol{f}_{\boldsymbol{g}_1}^{\mathrm{hom}} - \boldsymbol{f}_{\boldsymbol{g}_2}^{\mathrm{hom}} \right\|_{H^{-1}\left(\Omega^{\mathrm{3D}}, \partial\Omega_D^{\mathrm{3D}}\right)} +$$
$$+ \left\| \boldsymbol{A}_{\boldsymbol{g}_1}^{\mathrm{hom}} - \boldsymbol{A}_{\boldsymbol{g}_2}^{\mathrm{hom}} \right\|_{L^\infty(\Omega^{\mathrm{3D}})} \left\| \boldsymbol{u}_{\boldsymbol{g}_1}^0 \right\|_{H^1(\Omega^{\mathrm{3D}})}. \quad (1.39)$$

Assumption 2 guarantees that

$$\exists C_{\boldsymbol{u}^0} : \forall \boldsymbol{g} \in U_{\boldsymbol{g}}^2 \quad \left\| \boldsymbol{u}_{\boldsymbol{g}}^0 \right\|_{H^1(\Omega^{\mathrm{3D}})} \leq C_{\boldsymbol{u}_0},$$
$$\left\| \boldsymbol{f}_{\boldsymbol{g}_1}^{\mathrm{hom}} - \boldsymbol{f}_{\boldsymbol{g}_2}^{\mathrm{hom}} \right\|_{H^{-1}\left(\Omega^{\mathrm{3D}}, \partial\Omega_D^{\mathrm{3D}}\right)} \to 0, \text{ as } \boldsymbol{g}_1 \to \boldsymbol{g}_2.$$

By passage to the limit $\boldsymbol{g}_1 \to \boldsymbol{g}_2$, we arrive at the statement of the theorem. □

1.4.2 Equicontinuity of the two-scale convergence of the homogenization result

In this section the diffeomorphisms between the scaled domains $\Omega_{\boldsymbol{g}}^\varepsilon$ are considered. This time $\Omega_{\boldsymbol{g}_0}^\varepsilon$ is used as the reference domain and assumptions similar to Assumption 1 are used, but for a different diffeomorphism. Namely, the standard homogenization transformation of the argument $\boldsymbol{x}/\varepsilon$ and then multiplication of the function by ε, are used for the diffeomorphisms.

Recall that $\boldsymbol{T}_{\boldsymbol{g}}$ transforms the infinite set $\Omega_\infty^\mu(\boldsymbol{g}_0)$ into $\Omega_\infty^\mu(\boldsymbol{g})$. As usual in homogenization, the diffeomorphism, which transforms their scaled versions $\Omega_\infty^{\mu,\varepsilon}(\boldsymbol{g}_0)$ and $\Omega_\infty^{\mu,\varepsilon}(\boldsymbol{g})$, can be obtained by some proper scaling of $\boldsymbol{T}_{\boldsymbol{g}}$. Introduce the uniform scaling diffeomorphism $\boldsymbol{S}_c$. Observe that if $\boldsymbol{T}_{\boldsymbol{g}}$ satisfies (1.29), then

$$\mathfrak{T}_{\boldsymbol{g}}^\varepsilon = \boldsymbol{S}_\varepsilon \circ \boldsymbol{T}_{\boldsymbol{g}} \circ \boldsymbol{S}_{\frac{1}{\varepsilon}} \quad\quad\quad (1.40)$$

satisfies

$$\mathfrak{T}_{\boldsymbol{g}}^{\varepsilon}\left(\Omega_{\infty}^{\mu,\varepsilon}(\boldsymbol{g}_0)\right) = \Omega_{\infty}^{\mu,\varepsilon}(\boldsymbol{g}) \text{ and } \mathfrak{T}_{\boldsymbol{g}}^{\varepsilon}\left(S_{\infty}^{\mu,\varepsilon}(\boldsymbol{g}_0)\right) = S_{\infty}^{\mu,\varepsilon}(\boldsymbol{g}). \tag{1.41}$$

In classical notations, $\mathfrak{T}_{\boldsymbol{g}}^{\varepsilon}(\boldsymbol{x}) \equiv \varepsilon \boldsymbol{T}_{\boldsymbol{g}}\left(\frac{\boldsymbol{x}}{\varepsilon}\right)$. It is important that the determinant and cofactor of $D\mathfrak{T}_{\boldsymbol{g}}^{\varepsilon}$ are *not* scaled by ε, because

$$D\mathfrak{T}_{\boldsymbol{g}}^{\varepsilon}(\boldsymbol{x}) = D\boldsymbol{T}_{\boldsymbol{g}}\left(\frac{\boldsymbol{x}}{\varepsilon}\right).$$

It can be seen from the direct computation: $D\mathfrak{T}_{\boldsymbol{g}}^{\varepsilon} = D\boldsymbol{S}_{\varepsilon}D\boldsymbol{T}_{\boldsymbol{g}}D\boldsymbol{S}_{\frac{1}{\varepsilon}}$. Since $D\boldsymbol{S}_c = c\boldsymbol{I}$, the terms $D\boldsymbol{S}_{\varepsilon}$ and $D\boldsymbol{S}_{\frac{1}{\varepsilon}}$ cancel out. It follows that no additional scaling will enter the transformed integrals of weak formulations, and all the theorems on continuity with respect to $\boldsymbol{g}$ of the solutions of ε-problems (1.27) can be proved in exactly the same way as in Theorem 6. Further we will refer to Assumption 1 in the context of $\mathfrak{T}_{\boldsymbol{g}}^{\varepsilon}$. In such cases we mean that $\mathfrak{T}_{\boldsymbol{g}}^{\varepsilon}$ is defined according to (1.41), whereby the assumption holds for $\boldsymbol{T}_{\boldsymbol{g}}$.

Recall that our elasticity problems are stated for the domains of the form $\Omega_{\boldsymbol{g}} = \Omega \cap \Omega_{\infty}^{\mu,\varepsilon}(\boldsymbol{g})$, and we need the diffeomorphisms which transform $\Omega_{\boldsymbol{g}_0}$ into $\Omega_{\boldsymbol{g}}$, not just the scaled infinite periodic domains.

Assumption 4. *There exists a family of diffeomorphisms* $\boldsymbol{T}_{\boldsymbol{g}}^{\varepsilon}$ *satisfying the following conditions:*

1. $\boldsymbol{T}_{\boldsymbol{g}_0}^{\varepsilon} = \boldsymbol{I}$,

2. $\forall \boldsymbol{g} \in U_{\boldsymbol{g}}^2$, $\boldsymbol{T}_{\boldsymbol{g}}^{\varepsilon} \in W^{1,\infty}(\Omega_{\boldsymbol{g}_0})$,

3. $\forall \boldsymbol{g} \in U_{\boldsymbol{g}}^2$, $\boldsymbol{Q}_{\boldsymbol{g}}^{\varepsilon} = \left(\boldsymbol{T}_{\boldsymbol{g}}^{\varepsilon}\right)^{-1} \in W^{1,\infty}(\Omega_{\boldsymbol{g}_0})$,

4. $\forall \boldsymbol{g}_1, \boldsymbol{g}_2 \in U_{\boldsymbol{g}}^2$, $\left\|\boldsymbol{T}_{\boldsymbol{g}_1}^{\varepsilon} - \boldsymbol{T}_{\boldsymbol{g}_2}^{\varepsilon}\right\|_{W^{1,\infty}} \to 0$, *as* $\boldsymbol{g}_1 \to \boldsymbol{g}_2$,

5. $D\boldsymbol{T}_{\boldsymbol{g}}^{\varepsilon} \in C\left(\mathbb{R}^+ \times U_{\boldsymbol{g}}^2, L^{\infty}\left(\Omega_{\boldsymbol{g}_0}\right)\right)$, $\exists C_J > 0 : \forall \varepsilon \left\|D\boldsymbol{T}_{\boldsymbol{g}}^{\varepsilon}\right\|_{L^{\infty}\left(\Omega_{\boldsymbol{g}_0}\right)} \leq C_J$, *i.e. the Jacobi matrix is continuous with respect to* ε *and* $\boldsymbol{g}$, *and it is uniformly bounded with respect to* $\varepsilon > 0$.

Remark 8. Unfortunately, definition (1.40) does not ensure that $\mathfrak{T}_{\boldsymbol{g}}^{\varepsilon}\left(\Omega_{\boldsymbol{g}_0}\right) = \Omega_{\boldsymbol{g}}$. The problem is that the periodicity cells intersecting $\partial\Omega$ have to be transformed in a different way than the periodicity cells lying wholly in the interior. Such irregularities are common in studies of periodic media and usually it can be shown that the effect vanishes as $\varepsilon \to 0$.

The last condition of Assumption 4 is satisfiable. Observe that for any rectangular Ω with its sides parallel to the coordinate axes, there exists T_g such that $\mathfrak{T}_g^\varepsilon$ defined according to (1.40) actually satisfies all the conditions of Assumption 4, where the Jacobi matrix is not scaled by ε at all. For each fixed ε the restriction of $\mathfrak{T}_g^\varepsilon$ on the set of points of Ω, having distance to $\partial\Omega$ higher that the diameter of the periodicity cell, also satisfies the conditions. It remains to carefully extend $\mathfrak{T}_g^\varepsilon$ to the boundary layer. Nevertheless, we omit this procedure and make Assumption 4.

As in the previous section, all quantities are transformed to the reference domain Ω_{g_0}. Introduce the notations for the transported functions and their gradients as follows:

$$\mathfrak{u}_g^\varepsilon \equiv u_g^\varepsilon \circ T_g^\varepsilon,$$

$$\mathfrak{A}_g^\varepsilon \equiv A_g^\varepsilon \circ T_g^\varepsilon \left|\det\left(DT_g^\varepsilon\right)\right|,$$

$$\mathfrak{R}_g^\varepsilon \equiv R_g^\varepsilon \circ T_g^\varepsilon \left\|\operatorname{cof}\left(DT_g^\varepsilon\right)\nu\right\|,$$

$$\mathfrak{f}_g^\varepsilon \equiv f_g^\varepsilon \circ T_g^\varepsilon \left|\det\left(DT_g^\varepsilon\right)\right|,$$

$$\mathfrak{D}u_g^\varepsilon \equiv \nabla\left(u_g^\varepsilon \circ T_g^\varepsilon\right)\left(DT_g^\varepsilon\right)^{-1},$$

$$\mathfrak{e}(u_g^\varepsilon) \equiv \frac{1}{2}\left(\mathfrak{D}u_g^\varepsilon + \left(\mathfrak{D}u_g^\varepsilon\right)^T\right).$$

All these transported quantities are defined for $x \in \Omega_{g_0}$ for any $g \in U_g$. Then the closeness of functions $u_{g_1}^\varepsilon$ and $u_{g_2}^\varepsilon$ can be formulated in terms of the norm of the difference $\mathfrak{u}_{g_1}^\varepsilon - \mathfrak{u}_{g_2}^\varepsilon$.

This transformation notation is chosen in such way that each term of the weak formulation (1.27) on Ω_g^ε corresponds to the similar term on $\Omega_{g_0}^\varepsilon$. Namely, for any $g \in U_g^2$, $u \in H^1\left(\Omega_g^\varepsilon\right)$, and $v \in H^1\left(\Omega_g^\varepsilon\right)$,

$$\int_{\Omega_g^\varepsilon} A_g^\varepsilon e(u) : e(v)\, dy = \int_{\Omega_{g_0}^\varepsilon} \mathfrak{A}_g^\varepsilon(x)\mathfrak{e}(u) : \mathfrak{e}(v)\, dx,$$

$$\frac{1}{\varepsilon}\int_{S_{c,g}^\varepsilon} \left\langle R_g^\varepsilon\left[u\right],\left[v\right]\right\rangle ds_y = \frac{1}{\varepsilon}\int_{S_{c,g_0}^\varepsilon} \left\langle \mathfrak{R}_{g_0}^\varepsilon\left[\mathfrak{u}\right],\left[\mathfrak{v}\right]\right\rangle ds,$$

$$\int_{\Omega_g^\varepsilon} \left\langle f,v\right\rangle dy = \int_{\Omega_{g_0}^\varepsilon} \left\langle \mathfrak{f}_g,\mathfrak{v}\right\rangle dx.$$

Due to the non-degeneracy condition from Assumption 4, with this notation all the estimates of Poincare and Korn type for non-transported functions are true for the transported functions. The constants may change, but there exist universal constants such that the

estimates are true for all $\boldsymbol{g} \in U_{\boldsymbol{g}}^2$ by the same argument as in proof of Theorem 6.

Theorem 9. *Let* $\boldsymbol{u}_{\boldsymbol{g}}^\varepsilon$ *denote the solution of* (1.27). *The family of solutions* $\boldsymbol{u}_{\boldsymbol{g}}^\varepsilon$ *is uniformly equicontinuous with respect to* $\boldsymbol{g}$, *i.e. for any* $\eta > 0$ *there exists* $\delta(\eta) > 0$ *such that*

$$\sup_{\varepsilon>0} \left\| \mathfrak{u}_{\boldsymbol{g}_1}^\varepsilon - \mathfrak{u}_{\boldsymbol{g}_2}^\varepsilon \right\|_{H^1\left(\Omega_{\boldsymbol{g}_0}^\varepsilon\right)} \leq \eta$$

for any $\boldsymbol{g}_1$, $\boldsymbol{g}_2$, *provided that* $\|\boldsymbol{g}_1 - \boldsymbol{g}_2\| \leq \delta(\eta)$.

Proof. The proof is provided for non-homogeneous Dirichlet conditions. Consider the weak formulation for $\widehat{\boldsymbol{u}}_{\boldsymbol{g}}^\varepsilon = \boldsymbol{u}_{\boldsymbol{g}}^\varepsilon - \boldsymbol{k}_{\boldsymbol{g}}^\varepsilon$, where $\boldsymbol{k}_{\boldsymbol{g}}^\varepsilon \in H^1\left(\Omega_{\boldsymbol{g}}^\varepsilon\right)$ is the extension of the Dirichlet boundary condition into $\Omega_{\boldsymbol{g}}^\varepsilon$. Assume that its transported version is continuous with respect to $\boldsymbol{g}$, i.e. $\mathfrak{k}_{\boldsymbol{g}}^\varepsilon \in C(U_{\boldsymbol{g}}^2, H^{-1}(\Omega_{\boldsymbol{g}_0}^\varepsilon, \partial\Omega_{D,\boldsymbol{g}}^\varepsilon))$. By virtue of standard estimates on the norms of solution of elliptic problems, one obtains

$$\left\| \widehat{\mathfrak{u}}_{\boldsymbol{g}_1}^\varepsilon - \widehat{\mathfrak{u}}_{\boldsymbol{g}_2}^\varepsilon \right\|_{H^1\left(\Omega_{\boldsymbol{g}_0}^\varepsilon\right)} \leq$$

$$\leq C \left(\left\| \mathfrak{l}_{\boldsymbol{g}_1} - \mathfrak{l}_{\boldsymbol{g}_2} \right\|_{H^{-1}\left(\Omega_{\boldsymbol{g}_0}^\varepsilon\right)} + \left\| \mathfrak{l}_{\boldsymbol{g}_1}^\varepsilon \right\|_{C\left(U_{\boldsymbol{g}}^2, H^{-1}\left(\Omega_{\boldsymbol{g}_0}^\varepsilon\right)\right)} \left\| \mathfrak{A}_{\boldsymbol{g}_1}^\varepsilon - \mathfrak{A}_{\boldsymbol{g}_2}^\varepsilon \right\|_{\mathcal{L}\left(H^1\left(\Omega_{\boldsymbol{g}_0}^\varepsilon\right), H^{-1}\left(\Omega_{\boldsymbol{g}_0}^\varepsilon\right)\right)} \right),$$

where $\mathfrak{l}_{\boldsymbol{g}_1}^\varepsilon \in C\left(U_{\boldsymbol{g}}, H^{-1}\left(\Omega_{\boldsymbol{g}_0}^\varepsilon\right)\right)$ and constant C does not depend on ε, $\boldsymbol{g}_0$, $\boldsymbol{g}_1$, and $\boldsymbol{g}_2$. Since $\mathfrak{A}_{\boldsymbol{g}}^\varepsilon(\boldsymbol{x}) = \mathfrak{A}_{\boldsymbol{g}}(\varepsilon^{-1}\boldsymbol{x})$ for any $\boldsymbol{g} \in U_{\boldsymbol{g}}^2$,

$$\left\| \mathfrak{A}_{\boldsymbol{g}_1}^\varepsilon - \mathfrak{A}_{\boldsymbol{g}_2}^\varepsilon \right\|_{\mathcal{L}\left(H^1\left(\Omega_{\boldsymbol{g}_0}^\varepsilon\right), H^{-1}\left(\Omega_{\boldsymbol{g}_0}^\varepsilon\right)\right)} \leq$$

$$\leq \left\| \mathfrak{A}_{\boldsymbol{g}_1}^\varepsilon - \mathfrak{A}_{\boldsymbol{g}_2}^\varepsilon \right\|_{L^\infty\left(\Omega_{\boldsymbol{g}_0}^\varepsilon\right)} = \left\| \mathfrak{A}_{\boldsymbol{g}_1}^\varepsilon - \mathfrak{A}_{\boldsymbol{g}_2}^\varepsilon \right\|_{L^\infty\left(\mathrm{Y}_{\boldsymbol{g}_0}\right)} \to 0 \text{ as } \|\boldsymbol{g}_1 - \boldsymbol{g}_2\| \to 0, \forall \varepsilon > 0.$$

Recall that $\forall \boldsymbol{g} \in U_{\boldsymbol{g}}$

$$\left\| \mathfrak{l}_{\boldsymbol{g}} \right\|_{H^{-1}\left(\Omega_{\boldsymbol{g}_0}^\varepsilon\right)} \leq \left\| \mathfrak{f}_{\boldsymbol{g}}^\varepsilon \right\|_{H^{-1}\left(\Omega_{\boldsymbol{g}_0}^\varepsilon\right)} + \left\| \left| \det\left(D\boldsymbol{T}_{\boldsymbol{g}}^\varepsilon\right) \right| \mathfrak{D}(\boldsymbol{A}_{\boldsymbol{g}}^\varepsilon D\boldsymbol{k}_{\boldsymbol{g}}^\varepsilon) \right\|.$$

The continuity of the term with $\mathfrak{f}_{\boldsymbol{g}}^\varepsilon$ w.r.t. $\boldsymbol{g}$ follows directly from Assumption 1. See also Lemma 2.1 of Section 2.4 in Chapter 10 from [13]. To prove the continuity of the second term, introduce a new function

$$\psi_{\boldsymbol{g}}\left(\frac{\boldsymbol{x}}{\varepsilon}\right) = \left| \det\left(D\boldsymbol{T}_{\boldsymbol{g}}^\varepsilon\right) \right| \mathfrak{D}(\boldsymbol{A}_{\boldsymbol{g}}^\varepsilon D\boldsymbol{k}_{\boldsymbol{g}}^\varepsilon)\left(\frac{\boldsymbol{x}}{\varepsilon}\right).$$

Denote by $\mathrm{Y}_{\boldsymbol{m}}$ a zero-centered periodicity cell Y_0 shifted by vector $\boldsymbol{m} \in \mathbb{Z}^n$. The following relations chain is true:

$$
\sup_\varepsilon \int_\Omega \left| \boldsymbol{\psi}_{\boldsymbol{g}_1}\left(\frac{\boldsymbol{x}}{\varepsilon}\right) - \boldsymbol{\psi}_{\boldsymbol{g}_2}\left(\frac{\boldsymbol{x}}{\varepsilon}\right) \right|^2 dx \le \sup_\varepsilon \sum_{\varepsilon \mathrm{Y}_{\boldsymbol{m}} \subseteq \Omega} \int_{\varepsilon \mathrm{Y}_{\boldsymbol{m}}} \left| \boldsymbol{\psi}_{\boldsymbol{g}_1}\left(\frac{\boldsymbol{x}}{\varepsilon}\right) - \boldsymbol{\psi}_{\boldsymbol{g}_2}\left(\frac{\boldsymbol{x}}{\varepsilon}\right) \right|^2 dx =
$$

$$
= \sup_\varepsilon \varepsilon^n \sum_{\varepsilon \mathrm{Y}_{\boldsymbol{m}} \subseteq \Omega} \int_{\mathrm{Y}_{\boldsymbol{m}}} \left| \boldsymbol{\psi}_{\boldsymbol{g}_1}(\boldsymbol{\xi}) - \boldsymbol{\psi}_{\boldsymbol{g}_2}(\boldsymbol{\xi}) \right|^2 d\boldsymbol{\xi} \le
$$

$$
\le \sup_\varepsilon \left(\frac{|\Omega|}{|Y|} + \varepsilon \frac{|\partial\Omega| \max_{i=1,\dots,n} |\mathrm{Y}_{0i}|}{|Y|} \right) \int_{\mathrm{Y}} \left| \boldsymbol{\psi}_{\boldsymbol{g}_1}(\boldsymbol{\xi}) - \boldsymbol{\psi}_{\boldsymbol{g}_2}(\boldsymbol{\xi}) \right| d\boldsymbol{\xi} \le
$$

$$
\le \left(\frac{|\Omega|}{|\mathrm{Y}|} + \varepsilon_{\max} \frac{|\partial\Omega| \max_{i=1,\dots,n} |\mathrm{Y}_{0i}|}{|\mathrm{Y}|} \right) \int_{\mathrm{Y}} \left| \boldsymbol{\psi}_{\boldsymbol{g}_1}(\boldsymbol{\xi}) - \boldsymbol{\psi}_{\boldsymbol{g}_2}(\boldsymbol{\xi}) \right| d\boldsymbol{\xi}.
$$

Here $\varepsilon_{\max}$ can be assumed to be equal to 1. The last expression tends to zero as $\|\boldsymbol{g}_1 - \boldsymbol{g}_2\| \to 0$ if $\boldsymbol{\psi}_{\boldsymbol{g}}(\boldsymbol{\xi})$ is continuous with respect to $\boldsymbol{g}$. Indeed,

$$
\left\| \boldsymbol{\psi}_{\boldsymbol{g}_1} - \boldsymbol{\psi}_{\boldsymbol{g}_2} \right\|_{L^2(\mathrm{Y})} \le \left\| \boldsymbol{\mathfrak{A}}_{\boldsymbol{g}}^\varepsilon \right\|_{C\left(U_{\boldsymbol{g}}^2, L^\infty(\mathrm{Y})\right)} \left\| \boldsymbol{\mathfrak{D}} \boldsymbol{k}_{\boldsymbol{g}_1}^\varepsilon - \boldsymbol{\mathfrak{D}} \boldsymbol{k}_{\boldsymbol{g}_2}^\varepsilon \right\|_{L^2(\mathrm{Y})} +
$$

$$
\left\| \boldsymbol{\mathfrak{D}} \boldsymbol{k}_{\boldsymbol{g}}^\varepsilon \right\|_{C\left(U_{\boldsymbol{g}}^2, L^2(\mathrm{Y})\right)} \left\| \boldsymbol{\mathfrak{A}}_{\boldsymbol{g}_1} - \boldsymbol{\mathfrak{A}}_{\boldsymbol{g}_2} \right\|_{L^\infty(\mathrm{Y})} \to 0 \text{ as } \|\boldsymbol{g}_1 - \boldsymbol{g}_2\| \to 0.
$$

The a priori estimate also yields the uniform boundedness in $\boldsymbol{g}$. This concludes the proof. $\square$

The following theorem is a generalization of Arzela-Ascoli Theorem for the weak or two-scale topology.

Theorem 10. *Let $\{\mathfrak{u}_k^\varepsilon\}$ be a sequence of functions such that:*

1. *it is a uniformly bounded w.r.t. ε subset of $C(U_{\boldsymbol{g}}^2, L^2(\Omega_{\boldsymbol{g}_0}^\varepsilon))$,*

2. *it is uniformly equicontinuous in $L^2(\Omega_{\boldsymbol{g}_0}^\varepsilon)$.*

Then it contains a subsequence $\{\widehat{\mathfrak{u}}_k^\varepsilon\}$ which two-scale converges to a limit $\mathfrak{u}_{0,\boldsymbol{g}} \in C(U_{\boldsymbol{g}}^2, L^2(\Omega^{3D} \times Y))$, i.e. for any function $\psi(x,y) \in \mathcal{D}(\Omega^{3D}, C_{\mathrm{per}}^\infty(Y))$,

$$
\lim_{\varepsilon \to 0} \left| \int_{\Omega_{\boldsymbol{g}_0}^\varepsilon} \mathfrak{u}_{\boldsymbol{g}}^\varepsilon(\boldsymbol{x}) \psi(\boldsymbol{x}, \varepsilon^{-1}\boldsymbol{x}) \, d\boldsymbol{x} - \frac{1}{|Y|} \int_Y \mathfrak{u}_{0,\boldsymbol{g}}(\boldsymbol{x}, \boldsymbol{\xi}) \psi(\boldsymbol{x}, \boldsymbol{\xi}) \, d\boldsymbol{\xi} \right| \to 0.
$$

Proof. The proof is similar to the proof of Theorem 2.5.4 in [33]. Note that $U_{\boldsymbol{g}}^2$ contains a dense countable subset. Denote this subset by $\mathfrak{U}_{\boldsymbol{g}}$. Due to the boundedness of $\{\mathfrak{u}_k^\varepsilon\}$,

for each $\boldsymbol{g}_i \in U_{\boldsymbol{g}}^2$ it is possible to extract a two-scale convergent subsequence with the limit $\mathbf{u}_{0,\boldsymbol{g}_i} \in L^2\left(\Omega^{3D} \times Y\right)$ (see Theorem 1.2 in [3]). We proceed by the application of the Cantor diagonal procedure. Namely, for $\boldsymbol{g}_1 \in \mathfrak{U}_{\boldsymbol{g}}$ we extract from $\{\mathbf{u}_k^\varepsilon\}$ a subsequence $\left\{\mathbf{u}_{k_{i_1}}^\varepsilon\right\}$ which two-scale converges to $\mathbf{u}_{0,\boldsymbol{g}_1}$. From $\left\{\mathbf{u}_{k_{i_1}}^\varepsilon\right\}$ we extract a subsequence, two-scale converging for $\boldsymbol{g} = \boldsymbol{g}_2$ and so on for all $\boldsymbol{g}_i \in \mathfrak{U}_{\boldsymbol{g}}$. We finally arrive at the subsequence $\{\widehat{\mathbf{u}}_k^\varepsilon\}$ that two-scale converges to $\mathbf{u}_{0,\boldsymbol{g}_i}(\boldsymbol{x}, \boldsymbol{\xi})$ for all $\boldsymbol{g}_i \in \mathfrak{U}_{\boldsymbol{g}}$, $i \in \mathbb{N}$.

The continuity of the limit function $\mathbf{u}_{0,\boldsymbol{g}}(\boldsymbol{x}, \boldsymbol{\xi})$ with respect to $\boldsymbol{g}$ follows from the uniform equicontinuity of $\{\mathbf{u}_k^\varepsilon\}$ and density of $\mathfrak{U}_{\boldsymbol{g}}$. Indeed, for any $\boldsymbol{g}_i, \boldsymbol{g}_j \in \mathfrak{U}_{\boldsymbol{g}}$,

$$
\left\|\mathbf{u}_{0,\boldsymbol{g}_i}(\boldsymbol{x}, \boldsymbol{\xi}) - \mathbf{u}_{0,\boldsymbol{g}_j}(\boldsymbol{x}, \boldsymbol{\xi})\right\|_{L^2(\Omega \times Y)} \leq \lim_{\varepsilon \to 0} \left\|\widehat{\mathbf{u}}_{k,\boldsymbol{g}_i}^\varepsilon(\boldsymbol{x}) - \widehat{\mathbf{u}}_{k,\boldsymbol{g}_j}^\varepsilon(\boldsymbol{x})\right\|_{L^2(\Omega)} \leq
$$
$$
\leq \sup_\varepsilon \left\|\widehat{\mathbf{u}}_{k,\boldsymbol{g}_i}^\varepsilon(\boldsymbol{x}) - \widehat{\mathbf{u}}_{k,\boldsymbol{g}_j}^\varepsilon(\boldsymbol{x})\right\|_{L^2(\Omega)} \to 0 \text{ as } \left\|\boldsymbol{g}_i - \boldsymbol{g}_j\right\| \to 0. \quad (1.42)
$$

By the density of $\mathfrak{U}_{\boldsymbol{g}}$ in $U_{\boldsymbol{g}}^2$, for any $\boldsymbol{g} \in U_{\boldsymbol{g}}^2$ there exists a sequence $\{\boldsymbol{g}_i\} \in \mathfrak{U}_{\boldsymbol{g}}$ converging to $\boldsymbol{g}$. By (1.42), the sequence $\mathbf{u}_{0,\boldsymbol{g}_i}$ is fundamental in $L^2(\Omega^{3D} \times Y)$. Therefore, it has a limit which we denote by $\mathbf{u}_{0,\boldsymbol{g}}$. Note that by (1.42) again, this limit does not depend on the choice of the subsequence. Further, for any $\boldsymbol{g}_1, \boldsymbol{g}_2 \in U_{\boldsymbol{g}}$ we can choose two sequences from $\mathfrak{U}_{\boldsymbol{g}}$ and by application of (1.42) prove that

$$
\left\|\mathbf{u}_{0,\boldsymbol{g}_1}(\boldsymbol{x}, \boldsymbol{\xi}) - \mathbf{u}_{0,\boldsymbol{g}_2}(\boldsymbol{x}, \boldsymbol{\xi})\right\|_{L^2(\Omega^{3D} \times Y)} \leq \varepsilon.
$$

It remains to prove the point-wise two scale convergence for any $\boldsymbol{g} \in U_{\boldsymbol{g}}^2$. Indeed, for an arbitrary $\boldsymbol{g} \in U_{\boldsymbol{g}}^2$ pick a sequence $\{\boldsymbol{g}_k\}$ converging to $\boldsymbol{g}$. Let $\psi^\varepsilon \equiv \psi(\boldsymbol{x}, \boldsymbol{\xi})$, $\boldsymbol{\xi} = \varepsilon^{-1}\boldsymbol{x}$, $\psi \in \mathcal{D}\left(\Omega, C_{per}^\infty(Y)\right)$. Fix some $\varepsilon > 0$. We have

$$
\left|\left\langle \mathbf{u}_{\boldsymbol{g}}^\varepsilon, \psi^\varepsilon - \frac{1}{Y}\left\langle \mathbf{u}_{0,\boldsymbol{g}}, \psi\right\rangle_{L^2(Y)}\right\rangle_{L^2(\Omega)}\right| \leq \left\|\mathbf{u}_{\boldsymbol{g}}^\varepsilon - \mathbf{u}_{\boldsymbol{g}_k}^\varepsilon\right\|_{L^2(\Omega)} \|\psi^\varepsilon\|_{L^2(\Omega)} +
$$
$$
+ \left|\left\langle \mathbf{u}_{\boldsymbol{g}_k}^\varepsilon, \psi^\varepsilon - \frac{1}{Y}\left\langle \mathbf{u}_{0,\boldsymbol{g}_k}, \psi\right\rangle_{L^2(Y)}\right\rangle_{L^2(\Omega)}\right| + \frac{1}{Y}\left\|\mathbf{u}_{0,\boldsymbol{g}_k} - \mathbf{u}_{0,\boldsymbol{g}}\right\|_{L^2(\Omega \times Y)} \|\psi\|_{L^2(\Omega \times Y)}. \quad (1.43)
$$

Here $\|\psi^\varepsilon\|$ is bounded uniformly in ε. Due to the equicontinuity of $\mathbf{u}_{\boldsymbol{g}}^\varepsilon$ and continuity of $\mathbf{u}_{0,\boldsymbol{g}}$, one can choose $\boldsymbol{g}_k$ so close to $\boldsymbol{g}$ that the first and the third terms in the estimate (1.43) are less than δ. Finally, due to the point-wise two-scale convergence of $\mathbf{u}_{\boldsymbol{g}_k}^\varepsilon$ to $\mathbf{u}_{0,\boldsymbol{g}_k}$, one can choose $\varepsilon_0(\delta, \boldsymbol{g}_k)$ such that the second term in (1.43) is less than δ for any $\varepsilon < \varepsilon_0$. This

means that the left-hand side of (1.43) is less than 3δ and the convergence is proven.   □

1.5   Optimization problems statements

The textile-like material is modeled by a three-dimensional body made of the homogenized material. We clarify the relation between this body and the homogenized coefficients with the real textile and its properties further in this section.

The design space is always geometry parameter $\boldsymbol{g}$ defined in Section 1.2.2. For Poisson ratio optimization problem we consider $\boldsymbol{g}$ to be a constant function. For stress profile optimization problems we consider $\boldsymbol{g}$ to be an element of H^2, but prove the minimizer existence result when $U_{\boldsymbol{g}}$ is a compact set of C or when it is a bounded set in the space of Hölder functions $C^{0,1}$.

For each problem we discuss the objective functionals, prove existence of minimizers and describe the way to find their gradients. The gradients are used to run the projected gradient algorithm to obtain the minima, assuming that the gradient $\nabla_{\boldsymbol{g}}\boldsymbol{A}$ and the principal part of increment $\delta_{\boldsymbol{g}}\boldsymbol{A}$ are known. Later in Section 1.6.1 we show how they are computed.

1.5.1   Connection between three-dimensional and two-dimensional problems

Consider a textile-like material described in Section 1.2. Assume that it has width L_w, length L_h and the geometry consists of cells or meshes which are square in the in-plane subspace. This condition is true for the geometries described in Section 1.2. Assume that the side of the cells is ε_0, i.e. the textile-like material is a periodic or quasiperiodic structure with period ε_0.

We approximate the textile-like material with a three-dimensional body Π_{3D} of the homogenized medium described in Section 1.3.5. This body has the same length and width as the textile material. We use ε_0 for the thickness. There are two reasons for this. The first one is that Π_{3D} should model exactly one layer of the textile-like material. The second one is that Π_{3D} should consist of cubic cells, so that the homogenization results of Section 1.3.5 are applicable. Effectively, we take a single layer of the textile-like material and immerse it into a layer of soft matrix material of thickness ε_0. The plate obtained by this process is

then homogenized, and its in-plane elastic properties A_{ijkl}^{inp} are defined as follows:

$$A_{ijkl}^{\mathrm{inp}} = \varepsilon_0 \lim_{\delta \to 0} A_{ijkl}^{\mathrm{hom}}(\delta), \quad i, j, k, l \in \{1, 2\}.$$

1.5.2 Poisson's ratio optimization

The homogenized tensor is in general non-isotropic. However, if the geometry of the periodicity cell possesses certain symmetry properties, the homogenized tensor will be orthotropic (properties of the homogenized tensor are investigated in detail in [5]). Further in this part everywhere, where it is essential, the homogenized tensor is assumed to be orthotropic. Orthotropic elasticity Hooke's law in case of two dimensions has a form

$$\begin{pmatrix} \varepsilon_{11} \\ \varepsilon_{22} \\ 2\varepsilon_{12} \end{pmatrix} = \begin{pmatrix} 1/E_1 & -\nu_{21}/E_2 & 0 \\ -\nu_{12}/E_1 & 1/E_2 & 0 \\ 0 & 0 & 1/G_{12} \end{pmatrix} \begin{pmatrix} \sigma_{11} \\ \sigma_{22} \\ \sigma_{12} \end{pmatrix},$$

$$\begin{pmatrix} \sigma_{11} \\ \sigma_{22} \\ \sigma_{12} \end{pmatrix} = \begin{pmatrix} pE_1 & pE_1\nu_{21} & 0 \\ pE_2\nu_{12} & pE_2 & 0 \\ 0 & 0 & G_{12} \end{pmatrix} \begin{pmatrix} \varepsilon_{11} \\ \varepsilon_{22} \\ 2\varepsilon_{12} \end{pmatrix}, \text{ where } p = (1 - \nu_{12}\nu_{21})^{-1}. \quad (1.44)$$

Poisson's ratio ν_{12} characterizes contraction of the structure in the direction of axis Oy when stretched in the direction of axis Ox. Note that Poisson's ratios of an orthotropic material do not possess symmetry properties, i.e. in general $\nu_{12} \neq \nu_{21}$.

The in-plane Hooke's law is

$$\begin{pmatrix} \sigma_{11} \\ \sigma_{22} \\ \sigma_{12} \end{pmatrix} = \begin{pmatrix} \left[\boldsymbol{A_g^{\mathrm{inp}}}\right]_{1111} & \left[\boldsymbol{A_g^{\mathrm{inp}}}\right]_{1122} & \left[\boldsymbol{A_g^{\mathrm{inp}}}\right]_{1112} \\ \left[\boldsymbol{A_g^{\mathrm{inp}}}\right]_{1122} & \left[\boldsymbol{A_g^{\mathrm{inp}}}\right]_{2222} & \left[\boldsymbol{A_g^{\mathrm{inp}}}\right]_{2212} \\ \left[\boldsymbol{A_g^{\mathrm{inp}}}\right]_{1112} & \left[\boldsymbol{A_g^{\mathrm{inp}}}\right]_{2212} & \left[\boldsymbol{A_g^{\mathrm{inp}}}\right]_{1212} \end{pmatrix} \begin{pmatrix} \varepsilon_{11} \\ \varepsilon_{22} \\ 2\varepsilon_{12} \end{pmatrix}, \quad (1.45)$$

where the notation $\left[\boldsymbol{A_g^{\mathrm{inp}}}\right]_{ijkl}$ means the $ijkl$-th component of tensor $\boldsymbol{A_g^{\mathrm{inp}}}$. From (1.44) and (1.45) it is easy to see that the Poisson's ratios of the homogenized medium in 2D case are the following explicit functions of the homogenized coefficients:

$$\nu_{12} = \frac{\left[\boldsymbol{A_g^{\mathrm{inp}}}\right]_{1122}}{\left[\boldsymbol{A_g^{\mathrm{inp}}}\right]_{2222}} \quad \nu_{21} = \frac{\left[\boldsymbol{A_g^{\mathrm{inp}}}\right]_{1122}}{\left[\boldsymbol{A_g^{\mathrm{inp}}}\right]_{1111}}. \quad (1.46)$$

From Expressions (1.46) we immediately obtain the variation of ν_{12} and ν_{21}:

$$\delta_{\boldsymbol{g}}\nu_{12} = \frac{\delta_{\boldsymbol{g}}\left[\boldsymbol{A}_{\boldsymbol{g}}^{\mathrm{inp}}\right]_{1122}}{\left[\boldsymbol{A}_{\boldsymbol{g}}^{\mathrm{inp}}\right]_{2222}} - \frac{\left[\boldsymbol{A}_{\boldsymbol{g}}^{\mathrm{inp}}\right]_{1122}}{\left[\boldsymbol{A}_{\boldsymbol{g}}^{\mathrm{inp}}\right]_{2222}^{2}}\delta_{\boldsymbol{g}}\left[\boldsymbol{A}_{\boldsymbol{g}}^{\mathrm{inp}}\right]_{2222},$$

$$\delta_{\boldsymbol{g}}\nu_{21} = \frac{\delta_{\boldsymbol{g}}\left[\boldsymbol{A}_{\boldsymbol{g}}^{\mathrm{inp}}\right]_{1122}}{\left[\boldsymbol{A}_{\boldsymbol{g}}^{\mathrm{inp}}\right]_{1111}} - \frac{\left[\boldsymbol{A}_{\boldsymbol{g}}^{\mathrm{inp}}\right]_{1122}}{\left[\boldsymbol{A}_{\boldsymbol{g}}^{\mathrm{inp}}\right]_{1111}^{2}}\delta_{\boldsymbol{g}}\left[\boldsymbol{A}_{\boldsymbol{g}}^{\mathrm{inp}}\right]_{1111}.$$

At this point everything is available to run projected gradient method to optimize effective in-plane Poisson's ratios numerically. Therefore, for constant geometry, optimization of Poisson's ratios is reduced to simple optimization over the square $\boldsymbol{G}$. Due to the continuity of ν_{12} and ν_{21} with respect to the entries of $\boldsymbol{A}_{\boldsymbol{g}}^{\mathrm{inp}}$ and that $\left[\boldsymbol{A}_{\boldsymbol{g}}^{\mathrm{inp}}\right]_{1111} > 0$ and $\left[\boldsymbol{A}_{\boldsymbol{g}}^{\mathrm{inp}}\right]_{2222} > 0$, the existence of minimizers for ν_{12} and ν_{21} is obvious. In the section with numerical examples we show that the problem lacks convexity with respect to geometrical parameters and that the minimizer depends on the initial point of the minimization algorithm. Therefore, we do not discuss the uniqueness of the minimizers.

1.5.3   Effective pressure profile optimization

In this chapter we will work with non-periodic structures, at the same time using the results of the previous sections obtained for the periodic setting. The justification for this is that we apply Theorem 5 locally, i.e. we assume that the function $\boldsymbol{g}$ is no longer periodic and in the homogenized problems, tensor $\boldsymbol{A}_{\boldsymbol{g}}^{\mathrm{inp}}$ is no longer constant due to non-periodically changing geometry and should be computed at each point x from the corresponding cell problem. This approach is valid if the geometry does not change too quickly. It is enough to require that $\boldsymbol{g}(\boldsymbol{x})$ is a Lipschitz-continuous function with the Lipschitz constant independent of ε. See Section 5 of Chapter 3 in [5].

The effective pressure profile optimization problem is formulated as follows: find geometrical parameters $\boldsymbol{g} = (g_1, g_2)$ such that

$$J(\boldsymbol{g}) = \int_{\Omega} \boldsymbol{N}(\boldsymbol{A}_{\boldsymbol{g}}^{\mathrm{inp}}e(\boldsymbol{u}^0(\boldsymbol{g})) - \boldsymbol{\sigma}^{\star}) : (\boldsymbol{A}_{\boldsymbol{g}}^{\mathrm{inp}}e(\boldsymbol{u}^0(\boldsymbol{g})) - \boldsymbol{\sigma}^{\star})\,d\boldsymbol{x} \to \min_{\boldsymbol{g}}, \qquad (1.47)$$

where $\boldsymbol{N} \in \mathcal{T}^+(\Omega)$ does not depend on $\boldsymbol{g}$ and $\boldsymbol{u}^0(\boldsymbol{g})$ is the solution of the following 2D elasticity problem:

$$\begin{cases} -\nabla \cdot (\boldsymbol{A}_{\boldsymbol{g}}^{\text{inp}} e(\boldsymbol{u}^0)) = \boldsymbol{f} \text{ in } \Omega, \\ \boldsymbol{u}^0 = \boldsymbol{D}(\boldsymbol{x}) \text{ on } \partial\Omega_D, \\ \boldsymbol{A}_{\boldsymbol{g}}^{\text{inp}} e(\boldsymbol{u}^0)\boldsymbol{n} = 0 \text{ on } \partial\Omega_N. \end{cases} \tag{1.48}$$

This is a well-studied PDE-constrained optimization problem.

Theorem 11. *Let $\mathcal{V}$ be some compactly imbedded in $C(\Omega, \mathbb{R}^2)$ space and $U_{\boldsymbol{g}}$ be some bounded in $\mathcal{V}$ set. Then the problem (1.47)–(1.48), where $\boldsymbol{A}_{\boldsymbol{g}}^{\text{inp}}$ is defined according to (1.22)–(1.24), has a minimizer.*

Proof. We prove the theorem in four steps:

1. From Theorem 7 obtain that

$$\left\| \boldsymbol{A}_{\boldsymbol{g}_1}^{\text{inp}} - \boldsymbol{A}_{\boldsymbol{g}_2}^{\text{inp}} \right\|_{L^\infty} \to 0 \text{ as } \boldsymbol{g}_1 \to \boldsymbol{g}_2, \tag{1.49}$$

2. from Theorem 8 get

$$\left\| \boldsymbol{u}_{\boldsymbol{g}_1}^0 - \boldsymbol{u}_{\boldsymbol{g}_2}^0 \right\|_{H^1} \to 0 \quad \text{as} \quad \left\| \boldsymbol{A}_{\boldsymbol{g}_1}^{\text{inp}} - \boldsymbol{A}_{\boldsymbol{g}_2}^{\text{inp}} \right\|_{L^\infty} \to 0, \tag{1.50}$$

3. observe that $\left| J_{\boldsymbol{g}_1} - J_{\boldsymbol{g}_2} \right| \to 0$ as $\left\| \boldsymbol{u}_{\boldsymbol{g}_1}^0 - \boldsymbol{u}_{\boldsymbol{g}_2}^0 \right\|_{H^1} \to 0$, by using (1.49)–(1.50) obtain

$$\left| J_{\boldsymbol{g}_1} - J_{\boldsymbol{g}_2} \right| \to 0 \text{ as } \boldsymbol{g}_1 \to \boldsymbol{g}_2,$$

4. finally, since $U_{\boldsymbol{g}}$ is bounded in $\mathcal{V}$, by the compact imbedding result $\mathcal{V} \hookrightarrow C$, we observe that $U_{\boldsymbol{g}}$ is compact in C. But since J is continuous w.r.t. $\boldsymbol{g}$ converging in C-norm, the existence of the minimizer is provided by the classical Weierstrass theorem.

$\square$

Corollary 4. *Problem (1.47)–(1.48), where $\boldsymbol{A}_{\boldsymbol{g}}^{\text{inp}}$ is defined according to (1.22)–(1.24), has a minimizer, if $U_{\boldsymbol{g}}$ is a bounded set in either of the following spaces:*

1. *any finite-dimensional space of functions,*

   2. the space of Lipschitz-continuous functions $C^{0,1}(\Omega, \mathbb{R}^2)$,

   3. the Sobolev space $H^2\left(\Omega, \mathbb{R}^2\right)$.

Proof. In either of the three cases the spaces are compactly embedded in $C(\Omega, \mathbb{R}^2)$, thus Theorem 11 can be used directly. □

Remark 9. In Section 1.8 from numerical examples we observe that the problem is non-convex, and that the result of the gradient method depends on the initial approximation. Therefore, we do not discuss convexity of the functional and the uniqueness of the mini-mizer.

Assuming that increment $\delta_{\boldsymbol{g}} \boldsymbol{A}_{\boldsymbol{g}}^{\mathrm{inp}}(\boldsymbol{g})$ is available, derive gradient of $J(\boldsymbol{g})$. By the chain rule

$$
\delta_{\boldsymbol{g}} J = 2 \int_\Omega \boldsymbol{N}(\boldsymbol{A}_{\boldsymbol{g}}^{\mathrm{inp}}(\boldsymbol{g}) e(\boldsymbol{u}^0(\boldsymbol{g})) - \boldsymbol{\sigma}^\star) : (\delta_{\boldsymbol{g}} \boldsymbol{A}_{\boldsymbol{g}}^{\mathrm{inp}} \, e(\delta_{\boldsymbol{g}} \boldsymbol{u}^0(\boldsymbol{g})) - \boldsymbol{A}_{\boldsymbol{g}}^{\mathrm{inp}}(\boldsymbol{g}) \, e(\delta_{\boldsymbol{g}} \boldsymbol{u}^0(\boldsymbol{g}))) \, d\boldsymbol{x} =
$$
$$
= 2 \int_\Omega \boldsymbol{N}(\boldsymbol{A}_{\boldsymbol{g}}^{\mathrm{inp}}(\boldsymbol{g}) e(\boldsymbol{u}^0(\boldsymbol{g})) - \boldsymbol{\sigma}^\star) : (\delta_{\boldsymbol{g}} \boldsymbol{A}_{\boldsymbol{g}}^{\mathrm{inp}} \, e(\boldsymbol{u}^0(\boldsymbol{g}))) \, d\boldsymbol{x} -
$$
$$
+ 2 \int_\Omega \boldsymbol{N}(\boldsymbol{A}_{\boldsymbol{g}}^{\mathrm{inp}}(\boldsymbol{g}) e(\boldsymbol{u}^0(\boldsymbol{g})) - \boldsymbol{\sigma}^\star) : (\boldsymbol{A}_{\boldsymbol{g}}^{\mathrm{inp}}(\boldsymbol{g}) \, e(\delta_{\boldsymbol{g}} \boldsymbol{u}^0(\boldsymbol{g}))) \, d\boldsymbol{x}.
$$

Let us introduce the operator

$$
\boldsymbol{h}(\boldsymbol{g}) = \boldsymbol{A}_{\boldsymbol{g}}^{\mathrm{inp}}(\boldsymbol{g}) \boldsymbol{N}(\boldsymbol{A}_{\boldsymbol{g}}^{\mathrm{inp}}(\boldsymbol{g}) \, e(\boldsymbol{u}^0(\boldsymbol{g})) - \boldsymbol{\sigma}^\star), \tag{1.51}
$$

we have

$$
\delta_{\boldsymbol{g}} J = 2 \int_\Omega \boldsymbol{N}\left(\boldsymbol{A}_{\boldsymbol{g}}^{\mathrm{inp}}(\boldsymbol{g}) e(\boldsymbol{u}^0(\boldsymbol{g})) - \boldsymbol{\sigma}^\star\right) : \left(\delta_{\boldsymbol{g}} \boldsymbol{A}_{\boldsymbol{g}}^{\mathrm{inp}} \, e(\boldsymbol{u}^0(\boldsymbol{g}))\right) d\boldsymbol{x} - 2 \int_\Omega \boldsymbol{h}(\boldsymbol{g}) : e(\delta_{\boldsymbol{g}} \boldsymbol{u}^0(\boldsymbol{g})).
$$
$$
\tag{1.52}
$$

We will use integration by parts formula in the following form:

$$
\int_\Omega \langle \nabla \cdot \boldsymbol{A}e(\boldsymbol{u}), \boldsymbol{v} \rangle \, d\boldsymbol{x} = \int_{\partial\Omega} \langle \boldsymbol{A}e(\boldsymbol{u})\boldsymbol{n}, \boldsymbol{v} \rangle \, d\boldsymbol{s} - \int_\Omega \boldsymbol{A}e(\boldsymbol{u}) : e(\boldsymbol{v}) \, d\boldsymbol{x},
$$

This formula holds for any symmetric tensor $\boldsymbol{A} \in \mathcal{T}^+(\Omega)$, $\boldsymbol{u}$ and $\boldsymbol{v}$ from H^1, and for Ω with piecewise-Lipschitz boundary.

In (1.52) the function $\delta_{\boldsymbol{g}} \boldsymbol{u}^0$ is yet unknown. It can be found with application of increment operation to the weak form of the state equation (1.48). For any $\boldsymbol{g} \in U_{\boldsymbol{g}}$ and any $\boldsymbol{v} \in H^1(\Omega)$, $\boldsymbol{v} = 0$ on $\partial\Omega_D$

$$-\int_\Omega \boldsymbol{A}_{\boldsymbol{g}}^{\mathrm{inp}} e(\boldsymbol{u}^0) : e(\boldsymbol{v}) \, d\boldsymbol{x} + \int_\Omega \langle \boldsymbol{f}, \boldsymbol{v} \rangle \, d\boldsymbol{x} = 0.$$

With the assumption that $\boldsymbol{f}$ does not depend on $\boldsymbol{g}$, the application of increment operation yields

$$0 = \delta_{\boldsymbol{g}} \left(\int_\Omega \boldsymbol{A}_{\boldsymbol{g}}^{\mathrm{inp}} e(\boldsymbol{u}^0) : e(\boldsymbol{v}) \, d\boldsymbol{x} \right) = \int_\Omega \delta_{\boldsymbol{g}} \boldsymbol{A}_{\boldsymbol{g}}^{\mathrm{inp}} e(\boldsymbol{u}^0) : e(\boldsymbol{v}) \, d\boldsymbol{x} + \int_\Omega \boldsymbol{A}_{\boldsymbol{g}}^{\mathrm{inp}} e(\delta_{\boldsymbol{g}} \boldsymbol{u}^0) : e(\boldsymbol{v}) \, d\boldsymbol{x}.$$

Further, by partial integration we observe

$$0 = -\int_\Omega \delta_{\boldsymbol{g}} \boldsymbol{A}_{\boldsymbol{g}}^{\mathrm{inp}} e(\boldsymbol{u}^0) : e(\boldsymbol{v}) \, d\boldsymbol{x} - \int_\Omega \boldsymbol{A}_{\boldsymbol{g}}^{\mathrm{inp}} e(\delta_{\boldsymbol{g}} \boldsymbol{u}^0) : e(\boldsymbol{v}) \, d\boldsymbol{x} =$$

$$= -\int_{\partial\Omega_N} \langle \delta_{\boldsymbol{g}} \boldsymbol{A}_{\boldsymbol{g}}^{\mathrm{inp}} e(\boldsymbol{u}^0) \boldsymbol{n}, \boldsymbol{v} \rangle + \int_\Omega \langle \nabla \cdot \delta_{\boldsymbol{g}} \boldsymbol{A}_{\boldsymbol{g}}^{\mathrm{inp}} e(\boldsymbol{u}^0), \boldsymbol{v} \rangle - \int_\Omega \boldsymbol{A}_{\boldsymbol{g}}^{\mathrm{inp}} e(\delta_{\boldsymbol{g}} \boldsymbol{u}^0) : e(\boldsymbol{v}) \, d\boldsymbol{x}.$$

$$(1.53)$$

Here only $\delta_{\boldsymbol{g}} \boldsymbol{u}^0$ is unknown, therefore (1.53) can be considered as a weak formulation for a problem, from which $\delta_{\boldsymbol{g}} \boldsymbol{u}^0$ can be determined. The corresponding strong formulation is

$$\begin{cases} -\nabla \cdot (\boldsymbol{A}_{\boldsymbol{g}}^{\mathrm{inp}} e(\delta_{\boldsymbol{g}} \boldsymbol{u}^0)) = \nabla \cdot \delta_{\boldsymbol{g}} \boldsymbol{A}_{\boldsymbol{g}}^{\mathrm{inp}} e(\boldsymbol{u}^0) \text{ in } \Omega, \\ \boldsymbol{A}_{\boldsymbol{g}}^{\mathrm{inp}} e(\delta_{\boldsymbol{g}} \boldsymbol{u}^0) \boldsymbol{n} = -\delta_{\boldsymbol{g}} \boldsymbol{A}_{\boldsymbol{g}}^{\mathrm{inp}} e(\boldsymbol{u}^0) \boldsymbol{n} \text{ on } \partial\Omega_N, \\ \delta_{\boldsymbol{g}} \boldsymbol{u}^0 = 0 \text{ on } \partial\Omega_D. \end{cases} \qquad (1.54)$$

For some basis in the space, where $\boldsymbol{g}$ is defined, solutions of (1.52) and (1.54) can be found in order to to compose the gradient of J and run a descent method for optimization. This would implement the sensitivity approach.

It is possible to reduce the computational burden. Integrate by parts the unknown term of (1.52) and use the Dirichlet boundary condition of (1.54):

$$\int_\Omega \boldsymbol{h} : e(\delta_{\boldsymbol{g}} \boldsymbol{u}^0) = \int_{\partial\Omega_N} \langle \boldsymbol{h} \boldsymbol{n}, \delta_{\boldsymbol{g}} \boldsymbol{u}^0 \rangle \, d\boldsymbol{s} - \int_\Omega \langle \nabla \cdot \boldsymbol{h}, \delta_{\boldsymbol{g}} \boldsymbol{u}^0 \rangle \, d\boldsymbol{x} =$$

introduce function p such that $-\nabla \cdot (A_g^{\text{inp}} e(p)) = \nabla \cdot h$ and integrate the second term by parts,

$$= \int_{\partial \Omega_N} \langle hn, \delta_g u^0 \rangle \, ds + \int_\Omega \langle \nabla \cdot (A_g^{\text{inp}} e(p)), \delta_g u^0 \rangle =$$

$$= \int_{\partial \Omega_N} \langle (h + A_g^{\text{inp}} e(p)) \, n, \delta_g u^0 \rangle \, ds - \int_\Omega e(p) \colon A_g^{\text{inp}} e(\delta_g u^0) \, dx =$$

require that $hn + A_g^{\text{inp}} e(p)n = 0$ on $\partial \Omega_N$, the second term is integrated by parts

$$= -\int_{\partial \Omega} \langle p, A_g^{\text{inp}} e(\delta_g u^0)n \rangle \, ds + \int_\Omega \langle p, \nabla \cdot A_g^{\text{inp}} e(\delta_g u^0) \rangle \, dx =$$

as PDE of (1.54) states, $A_g^{\text{inp}} e(\delta_g u^0)$ can be replaced by $-\delta_g A_g^{\text{inp}} e(u^0)$,

$$= -\int_{\partial \Omega} \langle p, A_g^{\text{inp}} e(\delta_g u^0)n \rangle \, ds - \int_\Omega \langle p, \nabla \cdot \delta_g A_g^{\text{inp}} e(u^0) \rangle \, dx =$$

$$= -\int_{\partial \Omega} \langle p, (A_g^{\text{inp}} e(\delta_g u^0) + \delta_g A_g^{\text{inp}} e(u^0)) \, n \rangle \, ds + \int_\Omega \delta_g A_g^{\text{inp}} e(u^0) : e(p) \, dx =$$

require that $p = 0$ on $\partial \Omega_D$ and use the Neumann boundary condition of (1.54),

$$= \int_\Omega \delta_g A_g^{\text{inp}} e(u^0) : e(p) \, dx.$$

Summarizing all the conditions for p we see that it is the solution to the problem

$$\begin{cases} -\nabla \cdot (A_g^{\text{inp}} e(p)) = \nabla \cdot h \text{ in } \Omega, \\ p = 0 \text{ on } \partial \Omega_D, \\ A_g^{\text{inp}} e(p)n = -hn \text{ on } \partial \Omega_N. \end{cases}$$

Objective funtional's increment can be represented as

$$\delta_g J = 2 \int_\Omega N(A_g^{\text{inp}}(g)e(u^0(g)) - \sigma^\star) : (\delta_g A_g^{\text{inp}} e(u^0(g))) \, dx + 2 \int_\Omega \delta_g A_g^{\text{inp}} e(u^0) : e(p),$$

where tensor h is defined in (1.51). Solving (1.48), then computing h and p, and finally obtaining objective functional's increment is the adjoint approach and p is the adjoint state [22, 27].

Observe that it can be applied both to cases when the medium is periodic and not. The function $\delta_{\boldsymbol{g}} \boldsymbol{A}_{\boldsymbol{g}}^{\mathrm{inp}}$ as a function of the spatial coordinate is constant in the first case. In the non-periodic case this is no longer true, but the optimization approach described here still works with no change in the expressions.

1.6 Application of beam models at the level of cell problems

At the scale of cell problems we consider μ to be a small parameter and apply beam models. An investigation of elasticity problems on the domains parametrized in a similar way by two numbers ε and μ is available in [36], where the analysis is performed by the full asymptotic expansion for elasticity without Robin conditions.

In [38, 39, 51] it is observed that the limit strongly depends on the relation between ε and μ. In general, the homogenization approach leads to the second-order equations for the leading term if $\mu \sim \varepsilon^{\omega}$ for $\omega \in (0, 1/2)$. For such parameter values a transition to beam models can be justified as an asymptotic expansion of the cell problems with respect to the parameter μ.

The standard result in homogenization of elasticity problems on the nets found in [36] yields the problems on one-dimensional geometries of central segments of the cylinders of $\Omega_{\boldsymbol{g}}^{\mu,\varepsilon}$, i.e. on sets $\Gamma^{\varepsilon,\mu}(g_x, g_y)$. To account for Robin-type conditions at the contact interfaces, we introduce contact segments and work with $\Gamma^{\varepsilon,\mu c}(g_x, g_y)$.

1.6.1 Reduction to beam models at the level of cell problems

Introduce some additional geometric notation. Consider one-dimensional geometry of some cell Γ_Y^{μ}. Let n be some node of Γ_Y^{μ}. For an edge $e \in E(n)$ define $\gamma(e, n)$ to be the direction vector of the edge pointing from n. For each edge e define χ to be its longitudinal variable. In problems formulated on unions of segments, all derivatives with respect to χ mean derivatives along the corresponding edge. Define global base $(\boldsymbol{g}_1, \boldsymbol{g}_2, \boldsymbol{g}_3)$. For each edge e define local base $(\boldsymbol{l}_1^e, \boldsymbol{l}_2^e, \boldsymbol{l}_3^e)$. Introduce coordinate transformation matrix $\boldsymbol{C}^e$ (note that it depends neither on μ nor on ε) by the following rule:

$$(\boldsymbol{l}_1^e, \boldsymbol{l}_2^e, \boldsymbol{l}_3^e) = (\boldsymbol{g}_1, \boldsymbol{g}_2, \boldsymbol{g}_3)\boldsymbol{C}^e.$$

Following [36], we consider a behavior of the solution of the elasticity problem on a

finite net representing the periodicity cell, what corresponds to the case of $\mu \to 0$. The extension of these results to elasticity problems with Robin conditions at the contact interfaces for a particular geometry are obtained in [6]. In both works the limiting equations are of standard Euler-Bernoulli beam model type, while the Robin conditions result in nonstandard jump conditions at the interfaces.

1.6.2   Using full beams system instead of pure tensional system

According to Section 5.6 of [36], the coefficients of the homogenized equation can be obtained from problems of pure tension with periodic boundary conditions on Γ_Y^μ. However, for the uniqueness of the solution, we have to require that the underlying graph is geometrically rigid, independently of boundary conditions. This is undesirable for modeling of textiles, because any chain of straight segments modeling a curved yarn is ruled out by this condition.

For beam models with bending and torsion the situation is closer to standard elasticity, namely, it is enough to require that the structure is connected and that a complete Dirichlet condition is prescribed at any single node. It is proved in Corollary 5. Thus bending and torsion provide some sort of regularization, what renders these systems more attractable for numerical experiments. In the sequel we use the beam systems of equations from Section 4.4.1 of [36] augmented with jump conditions (1.57).

Cell problems were already introduced in Section 1.3.5 in the form (1.23). The cell problems are indexed by two numbers $i \in \{1,2,3\}$ and $j \in \{1,2,3\}$. For the in-plane properties, only problems for $i \in \{1,2\}$ and $j \in \{1,2\}$ are of interest. For beam models they

are formulated as follows: find $\boldsymbol{u}_{ij} \in \Gamma_Y \to \mathbb{R}^{1\times 6}$, $i,j \in \{1,2\}$ such that

$$
\begin{cases}
\text{at each edge } e \text{ define } \boldsymbol{u}_{ij}^e \in [0; l^e] \to \mathbb{R}^{1\times 4}, \ 1 \le i \le 2, \ 1 \le j \le 2, \\
\left[\boldsymbol{u}_{ij}^e\right]_1 \in H^1\left([0; l^e]\right), \ \left[\boldsymbol{u}_{ij}^e\right]_2 \in H^2\left([0; l^e]\right), \ \left[\boldsymbol{u}_{ij}^e\right]_3 \in H^2\left([0; l^e]\right), \ \left[\boldsymbol{u}_{ij}^e\right]_4 \in H^1\left([0; l^e]\right), \\
\text{equilibrium conditions on edges hold:} \\
E^e \mathcal{A}^e \dfrac{d^2}{d\chi^2}\left[\boldsymbol{u}_{ij}^e\right]_1 = 0, \\
E^e \mathcal{I}_2^e \dfrac{d^4}{d\chi^4}\left[\boldsymbol{u}_{ij}^e\right]_2 = 0, \\
E^e \mathcal{I}_3^e \dfrac{d^4}{d\chi^4}\left[\boldsymbol{u}_{ij}^e\right]_3 = 0, \\
G^e \mathcal{M}^e \dfrac{d^2}{d\chi^2}\left[\boldsymbol{u}_{ij}^e\right]_4 = 0, \\
\text{force balance conditions in nodes hold:} \\
\sum_{e\in E(n)} E^e \boldsymbol{C}^e \left(\mathcal{A}^e\left(\left[\boldsymbol{u}_{ij}^e\right]_1 + (\boldsymbol{C}^e)^T \boldsymbol{S}_{ij}\right)'_\chi \quad \mathcal{I}_2^e\left(\left[\boldsymbol{u}_{ij}^e\right]_2\right)'''_\chi \quad \mathcal{I}_3^e\left(\left[\boldsymbol{u}_{ij}^e\right]_3\right)'''_\chi\right)^T = 0, \\
\text{moment balance conditions in nodes hold:} \\
\sum_{e\in E(n)} \boldsymbol{C}^e \left(G^e \mathcal{M}^e \left(\left[\boldsymbol{u}_{ij}^e\right]_4\right)'_\chi \quad -E^e \mathcal{I}_2^e\left(\left[\boldsymbol{u}_{ij}^e\right]_3\right)''_\chi \quad E^e \mathcal{I}_3^e\left(\left[\boldsymbol{u}_{ij}^e\right]_2\right)''_\chi\right)^T = 0, \\
\text{jump conditions at the contact interfaces given by (1.57), hold} \\
\text{periodic w.r.t. the periodicity cell boundary conditions hold:} \\
[\boldsymbol{u}_{ij}]_{1:3} \equiv \boldsymbol{C}^e \left[\boldsymbol{u}_{ij}^e\right]_{1:3} \text{ and } [\boldsymbol{u}_{ij}]_{4:6} \equiv \boldsymbol{C}^e \begin{pmatrix} \left[\boldsymbol{u}_{ij}^e\right]_4 \\ -\dfrac{d}{d\chi}\left[\boldsymbol{u}_{ij}^e\right]_3 \\ \dfrac{d}{d\chi}\left[\boldsymbol{u}_{ij}^e\right]_2 \end{pmatrix} \text{ are periodic,}
\end{cases}
$$

$$(1.55)$$

where

$$
\boldsymbol{S}_{11} = \begin{pmatrix} x_1 \\ 0 \end{pmatrix}, \quad \boldsymbol{S}_{12} = \begin{pmatrix} 0 \\ x_1 \end{pmatrix}, \quad \boldsymbol{S}_{21} = \begin{pmatrix} x_2 \\ 0 \end{pmatrix}, \quad \boldsymbol{S}_{22} = \begin{pmatrix} 0 \\ x_2 \end{pmatrix}.
$$

In this system χ is the longitudinal coordinate of an element. Constants $\mathcal{A}^e$, $\mathcal{I}_2^e$, $\mathcal{I}_3^e$, and $\mathcal{M}^e$ are area of the cross-section of the element, its area moments with respect to the second and the third axes of the element, and its polar area moment respectively. For a beam of circular cross-section of radius r, $\mathcal{A}^e = \pi r^2$, $\mathcal{I}_2^e = \mathcal{I}_3^e = \pi r^4/4$, and $\mathcal{M}^e = \pi r^4/2$. Elastic constants E^e and G^e are Young's and shear moduli of the element's material. For any vector

v notation $[v]_i$ means the i-th component of v and for $j \geq i$, $[v]_{i:j}$ is the sub-vector of v from its i-th component to its j-th component, i.e. $[v]_{i:j} \equiv \begin{pmatrix} v_i & v_{i+1} & \dots & v_j \end{pmatrix}$.

It will be convenient to consider functions $m_{ij} = u_{ij} + S_{ij}$ instead of u_{ij}. It is easy to check that since u_{ij} satisfy (1.55), m_{ij} solve the following problem:

$$
\left\{
\begin{aligned}
&\text{at each edge } e \text{ define } m_{ij}^e \in [0; l^e] \to \mathbb{R}^{1\times 4}, \ 1 \leq i \leq 2, \ 1 \leq j \leq 2, \\
&\left[m_{ij}^e\right]_1 \in H^1\left([0; l^e]\right), \ \left[m_{ij}^e\right]_2 \in H^2\left([0; l^e]\right), \ \left[m_{ij}^e\right]_3 \in H^2\left([0; l^e]\right), \ \left[m_{ij}^e\right]_4 \in H^1\left([0; l^e]\right), \\
&m_{ij}^e \in \mathbb{R}^1 \to \mathbb{R}^{1\times 4}, \ 1 \leq i \leq 2, \ 1 \leq j \leq 2 \\
&\text{equilibrium conditions on edges hold:} \\
&E^e \mathcal{A}^e \frac{d^2}{d\chi^2}\left[m_{ij}^e\right]_1 = 0, \\
&E^e \mathcal{I}_2^e \frac{d^4}{d\chi^4}\left[m_{ij}^e\right]_2 = 0, \\
&E^e \mathcal{I}_3^e \frac{d^4}{d\chi^4}\left[m_{ij}^e\right]_3 = 0, \\
&G^e \mathcal{M}^e \frac{d^2}{d\chi^2}\left[m_{ij}^e\right]_4 = 0, \\
&\text{force balance conditions in nodes hold:} \\
&\sum_{e\in E(n)} E^e C^e \left(\mathcal{A}^e \left(\left[m_{ij}^e\right]_1\right)_\chi' \quad \mathcal{I}_2^e \left(\left[m_{ij}^e\right]_2\right)_\chi''' \quad \mathcal{I}_3^e \left(\left[m_{ij}^e\right]_3\right)_\chi''' \right)^T = 0, \\
&\text{moment balance conditions in nodes hold:} \\
&\sum_{e\in E(n)} C^e \left(G^e \mathcal{M}^e \left(\left[m_{ij}^e\right]_4\right)_\chi' \quad -E^e \mathcal{I}_2^e \left(\left[m_{ij}^e\right]_3\right)_\chi'' \quad E^e \mathcal{I}_3^e \left(\left[m_{ij}^e\right]_2\right)_\chi'' \right)^T = 0, \\
&\text{jump conditions at the contact interfaces given by (1.57),} \\
&\text{periodic w.r.t. the periodic boundary conditions hold:} \\
&[u_{ij}]_{1:3} \equiv C^e \left(\left[m_{ij}^e\right]_{1:3} - S_{ij}\right) \text{ and } [u_{ij}]_{4:6} \equiv C^e \begin{pmatrix} \left[m_{ij}^e\right]_4 \\ -\frac{d}{d\chi}\left[m_{ij}^e\right]_3 \\ \frac{d}{d\chi}\left[m_{ij}^e\right]_2 \end{pmatrix} \text{ are periodic.}
\end{aligned}
\right.
$$

$$(1.56)$$

From general asymptotic analysis it follows that adding non-scaled bending components to purely tensional system from [36] does not affect the leading terms of the full asymptotic expansion. Therefore, solutions of systems with bending and torsion instead of solutions of purely tensional systems can be used for computation of the coefficients of the homogenized tensor without any modifications.

A remarkable feature of the problem (1.56) is that its solution is a piecewise-polynomial function of the third order. This means that the corresponding finite element schemes yield the exact solutions for this problem.

1.6.3 Introducing contact conditions

In the limit problem Robin boundary conditions are represented by jump conditions for the derivatives of the components of displacement across the points, closest to the contact interface, see [6]. We consider a more general case of the jump conditions.

Recall that each segment of $\Gamma_Y^\mu(g_x, g_y)$ corresponds to an elastic cylinder in $\Omega_\infty^\mu(g_x, g_y) \cap Y$. This is not true for $\Gamma_Y^{\mu c}(g_x, g_y)$, where some segments correspond to locations of the contact between the cylinders. We will refer to the ends of such segments as to contact nodes. By construction of $\Gamma_Y^{\mu c}(g_x, g_y)$, contact nodes never connect two non-parallel non-contact segments. Therefore, for all non-contact segments adjacent to the same contact node the local coordinate systems have the same bases.

Consider a single contact segment S and two pairs of segments entering its two contact nodes n_1 and n_2. Denote their coordinate transformation matrices by $\boldsymbol{C}_1$ and $\boldsymbol{C}_2$. Define contact coordinate system as a system with origin in the center of S and its first basis vector aligned with S. The other two basis vectors can be any such that the contact coordinate system is orthonormal. Let $\boldsymbol{C}_c$ be the coordinate transformation matrix. Denote the local displacement components of the segments entering n_1 by u_i, $1 \leq i \leq 4$ and the components entering n_2 by v_i, $1 \leq i \leq 4$.

Remark 10. Asymptotic dimension reduction for 3D problem of (1.24) was considered for a beam in contact with a rigid foundation in [6]. With the appropriate choice of matrices $\boldsymbol{P}_f$ and $\boldsymbol{P}_M$ the jump conditions presented below in (1.57) coincide with the conditions of [6] for bending and tensional components, the torsional component in the work vanishes due to scaling effects. It is remarkable, that the values obtained in [6] are bound to the corresponding inertia moments of the contact interface, which is assumed to be known. We choose the coefficients for our numerical experiments accordingly.

We use the following jump conditions at n_1 and n_2:

$$\Lambda(\boldsymbol{w}) = -\boldsymbol{Q}^T \left(\boldsymbol{T}_f^T \boldsymbol{P}_f \boldsymbol{T}_f + \boldsymbol{T}_M^T \boldsymbol{P}_M \boldsymbol{T}_M \right) \boldsymbol{Q} \boldsymbol{w}, \text{ where}$$

$$\boldsymbol{P}_M = \begin{pmatrix} G_1 & 0 & 0 \\ 0 & G_2 & 0 \\ 0 & 0 & G_3 \end{pmatrix}, \ \boldsymbol{V}_i = \begin{pmatrix} 0 & z_i^c & -y_i^c \\ -z_i^c & 0 & x_i^c \\ y_i^c & -x_i^c & 0 \end{pmatrix}, \ \delta_c^{-1} > 0, \ G > 0, \ G_N > 0, \ G_T > 0,$$

$$\boldsymbol{T}_f = \begin{pmatrix} \boldsymbol{I}_3 & \boldsymbol{V}_1 & -\boldsymbol{I}_3 & -\boldsymbol{V}_2 \end{pmatrix}, \qquad \boldsymbol{P}_f = \begin{pmatrix} \delta_c^{-1} & 0 & 0 \\ 0 & G & 0 \\ 0 & 0 & G \end{pmatrix},$$

$$\boldsymbol{T}_M = \begin{pmatrix} 0 & \boldsymbol{I}_3 & 0 & -\boldsymbol{I}_3 \end{pmatrix},$$

(1.57)

$$\Lambda(\boldsymbol{w}) = \begin{pmatrix} [EAu_1']_{n_1} \\ [EIu_2''']_{n_1} \\ [EIu_3''']_{n_1} \\ [GJu_4']_{n_1} \\ -[EIu_3'']_{n_1} \\ [EIu_2'']_{n_1} \\ [EAv_1']_{n_2} \\ [EIv_2''']_{n_2} \\ [EIv_3''']_{n_2} \\ [GJv_4']_{n_2} \\ -[EIv_3'']_{n_2} \\ [EIv_2'']_{n_2} \end{pmatrix}, \ \boldsymbol{w} = \begin{pmatrix} u_1 \\ u_2 \\ u_3 \\ u_4 \\ -u_3' \\ u_2' \\ v_1 \\ v_2 \\ v_3 \\ v_4 \\ -v_3' \\ v_2' \end{pmatrix}, \ \boldsymbol{Q} = \begin{pmatrix} C_c^T C_1 & 0 & 0 & 0 \\ 0 & C_c^T C_1 & 0 & 0 \\ 0 & 0 & C_c^T C_2 & 0 \\ 0 & 0 & 0 & C_c^T C_2 \end{pmatrix}. \quad (1.58)$$

Here $\boldsymbol{r}_1 = (x_1, y_1, z_1)$ is the radius-vector of n_1 in the contact coordinate system, $\boldsymbol{r}_2 = (x_2, y_2, z_2)$ — the radius vector of n_2. Note that matrices $\boldsymbol{P}_f$ and $\boldsymbol{P}_M$ are positive-definite.

Remark 11. Coefficient δ_c^{-1} corresponds to the penalization of the normal penetration of the beams, G corresponds to the penalization of the tangential relative displacement of the beams. Rotational coefficients G_1, G_2 and G_3 correspond to the penalization of the rotational relative displacement in the tangential and two normal planes at the contact point of the cylinders. Roughly speaking, if the following conditions hold: $\delta_c^{-1} \gg E \gg G$,

$G_1 \gg E \gg G_2 = G_3$, where E is the Young's modulus of the material, then conditions (1.57) will penalize the normal penetration much stronger than the tangential relative displacement. At the same time, the elastic energy term will penalize the deforming elastic displacements weaker than the jump conditions penalize the normal penetration and stronger than the tangential relative displacement. Such behaviour is desirable if friction is approximated with conditions (1.57). The coefficients in our numerical experiments are chosen accordingly.

The corresponding term in the energy of the system reflecting the Robin term in (1.22) is

$$J_f(\boldsymbol{w}) + J_M(\boldsymbol{w}) = \frac{1}{2}(\boldsymbol{Q}\boldsymbol{w})^T(\boldsymbol{T}_f^T \boldsymbol{P}_f \boldsymbol{T}_f + \boldsymbol{T}_M^T \boldsymbol{P}_M \boldsymbol{T}_M)(\boldsymbol{Q}\boldsymbol{w}). \tag{1.59}$$

Remark 12. Note that vector $\boldsymbol{w}$ contains the degrees of freedom of the elastic elements being in contact in their local coordinate system. The matrices for the numerical scheme differ from (1.59) in coordinate transformation matrices (see (1.65)).

We thus augment the system (1.55) with conditions (1.57) to model contact.

1.6.4 Variational formulation of 1D problem

We extend the definition of test functions from PF_2 from Chapter 4 of [36]:

Definition 1. A four-dimensional function Ψ belongs to class $\mathcal{H}(\Gamma_Y^\mu(g_x, g_y))$, iff:

1. Ψ is Y-periodic,

2. for any segment e of $\Gamma_Y^\mu(g_x, g_y)$, $[\Psi]_{1,4} \in H^1(e)$, $[\Psi]_{2,3} \in H^2(e)$,

3. for all internal nodes n of $\Gamma_Y^\mu(g_x, g_y)$ for all pairs of segments $e_1, e_2 \in E(n)$ the matching conditions are satisfied:

$$\boldsymbol{C}^{e_1}\begin{pmatrix} [\Psi^{e_1}]_1 \\ [\Psi^{e_1}]_2 \\ [\Psi^{e_1}]_3 \end{pmatrix} = \boldsymbol{C}^{e_2}\begin{pmatrix} [\Psi^{e_2}]_1 \\ [\Psi^{e_2}]_2 \\ [\Psi^{e_2}]_3 \end{pmatrix}, \quad \boldsymbol{C}^{e_1}\begin{pmatrix} [\Psi^{e_1}]_4 \\ -d[\Psi^{e_1}]_3/d\chi \\ d[\Psi^{e_1}]_2/d\chi \end{pmatrix} = \boldsymbol{C}^{e_2}\begin{pmatrix} [\Psi^{e_2}]_4 \\ -d[\Psi^{e_2}]_3/d\chi \\ d[\Psi^{e_2}]_2/d\chi \end{pmatrix},$$

The following assumption mimics Poincare's inequality on $\Gamma_Y^\mu(g_x, g_y)$:

Assumption 5. *the following inequality holds:*

$$\int_{\Gamma_Y^\mu(g_x,g_y)} \left([\Psi^e]_1^2 + \left(\frac{d[\Psi^e]_2}{d\chi} \right)^2 + \left(\frac{d[\Psi^e]_3}{d\chi} \right)^2 + [\Psi^e]_4^2 \right) d\chi \leq$$

$$\leq \mathcal{C} \int_{\Gamma_Y^\mu(g_x,g_y)} \left(\left(\frac{d[\Psi^e]_1}{d\chi} \right)^2 + \left(\frac{d^2[\Psi^e]_2}{d\chi^2} \right)^2 + \left(\frac{d^2[\Psi^e]_3}{d\chi^2} \right)^2 + \left(\frac{d[\Psi^e]_4}{d\chi} \right)^2 \right) d\chi.$$

The homogenized coefficients are computed from the bilinear form of the problem (1.55)–(1.57):

$$a_{1D}(\boldsymbol{u}, \boldsymbol{v}) = \sum_e \left(\int_e E^e \mathcal{A}^e \frac{d\boldsymbol{u}_1^e}{d\chi} \frac{dv_1^e}{d\chi} d\chi + \int_e E^e \mathcal{I}_2^e \frac{d^2\boldsymbol{u}_2^e}{d\chi^2} \frac{d^2v_2^e}{d\chi^2} d\chi + \int_e E^e \mathcal{I}_3^e \frac{d^2\boldsymbol{u}_3^e}{d\chi^2} \frac{d^2v_3^e}{d\chi^2} d\chi + $$
$$+ \int_e G^e \mathcal{M}^e \frac{d\boldsymbol{u}_4^e}{d\chi} \frac{dv_4^e}{d\chi} d\chi \right) + \sum_c \boldsymbol{w}^T(\boldsymbol{u}) \boldsymbol{\mathcal{P}}_c \boldsymbol{w}(\boldsymbol{v}), \quad \text{for } \boldsymbol{u}, \boldsymbol{v} \in \mathcal{H}\left(\Gamma_Y^\mu(g_x, g_y) \right), \tag{1.60}$$

where

$$\boldsymbol{\mathcal{P}}_c = \boldsymbol{Q}_c^T (\boldsymbol{T}_{fc}^T \boldsymbol{P}_{fc} \boldsymbol{T}_{fc} + \boldsymbol{T}_{Mc}^T \boldsymbol{P}_{Mc} \boldsymbol{T}_{Mc}) \boldsymbol{Q}_c \tag{1.61}$$

is built according to (1.57) and (1.59) with matrices $\boldsymbol{Q}$ and $\boldsymbol{V}_i$ obtained from the geometry of the segments entering nodes c. Introduce homogenized coefficients computed from the beam models as

$$\widehat{A}_{ijkl}^{\text{hom}} = a_{1D}(\boldsymbol{m}_{ij}, \boldsymbol{m}_{kl}). \tag{1.62}$$

Remark 13. We do not consider the important question of convergence of the coefficients computed from 1.22 and from 1.62. For the problems without Robin boundary conditions, such convergence is a direct corollary of dimension reduction results, see Chapter 5 in [36].

1.6.5 Homogenization of quasiperiodic structures

The homogenization approach works in a more general setting for non-periodic structures. The scheme of the method does not change in the sense that the limiting problem is a continuum problem, but the homogenized tensor is not constant anymore. At each point of the limiting continuum problem it has to be computed from the solution of a coordinate-dependent cell problem, i.e. for non-periodic medium one has to solve potentially infinitely

many cell problems. In numerics we use piecewise affine interpolation of the homogenized tensor on a fixed grid, at each point of which we solve a cell problem.

1.6.6 Properties of the beam problems

In this section we assume that $\Gamma_Y^c(g_x, g_y)$ is a connected periodic graph. On this graph we solve a problem of type (1.55) with contact conditions (1.57). Each edge of $\Gamma_Y^c(g_x, g_y)$ corresponds to either an elastic element or a contact pair.

We explicitly check that the kernel of stiffness matrices for segments representing beams and contact pairs is a standard rigid displacements field with small rotations. Then we show that periodical boundary conditions rule out the rotational rigid displacements part. Thus, to ensure that cell problems for such structures have unique solutions, it is enough to define spatial displacements for any single node of the structure. Note that the solutions of beam problems are continuous polynomials, and the spaces in variational formulation (1.60) consist of absolutely continuous functions. For such problems fixation of displacements at any single point makes sense.

We solve the cell problems in the form with zero right-hand sides. In this case functions M_{ij} are piecewise-polynomial functions of the third order on $\Gamma_Y(g_x, g_y)$. Their coefficients are algebraic functions of the degrees of freedom considered in the standard FEM schemes for beams. Therefore, the analysis of uniqueness and the kernel structure for such problems can be obtained from the properties of the corresponding stiffness matrices.

Kernel structure of the elastic part

In this section the following notation will be used: for a matrix $\boldsymbol{A}$, $[\boldsymbol{A}]_{i_1:i_2,j_1:j_2}$, $i_1 \leq i_2$, $j_1 \leq j_2$ is the submatrix with lines from i_1 to i_2 and columns from j_1 to j_2. For example,

$$\boldsymbol{A} = \begin{pmatrix} 1 & 2 & 3 & 4 \\ 5 & 6 & 7 & 8 \\ 9 & 10 & 11 & 12 \\ 13 & 14 & 15 & 16 \end{pmatrix}, \qquad [\boldsymbol{A}]_{2:3,2:4} = \begin{pmatrix} 6 & 7 & 8 \\ 10 & 11 & 12 \end{pmatrix}.$$

Consider a single term of the first sum in (1.60) or a single segment (1.55). It will be referred to as a single elastic element e of $\Gamma_Y(g_x, g_y)$. Further in this section we omit e as a subscript or index when refer to inertia moments and elastic constants. The corresponding

stiffness matrix $\mathbf{K}^e$ of e has the following form:

$$\mathbf{K}^e = \Xi^e \mathbf{G}^e \left(\Xi^e\right)^T,$$

where $\mathbf{G}_e$ is

$$
\begin{pmatrix}
\frac{E\mathcal{A}}{l} & 0 & 0 & 0 & 0 & 0 & -\frac{E\mathcal{A}}{l} & 0 & 0 & 0 & 0 & 0 \\
0 & 12\frac{E\mathcal{I}_2}{l^3} & 0 & 0 & 0 & 6\frac{E\mathcal{I}_2}{l^2} & 0 & -12\frac{E\mathcal{I}_2}{l^3} & 0 & 0 & 0 & 6\frac{E\mathcal{I}_2}{l^2} \\
0 & 0 & 12\frac{E\mathcal{I}_3}{l^3} & 0 & -6\frac{E\mathcal{I}_3}{l^2} & 0 & 0 & 0 & -12\frac{E\mathcal{I}_3}{l^3} & 0 & -6\frac{E\mathcal{I}_3}{l^2} & 0 \\
0 & 0 & 0 & \frac{G\mathcal{M}}{l} & 0 & 0 & 0 & 0 & 0 & -\frac{G\mathcal{M}}{l} & 0 & 0 \\
0 & 0 & -6\frac{E\mathcal{I}_3}{l^2} & 0 & 4\frac{E\mathcal{I}_3}{l} & 0 & 0 & 0 & 6\frac{E\mathcal{I}_3}{l^2} & 0 & 2\frac{E\mathcal{I}_3}{l} & 0 \\
0 & 6\frac{E\mathcal{I}_2}{l^2} & 0 & 0 & 0 & 4\frac{E\mathcal{I}_2}{l} & 0 & -6\frac{E\mathcal{I}_2}{l^2} & 0 & 0 & 0 & 2\frac{E\mathcal{I}_2}{l} \\
-\frac{E\mathcal{A}}{l} & 0 & 0 & 0 & 0 & 0 & \frac{E\mathcal{A}}{l} & 0 & 0 & 0 & 0 & 0 \\
0 & -12\frac{E\mathcal{I}_2}{l^3} & 0 & 0 & 0 & -6\frac{E\mathcal{I}_2}{l^2} & 0 & 12\frac{E\mathcal{I}_2}{l^3} & 0 & 0 & 0 & -6\frac{E\mathcal{I}_2}{l^2} \\
0 & 0 & -12\frac{E\mathcal{I}_3}{l^3} & 0 & 6\frac{E\mathcal{I}_3}{l^2} & 0 & 0 & 0 & 12\frac{E\mathcal{I}_3}{l^3} & 0 & 6\frac{E\mathcal{I}_3}{l^2} & 0 \\
0 & 0 & 0 & -\frac{G\mathcal{M}}{l} & 0 & 0 & 0 & 0 & 0 & \frac{G\mathcal{M}}{l} & 0 & 0 \\
0 & 0 & -6\frac{E\mathcal{I}_3}{l^2} & 0 & 2\frac{E\mathcal{I}_3}{l} & 0 & 0 & 0 & 6\frac{E\mathcal{I}_3}{l^2} & 0 & 4\frac{E\mathcal{I}_3}{l} & 0 \\
0 & 6\frac{E\mathcal{I}_2}{l^2} & 0 & 0 & 0 & 2\frac{E\mathcal{I}_2}{l} & 0 & -6\frac{E\mathcal{I}_2}{l^2} & 0 & 0 & 0 & 4\frac{E\mathcal{I}_2}{l}
\end{pmatrix},
$$

$\Xi_e = \operatorname{diag}(\boldsymbol{C}^e, \boldsymbol{C}^e, \boldsymbol{C}^e, \boldsymbol{C}^e)$.

Lemma 3. *The kernel of $\mathbf{G}^e$ is given by*

$$
\ker_{\mathrm{L}} = \bigcup_{\substack{\boldsymbol{s}\in\mathbb{R}^3 \\ \boldsymbol{\theta}\in\mathbb{R}^3}}
\begin{pmatrix}
\boldsymbol{s} \\
\boldsymbol{\theta} \\
\boldsymbol{s} + \boldsymbol{W}(\boldsymbol{\theta})\boldsymbol{l} \\
\boldsymbol{\theta}
\end{pmatrix},
\boldsymbol{l} = \begin{pmatrix} l \\ 0 \\ 0 \end{pmatrix}, \
\boldsymbol{W}(\boldsymbol{\theta}) = \begin{pmatrix}
0 & -\theta_z & \theta_y \\
\theta_z & 0 & -\theta_x \\
-\theta_y & \theta_x & 0
\end{pmatrix}, \ \boldsymbol{\theta}\in\mathbb{R}^3.
$$

where $\boldsymbol{s}$ are spatial displacements and $\boldsymbol{\theta}$ are angular displacements.

The kernel of $\mathbf{K}^e$ is given by

$$
\mathrm{ker_G} = \bigcup_{\substack{s \in \mathbb{R}^3 \\ \boldsymbol{\theta} \in \mathbb{R}^3}} \begin{pmatrix} s \\ \boldsymbol{\theta} \\ s + \boldsymbol{W}(\boldsymbol{\theta})\boldsymbol{C}^e l \\ \boldsymbol{\theta} \end{pmatrix}, l = \begin{pmatrix} l \\ 0 \\ 0 \end{pmatrix}, \boldsymbol{W}(\boldsymbol{\theta}) = \begin{pmatrix} 0 & -\theta_z & \theta_y \\ \theta_z & 0 & -\theta_x \\ -\theta_y & \theta_x & 0 \end{pmatrix}, \boldsymbol{\theta} \in \mathbb{R}^3. \quad (1.63)
$$

Proof. Due to non-degeneracy of Ξ_e, $\mathrm{rank}\,(\mathbf{K}^e) = \mathrm{rank}\,(\mathbf{G}^e)$. By direct calculation we observe that $\det\left([\mathbf{G}^e]_{1:6,1:6}\right) = \det\left([\mathbf{G}^e]_{7:12,7:12}\right) = 144\mathcal{A}E^5 G\mathcal{I}_2^2\mathcal{I}_3^2\mathcal{M}l^{-10} > 0$. This means that $\mathrm{rank}\,(\mathbf{K}^e) = \mathrm{rank}\,(\mathbf{G}^e) \geq 6$. Further, by direct computation one can verify that

$$
\mathbf{G}^e v = 0, v = \begin{pmatrix} s \\ \boldsymbol{\alpha} \\ s + \boldsymbol{W}(\boldsymbol{\alpha})l \\ \boldsymbol{\alpha} \end{pmatrix} \quad \forall s \in \mathbb{R}^3, \quad \forall \boldsymbol{\alpha} \in \mathbb{R}^3.
$$

Note that by special choice of $\boldsymbol{\alpha}$, s, $\boldsymbol{\theta}$ it is possible to obtain six linearly independent full displacement vectors v. It follows that $\dim\,(\ker\,(\mathbf{K}^e)) = \dim\,(\ker\,(\mathbf{G}^e)) \geq 6$, but since $\mathrm{rank}\,(\mathbf{K}^e) = \mathrm{rank}\,(\mathbf{G}^e) \geq 6$, we conclude that $\dim\,(\ker\,(\mathbf{K}^e)) = \dim\,(\ker\,(\mathbf{G}^e)) = 6$ and that $\ker\,(\mathbf{G}^e) = \mathrm{ker_L}$.

To prove that $\mathrm{ker_G} = \ker\,(\mathbf{K}^e)$, observe that $\mathrm{ker_G}$ is basically a transformation of $\mathrm{ker_L}$ to the global coordinate system, i.e. for any $s_g \in \mathbb{R}^3$, $\boldsymbol{\theta}_g \in \mathbb{R}^3$ there exist s and $\boldsymbol{\theta}$, such that:

$$
s_g = \boldsymbol{C}^e s, \; \boldsymbol{\theta}_g = \boldsymbol{C}^e \boldsymbol{\theta}, \; \boldsymbol{W}(\boldsymbol{\theta}_g) = \boldsymbol{C}^e \boldsymbol{W}(\boldsymbol{\theta})\,(\boldsymbol{C}^e)^T. \quad (1.64)
$$

The transformation rule for $\boldsymbol{W}(\boldsymbol{\theta}_g)$ follows from the standard rules of transformation of linear operators and properties of vector product. Further, consider vector

$$
v_g = \begin{pmatrix} s_g \\ \boldsymbol{\theta}_g \\ s_g + \boldsymbol{W}(\boldsymbol{\theta}_g)\boldsymbol{C}^e l \\ \boldsymbol{\theta}_g \end{pmatrix} = \begin{pmatrix} \boldsymbol{C}^e s \\ \boldsymbol{C}^e \boldsymbol{\theta} \\ \boldsymbol{C}^e s + \boldsymbol{C}^e \boldsymbol{W}(\boldsymbol{\theta})\,(\boldsymbol{C}^e)^T \boldsymbol{C}^e l \\ \boldsymbol{C}^e \boldsymbol{\theta} \end{pmatrix} = \Xi^e v.
$$

To show that it is in $\ker(\mathbf{K}^e)$, show that the corresponding product is zero:

$$\mathbf{K}^e \boldsymbol{v}_g = \Xi^e \mathbf{G}^e \left(\Xi^e\right)^T \Xi^e \boldsymbol{v} = \Xi^e \mathbf{G}^e \boldsymbol{v} = 0.$$

This proves that $\ker_{\mathrm{G}} \subseteq \ker(\mathbf{K}^e)$. However, due to the bijectivity of the transformations in (1.64) and $\ker_{\mathrm{L}} = \ker(\mathbf{G}^e)$, it follows that $\ker_{\mathrm{G}} = \ker(\mathbf{K}^e)$. $\qquad\square$

Kernel structure of contact part

In this section the results similar to those of the previous section are proved. Denote a single contact pair element of $\Gamma_Y^c(g_x, g_y)$ by c. The corresponding stiffness matrix $\mathbf{G}^c$ of c is similar to $\mathcal{P}_c$, the only difference is a coordinate transformation matrix: for (1.61) degrees of freedom are specified in the local coordinate systems of the elastic elements in contact, while for $\mathbf{G}^c$ degrees of freedom have to be specified in the coordinate system of the contact element. We have:

$$\begin{aligned}
\mathbf{G}^c &= \boldsymbol{T}_{fc}^T \boldsymbol{P}_{fc} \boldsymbol{T}_{fc} + \boldsymbol{T}_{Mc}^T \boldsymbol{P}_{Mc} \boldsymbol{T}_{Mc}, \\
\mathbf{K}^c &= \boldsymbol{Q}_{cg}^T (\boldsymbol{T}_{fc}^T \boldsymbol{P}_{fc} \boldsymbol{T}_{fc} + \boldsymbol{T}_{Mc}^T \boldsymbol{P}_{Mc} \boldsymbol{T}_{Mc}) \boldsymbol{Q}_{cg}, \\
\boldsymbol{Q}_{cg} &= \mathrm{diag}(\boldsymbol{C}_c^T, \boldsymbol{C}_c^T, \boldsymbol{C}_c^T, \boldsymbol{C}_c^T).
\end{aligned} \tag{1.65}$$

Further the following elementary representation of vector product will be helpful:

Lemma 4. *for any* $\boldsymbol{\omega} \in \mathbb{R}^3$, $\boldsymbol{r} \in \mathbb{R}^3$

$$\begin{pmatrix} 0 & -\omega_3 & \omega_2 \\ \omega_3 & 0 & -\omega_1 \\ -\omega_2 & \omega_1 & 0 \end{pmatrix} \begin{pmatrix} r_1 \\ r_2 \\ r_3 \end{pmatrix} = [\boldsymbol{\omega} \times \boldsymbol{r}] = \begin{pmatrix} 0 & r_3 & -r_2 \\ -r_3 & 0 & r_1 \\ r_2 & -r_1 & 0 \end{pmatrix} \begin{pmatrix} \omega_1 \\ \omega_2 \\ \omega_3 \end{pmatrix} \tag{1.66}$$

Lemma 5. *The* $\ker_{\mathrm{L}} = \ker(\mathbf{G}^c)$, $\ker_{\mathrm{G}} = \ker(\mathbf{K}^c)$ *where*

$$\ker_{\mathrm{L}} = \bigcup_{\substack{\boldsymbol{s} \in \mathbb{R}^3 \\ \boldsymbol{\theta} \in \mathbb{R}^3}} \begin{pmatrix} \boldsymbol{s} \\ \boldsymbol{\theta} \\ \boldsymbol{s} + \boldsymbol{W}(\boldsymbol{\theta})(\boldsymbol{r}_{1l} - \boldsymbol{r}_{2l}) \\ \boldsymbol{\theta} \end{pmatrix},$$

where $\boldsymbol{s}$ are spatial displacements and $\boldsymbol{\theta}$ are angular displacements, and $\boldsymbol{r}_{ig}$, $i = 1, 2$, are the

radius-vectors of the nodes of the elastic elements in contact in the contact coordinate system.

The kernel of $\mathbf{K}^c$ is given by

$$\ker_{\mathrm{G}} = \bigcup_{\substack{s \in \mathbb{R}^3 \\ \theta \in \mathbb{R}^3}} \begin{pmatrix} s \\ \theta \\ s + W(\theta)(r_{1g} - r_{2g}) \\ \theta \end{pmatrix}, \tag{1.67}$$

where r_{ig} are the radius-vectors the nodes of the elastic elements in contact in the global coordinate system.

Moreover

$$\det\left([\mathbf{G}^c]_{1:6,1:6}\right) > 0, \det\left([\mathbf{G}^c]_{7:12,7:12}\right) > 0, \det\left([\mathbf{K}^c]_{1:6,1:6}\right) > 0, \det\left([\mathbf{K}^c]_{7:12,7:12}\right) > 0. \tag{1.68}$$

Proof. It is obvious that $\mathbf{G}^c$ and $\mathbf{K}^c$ are positive-semidefinite matrices. Recall that for any positive-semidefinite $\boldsymbol{A}$, $\boldsymbol{v} \in \ker(\boldsymbol{A}) \Leftrightarrow \langle \boldsymbol{v}, \boldsymbol{A}\boldsymbol{v} \rangle = 0$. Further, note that both terms in (1.65) of $\mathbf{G}^c$ are positive-semidefinite. Therefore, $\boldsymbol{v} \in \ker(\mathbf{G}^c)$ iff $\langle \boldsymbol{v}, \boldsymbol{T}_{Mc}^T \boldsymbol{P}_{Mc} \boldsymbol{T}_{Mc} \boldsymbol{v} \rangle = 0$ and $\langle \boldsymbol{v}, \boldsymbol{T}_{fc}^T \boldsymbol{P}_{fc} \boldsymbol{T}_{fc} \boldsymbol{v} \rangle = 0$.

Observe that due to the structure of matrix $\boldsymbol{T}_{Mc}$, for any $\boldsymbol{s}, \boldsymbol{t}, \boldsymbol{\alpha}, \boldsymbol{\beta} \in \mathbb{R}^{3 \times 1}$ for the second term the following is true:

$$\begin{pmatrix} \boldsymbol{s}^T & \boldsymbol{\alpha}^T & \boldsymbol{t}^T & \boldsymbol{\beta}^T \end{pmatrix} \boldsymbol{T}_{Mc}^T \boldsymbol{P}_{Mc} \boldsymbol{T}_{Mc} \begin{pmatrix} \boldsymbol{s}^T & \boldsymbol{\alpha}^T & \boldsymbol{t}^T & \boldsymbol{\beta}^T \end{pmatrix}^T \equiv (\boldsymbol{\alpha} - \boldsymbol{\beta})^T \boldsymbol{P}_{Mc} (\boldsymbol{\alpha} - \boldsymbol{\beta}).$$

Since $\boldsymbol{P}_{Mc} > 0$, this implies the following: $\begin{pmatrix} \boldsymbol{s}^T & \boldsymbol{\alpha}^T & \boldsymbol{t}^T & \boldsymbol{\beta}^T \end{pmatrix} \in \ker(\mathbf{G}^c)$ if and only if $\boldsymbol{\alpha} = \boldsymbol{\beta}$, i.e. the angular components of the upper and the lower halves of $\boldsymbol{v}$ coincide. For such vectors the first term can be written as follows:

$$\begin{pmatrix} \boldsymbol{s}^T & \boldsymbol{\alpha}^T & \boldsymbol{t}^T & \boldsymbol{\alpha}^T \end{pmatrix} \boldsymbol{T}_{fc}^T \boldsymbol{P}_{fc} \boldsymbol{T}_{fc} \begin{pmatrix} \boldsymbol{s}^T & \boldsymbol{\alpha}^T & \boldsymbol{t}^T & \boldsymbol{\alpha}^T \end{pmatrix}^T \equiv$$
$$\equiv (\boldsymbol{s} - \boldsymbol{t} + (\boldsymbol{V}_1 - \boldsymbol{V}_2)\boldsymbol{\alpha})^T \boldsymbol{P}_{fc} (\boldsymbol{s} - \boldsymbol{t} + (\boldsymbol{V}_1 - \boldsymbol{V}_2)\boldsymbol{\alpha}).$$

Since $\boldsymbol{P}_{fc} > 0$, this is zero if and only if $\boldsymbol{t} = \boldsymbol{s} + (\boldsymbol{V}_1 - \boldsymbol{V}_2)\boldsymbol{\alpha}$. Recall that by the construction of $\boldsymbol{V}_1$ and $\boldsymbol{V}_2$, and by (1.66), one has $(\boldsymbol{V}_1 - \boldsymbol{V}_2)\boldsymbol{\alpha} = [\boldsymbol{\alpha} \times (\boldsymbol{r}_{1l} - \boldsymbol{r}_{2l})] = \boldsymbol{W}(\boldsymbol{\alpha})(\boldsymbol{r}_{1l} - \boldsymbol{r}_{2l})$. This proves $\ker(\mathbf{G}^c) = \ker_{\mathrm{L}}$. Proof of $\ker(\mathbf{K}^c) = \ker_{\mathrm{G}}$ can be obtained from $\ker(\mathbf{G}^c) = \ker_{\mathrm{L}}$

in exactly the same way as in Lemma 3.

To prove (1.68), let us compute the determinants explicitly:

$$\det\left([\mathbf{G}^c]_{1:6,1:6}\right) = \det\left([\mathbf{G}^c]_{7:12,7:12}\right) = \det\left([\mathbf{K}^c]_{1:6,1:6}\right) = \det\left([\mathbf{K}^c]_{7:12,7:12}\right) =$$
$$= \delta_c^{-1} G^2 G_N G_T^2 > 0.$$

$\square$

Solution structure for systems of elastic and contact elements

Lemma (3) and lemma (5) show that contact and elastic elements possess the same kernel structure. The twelve-by-one kernel vectors are obtained by the substitution of coordinates of the end nodes of the elements into some rigid displacements field

$$\mathfrak{R}_{\boldsymbol{s},\boldsymbol{\theta}}(\boldsymbol{x}) = \boldsymbol{s} + [\boldsymbol{\theta} \times \boldsymbol{x}] = \boldsymbol{s} + \boldsymbol{W}(\boldsymbol{\theta})\boldsymbol{x},$$

where $\boldsymbol{x}$ is a point in space and $\boldsymbol{s}$ and $\boldsymbol{\theta}$ are six parameters defining the rigid displacements field. In this section we prove that for a connected structure of elements the kernel of the corresponding stiffness matrix is obtained in the same way as for individual elements. The only difference is that instead of twelve-by-one vectors one has to deal with vectors having total number of nodes multiplied by six components. From now on, the exact type of an element (contact/elastic) will not be important. We will not distinguish between them and use just the term "element".

Under the term "system of elements" we understand any connected graph Γ, such that each edge of it is an element. Denote the set of nodes of Γ by N. For each node $n \in N$ its reference six-dimensional position $\left(\boldsymbol{x}_n^T \quad \boldsymbol{\alpha}_n^T\right)^T$, $\boldsymbol{x} \in \mathbb{R}^3$, $\boldsymbol{\alpha} \in \mathbb{R}^3$ is defined, and six-dimensional displacement $\boldsymbol{q}_n \in \mathbb{R}^6$ is to find from the statements of type (1.55). Denote the vector of all the degrees of freedom by $\boldsymbol{q}_{\text{tot}}$. In each statement of this section we specify boundary conditions explicitly, no other boundary conditions are implied.

The global stiffness matrix $\mathbf{K}^\Gamma$ for Γ is obtained from matrices $\mathbf{K}^c$ and $\mathbf{K}^e$ by the standard procedure used in FEM methods.

Lemma 6. *For any connected system of elements its kernel space* $\ker\left(\mathbf{K}^\Gamma\right)$ *is defined by*

$$\boldsymbol{q}_n = \begin{pmatrix} \boldsymbol{s} + \boldsymbol{W}(\boldsymbol{\theta})\boldsymbol{x}_n \\ \boldsymbol{\theta} \end{pmatrix}, \text{ for any } \boldsymbol{s} \in \mathbb{R}^3, \ \boldsymbol{\theta} \in \mathbb{R}^3. \qquad (1.69)$$

Proof. First note that for any element d, either plastic or elastic, (1.69) yields a vector from (1.63) or (1.67). Indeed, let n_1 and n_2 be the two nodes of d and consider displacement vector according to (1.69). By elementary transformations it can be transformed to the forms (1.63) and (1.67):

$$\begin{pmatrix} \boldsymbol{s} + \boldsymbol{W}(\boldsymbol{\theta})\boldsymbol{x}_{n_1} \\ \boldsymbol{\theta} \\ \boldsymbol{s} + \boldsymbol{W}(\boldsymbol{\theta})\boldsymbol{x}_{n_2} \\ \boldsymbol{\theta} \end{pmatrix} = \begin{pmatrix} \boldsymbol{s} + \boldsymbol{W}(\boldsymbol{\theta})\boldsymbol{x}_{n_1} \\ \boldsymbol{\theta} \\ \boldsymbol{s} + \boldsymbol{W}(\boldsymbol{\theta})\boldsymbol{x}_{n_1} + \boldsymbol{W}(\boldsymbol{\theta})(\boldsymbol{x}_{n_2} - \boldsymbol{x}_{n_1}) \\ \boldsymbol{\theta} \end{pmatrix} = \begin{pmatrix} \boldsymbol{s}' \\ \boldsymbol{\theta} \\ \boldsymbol{s}' + \boldsymbol{W}(\boldsymbol{\theta})(\boldsymbol{x}_{n_2} - \boldsymbol{x}_{n_1}) \\ \boldsymbol{\theta} \end{pmatrix}.$$

Note that for an elastic element $\boldsymbol{x}_{n_2} - \boldsymbol{x}_{n_1} = \pm \boldsymbol{C}^e \boldsymbol{l}$ and for a contact element $\boldsymbol{s}_{n_2} - \boldsymbol{x}_{n_1} = \pm(\boldsymbol{r}_{1g} - \boldsymbol{r}_{2g})$. Therefore, vectors of the form (1.69) belong to the kernels of single elements and thus are in $\ker\left(\mathbf{K}^\Gamma\right)$.

Show that matrix $\mathbf{K}^\Gamma$ has a non-degenerate submatrix of rank $6\,|N| - 6$. To prove this, consider a system of linear algebraic equations $\mathbf{K}^\Gamma \boldsymbol{v} = 0$. Since $\mathbf{K}^\Gamma$ and all its constituent matrices are positive-semidefinite, this implies that for any element d

$$\mathbf{K}^d \boldsymbol{v}_d = 0 \ \forall\, d, \qquad (1.70)$$

where $\boldsymbol{v}_d$ are twelve degrees of freedom of the nodes incident to d.

Fix all six degrees of freedom of any node $n \in N$. Consider set of all elements incident to n D_n. For each d let n_d be the second node of d which does not coincide with n. By Lemma 3 and Lemma 5, $\det\left(\left[\mathbf{G}^d\right]_{1:6,1:6}\right) = \det\left(\left[\mathbf{G}^d\right]_{7:12,7:12}\right) > 0$. But together with (1.70) this implies that for any d all degrees of freedom of n_d are uniquely defined from (1.70). We can repeat this reasoning for n_d and due to the connectedness of Γ this way we are able to prove that all degrees of freedom are uniquely defined. This implies that the system of equations $\mathbf{K}^\Gamma \boldsymbol{v} = 0$ is non-degenerate for any subset of variables not containing all degrees of freedom of some single node. But any such subsystem is of rank $6\,|N| - 6$.

Finally, since $\mathbf{K}^\Gamma$ contains a submatrix of rank $6\,|N| - 6$ and has size $6\,|N|$, its kernel can be at most of dimensionality six. Since the subspace defined by (1.69) has dimensionality

six, we conclude that it defines the whole $\ker\left(\mathbf{K}^{\Gamma}\right)$. $\square$

Corollary 5. *For any connected system of elements a problem of type* (1.55) *with any boundary conditions fixing all degrees of freedom in any single node possesses a unique solution.*

Consider a connected system of elements $\Gamma^{Y} \subseteq Y$ such that it is possible to prescribe periodic boundary conditions with respect to the periodicity cell Y. Moreover, assume that Γ^{Y} has at least one node at each face of Y. For simplicity we assume that Y is a unit cube.

Lemma 7. *All vectors from* (1.69) *satisfying periodicity conditions for* Γ_{Y} *have zero rotational part, i.e. if v is a vector of all nodal displacements and there exist $s \in \mathbb{R}^{3}$, $\boldsymbol{\theta} \in \mathbb{R}^{3}$ such that for each n*

$$q_n = \begin{pmatrix} s + W(\boldsymbol{\theta})x_n \\ \boldsymbol{\theta} \end{pmatrix},$$

then $\boldsymbol{\theta} = 0$. In other words, all vectors from (1.69) *satisfying periodicity conditions for Γ^{Y} are spatial shifts.*

Proof. By the assumptions on Γ^{Y}, there exist three pairs of nodes (n_{x-}, n_{x+}), (n_{y-}, n_{y+}) and (n_{z-}, n_{z+}) such that

$$x_{x+} = x_{x-} + \begin{pmatrix} 1 \\ 0 \\ 0 \end{pmatrix}, \ \ x_{y+} = x_{y-} + \begin{pmatrix} 0 \\ 1 \\ 0 \end{pmatrix}, \ \ x_{z+} = x_{z-} + \begin{pmatrix} 0 \\ 0 \\ 1 \end{pmatrix}.$$

Periodic boundary conditions imply that $q_{x-} = q_{x+}$, $q_{y-} = q_{y+}$ and $q_{z-} = q_{z+}$. By the substitution of (1.69) in these three conditions we arrive at

$$W(\boldsymbol{\theta}) \begin{pmatrix} 1 \\ 0 \\ 0 \end{pmatrix} = \begin{pmatrix} 0 \\ \theta_3 \\ -\theta_2 \end{pmatrix} = \begin{pmatrix} 0 \\ 0 \\ 0 \end{pmatrix}, \ W(\boldsymbol{\theta}) \begin{pmatrix} 0 \\ 1 \\ 0 \end{pmatrix} = \begin{pmatrix} -\theta_3 \\ 0 \\ \theta_1 \end{pmatrix} = \begin{pmatrix} 0 \\ 0 \\ 0 \end{pmatrix},$$

$$W(\boldsymbol{\theta}) \begin{pmatrix} 0 \\ 0 \\ 1 \end{pmatrix} = \begin{pmatrix} \theta_2 \\ -\theta_1 \\ 0 \end{pmatrix} = \begin{pmatrix} 0 \\ 0 \\ 0 \end{pmatrix}.$$

It follows that $\boldsymbol{\theta} = \mathbf{0}$. $\square$

Remark 14. Note that for the statement of Lemma 7 to be true it is enough to require that Γ^Y has at least one node at each face from any set of two non-coincident pairs of the opposite faces of Y.

Corollary 6. *A problem of type* (1.55) *with periodical boundary conditions and all spatial displacement components defined at certain node of* Γ^Y *possesses a unique solution.*

Corollary 7. *Assume that the coordinate transformation matrices* $\boldsymbol{C}^e$ *are continuously differentiable with respect to* $\boldsymbol{g}$. *Then*

$$\widehat{A}_{ijkl}^{\mathrm{hom}}(\boldsymbol{g}) \in C^1(U_{\boldsymbol{g}}).$$

Proof. From differentiability of the coordinate transformation matrices we immediately obtain the differentiability of the stiffness matrices. Further, by Corollary 6, the solutions to the cell problems are the solutions of some linear systems of equations, with the systems' matrices non-degenerate uniformly in $\boldsymbol{g} \in U_{\boldsymbol{g}}$ and continuously differentiable with respect to $\boldsymbol{g}$. It follows that the solutions of the cell problems are themselves continuously differentiable with respect to $\boldsymbol{g}$. Finally, $\widehat{A}_{ijkl}^{\mathrm{hom}}(\boldsymbol{g})$ are differentiable as products of continuously differentiable functions. $\square$

Derivatives of the solution and the homogenized tensor

The crucial point is that beam approximations reduce the cell problems to systems of linear algebraic equations with uniformly non-degenerate matrix depending in some non-linear manner on $\boldsymbol{g}$. This allows us not only to benefit from the problem's simplicity, but also to obtain the derivatives of the solution with respect to $\boldsymbol{g}$, which are necessary to obtain $\delta_{\boldsymbol{g}} \widehat{\boldsymbol{A}}_{\boldsymbol{g}}^{\mathrm{inp}}$. We achieve this with automatic symbolic differentiation of the FEM system of equations.

Assume that the conditions of Corollary 7 hold. Derive the algorithm to obtain derivatives of the effective tensor given by (1.22) with respect to design parameters $\boldsymbol{g}$.

Note that the right-hand sides of beam equations (1.56) are zeros, and thus the FEM procedure with Lagrangian polynomials yields the exact solution of the beam structure problem. It follows that solutions of the cell problems are polynomials parametrized by the

solution $\boldsymbol{w}_{ij}^{\mathrm{FEM}}(\boldsymbol{g})$ of the corresponding FEM system

$$\boldsymbol{K}_{ij}(\boldsymbol{g})\boldsymbol{w}_{ij}^{\mathrm{FEM}}(\boldsymbol{g}) = \boldsymbol{f}_{ij}^{\mathrm{FEM}}(\boldsymbol{g}). \tag{1.71}$$

This system holds for all values of $\boldsymbol{g}$. Hence we can apply the increment operator $\delta_{\boldsymbol{g}}$ to it and arrive at

$$\delta_{\boldsymbol{g}}\boldsymbol{K}_{ij}(\boldsymbol{g})\boldsymbol{w}_{ij}^{\mathrm{FEM}}(\boldsymbol{g}) + \boldsymbol{K}_{ij}(\boldsymbol{g})\delta_{\boldsymbol{g}}\boldsymbol{w}_{ij}^{\mathrm{FEM}}(\boldsymbol{g}) = \delta_{\boldsymbol{g}}\boldsymbol{f}_{ij}^{\mathrm{FEM}}(\boldsymbol{g}). \tag{1.72}$$

Matrices $\boldsymbol{K}_{ij}(\boldsymbol{g})$ are non-linear but explicitly known functions of $\boldsymbol{g}$. Therefore, it is possible to compose $\boldsymbol{K}_{ij}$ symbolically and obtain $\delta_{\boldsymbol{g}}\boldsymbol{K}_{ij}(\boldsymbol{g})$ using symbolic differentiation. The same can be done with the right-hand side $\boldsymbol{f}_{ij}^{\mathrm{FEM}}(\boldsymbol{g})$ to obtain $\delta_{\boldsymbol{g}}\boldsymbol{f}_{ij}^{\mathrm{FEM}}(\boldsymbol{g})$. However, it is very difficult to solve system (1.71) symbolically and then find $\boldsymbol{w}_{ij}^{\mathrm{FEM}}$ by symbolic differentiation.

We overcome this obstacle using (1.72). Rewrite it as a linear system with respect to $\delta_{\boldsymbol{g}}\boldsymbol{w}_{ij}^{\mathrm{FEM}}(b\boldsymbol{g})$:

$$\boldsymbol{K}_{ij}(\boldsymbol{g})\delta_{\boldsymbol{g}}\boldsymbol{w}_{ij}^{\mathrm{FEM}}(\boldsymbol{g}) = \delta_{\boldsymbol{g}}\boldsymbol{f}_{ij}^{\mathrm{FEM}}(\boldsymbol{g}) - \delta_{\boldsymbol{g}}\boldsymbol{K}_{ij}(\boldsymbol{g})\boldsymbol{w}_{ij}^{\mathrm{FEM}}(\boldsymbol{g}). \tag{1.73}$$

Note that if $\boldsymbol{w}_{ij}^{\mathrm{FEM}}(\boldsymbol{g})$ is found numerically from (1.71), then all terms on the right-hand side of (1.73) are known and it can be solved numerically to find $\delta_{\boldsymbol{g}}\boldsymbol{w}_{ij}^{\mathrm{FEM}}$ numerically. This way we can find the derivatives of the cell problems' solutions for beams for any fixed $\boldsymbol{g}$.

To obtain the derivatives of the homogenized tensor, observe that since the FEM procedure yields exact solutions of the cell problems, expressions (1.22) for the entries of the homogenized tensor can be computed symbolically with respect to $\boldsymbol{w}_{ij}^{\mathrm{FEM}}(\boldsymbol{g})$ and $\boldsymbol{g}$. Denote the symbolic expressions obtained as $\widehat{\boldsymbol{A}}_{\mathrm{sym}}^{\mathrm{inp}}$. Therefore, by the chain rule it is possible to obtain increments of the homogenized tensor:

$$\delta_{\boldsymbol{g}}\widehat{\boldsymbol{A}}_{\boldsymbol{g}}^{\mathrm{inp}}(\boldsymbol{g}) = \delta_{\boldsymbol{g}}\widehat{\boldsymbol{A}}_{\mathrm{sym}}^{\mathrm{inp}}(\boldsymbol{w}_{ij}^{\mathrm{FEM}}(\boldsymbol{g}),\boldsymbol{g}) = \delta_{\boldsymbol{w}}\widehat{\boldsymbol{A}}_{\mathrm{sym}}^{\mathrm{inp}}\delta_{\boldsymbol{g}}\boldsymbol{w}_{ij}^{\mathrm{FEM}}(\boldsymbol{g}) + \delta_{\boldsymbol{g}}\widehat{\boldsymbol{A}}_{\mathrm{sym}}^{\mathrm{inp}} \tag{1.74}$$

and evaluate the expressions obtained for any fixed value of $\boldsymbol{g}$.

1.7   Summary of the optimization algorithm

A single step of a gradient-type method for the effective stress profile optimization problem is presented in Figure 1.5. Assume that approximation $\boldsymbol{g}_n$ is available. From $\boldsymbol{g}_n$ we get the
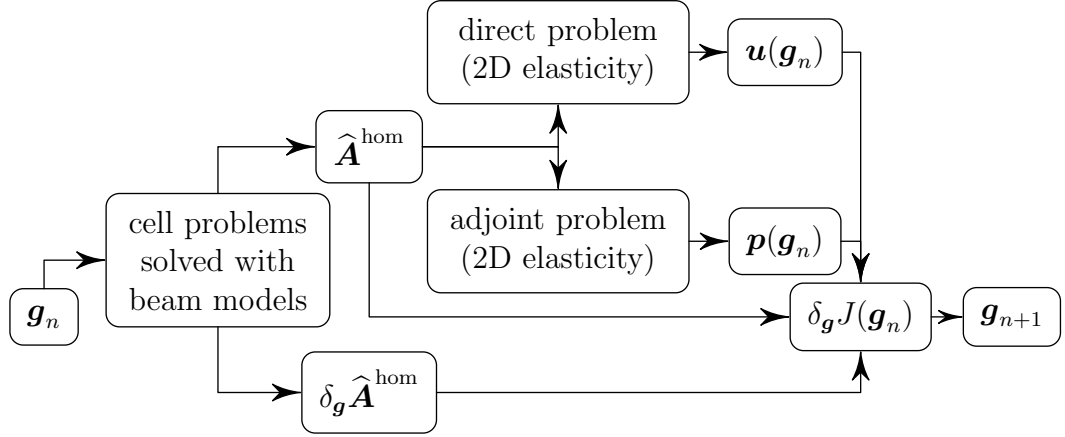
Figure 1.5: A brief scheme of the stress profile optimization algorithm

homogenized properties with help of beam the models. Then we plug the obtained tensor into the direct and adjoint problems, which are of 2D elasticity type. Form these problems we obtain state $\boldsymbol{u}(\boldsymbol{g}_n)$ and adjoint state $\boldsymbol{p}(\boldsymbol{g}_n)$, which are used to get the gradient of the objective functional. Finally, the gradient is used to compute the next approximation of the optimal solution $\boldsymbol{g}_{n+1}$. The loop is repeated until some convergence criteria is met.

1.8 Numerical examples.

In the examples presented below we use a rubber-like material with Young's modulus $E = 1.5 \cdot 10^7 \mathrm{Pa}$ and Poisson's ratio $\nu = 0.49$ (we cannot use the ideally incompressible value 0.5 due to non-invertibility of Hooke's law, we take 0.49 as an approximation), see Chapter 1 in [28]. The horizontal period ε_0 of the fabric is $1.91 \mathrm{mm}$, i.e. $1.91 \cdot 10^{-3} \mathrm{m}$. We use value $3 \cdot 10^8$ for the normal penetration coefficient δ_c^{-1} and $3 \cdot 10^3$ for the tangential penetration coefficient G. Angular penalization coefficients are chosen according to the following rule: $G_1 = 375$, $G_2 = G_3 = 1.875 \cdot 10^7$, all penalization coefficients are given in SI unit system.

Examples of the homogenized structures can be seen in Figures 1.6–1.7. The stress tensor is given in $\mathrm{N/m}$, the proper unit for stress tensors in two dimensions. The displacement field and local longitudinal stresses for cell problems are presented in Figure 1.8. We do not provide scale and legend for this figure because the color scales are local and different for each single element.

Out of six independent components of the in-plane elasticity tensor, two were always
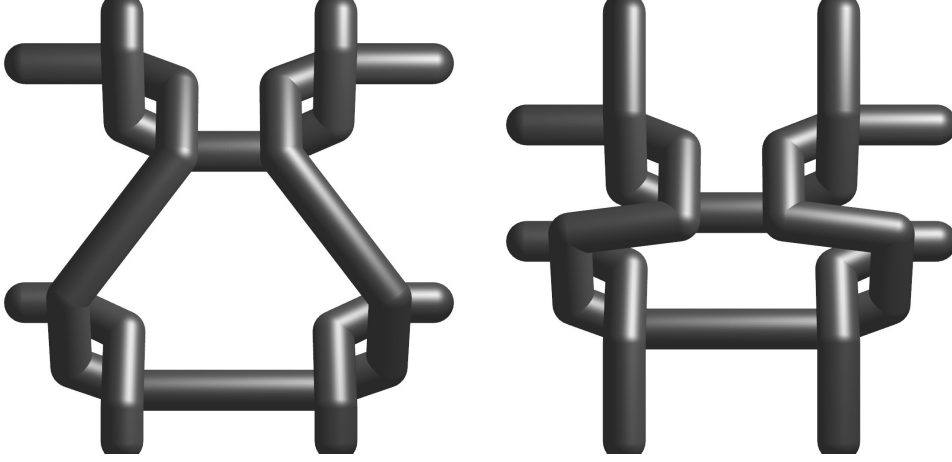
$$\begin{pmatrix} 3.68 \cdot 10^2 & 0 & 0 & 0.20 \cdot 10^2 \\ 0 & 3.02 \cdot 10^2 & 0.20 \cdot 10^2 & 0 \\ 0 & 0.20 \cdot 10^2 & 3.02 \cdot 10^2 & 0 \\ 0.20 \cdot 10^2 & 0 & 0 & 3.04 \cdot 10^2 \end{pmatrix}, \begin{pmatrix} 1.84 \cdot 10^2 & 0 & 0 & 0.14 \cdot 10^2 \\ 0 & 1.35 \cdot 10^2 & 0.14 \cdot 10^2 & 0 \\ 0 & 0.14 \cdot 10^2 & 1.35 \cdot 10^2 & 0 \\ 0.14 \cdot 10^2 & 0 & 0 & 1.59 \cdot 10^2 \end{pmatrix}$$

Figure 1.6: Geometry and homogenized tensor for $x = 0.5$, $y = 0.5$ and $x = 0.5$, $y = 0.8$.

zeros. This is not uncommon for the homogenized elasticity tensor, since it is proven that if the periodicity cell has some symmetry properties, then certain entries of the homogenized tensor will be zeros, see Chapter 6 of [5]. The other four components are shown in Figure 1.9.

Out of these four components, A_{1111}^{inp}, A_{1122}^{inp}, and A_{2222}^{inp} are very much alike in the shape, but the difference in the magnitude is up to 20%. In our stress profile optimization example, we optimize specifically for the xx component of the stress. In such a setting, the major role is played by the component A_{1111}^{inp}. It is maximal for $\boldsymbol{g}^{\mathrm{max}} \approx (0.723, 0.8)$, $A_{1111\,\mathrm{max}}^{\mathrm{inp}} \approx 421.613$, and is minimal for $\boldsymbol{g}^{\mathrm{min}} \approx (0.4, 0.8)$, $A_{1111\,\mathrm{min}}^{\mathrm{inp}} \approx 132.081$. These values will be helpful during the analysis of the results of the profile optimization problem, where at the areas of high desired stress, the local geometries close to $\boldsymbol{g}^{\mathrm{max}}$ are expected, and at the areas of low desired stress, the local geometries close to $\boldsymbol{g}_{\mathrm{min}}$ are expected. We will also use these values as initial approximations for our optimization procedure. Another useful conclusion to draw from the figure is that the optimization problems involving $\boldsymbol{A}^{\mathrm{inp}}$ are essentially non-convex, but it is likely that gradient-type methods will wander in valleys on the left and on the right of the maximal hill clearly visible in the figure.
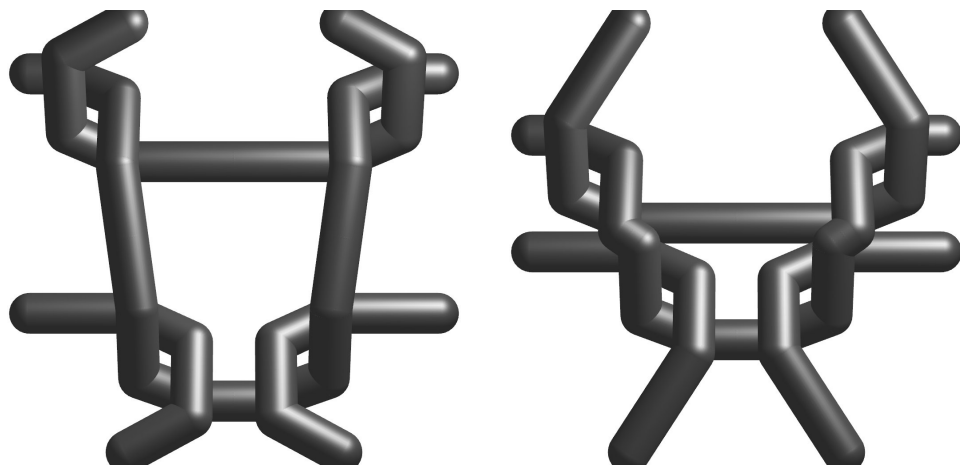
$$\begin{pmatrix} 2.31 \cdot 10^2 & 0 & 0 & 0.20 \cdot 10^2 \\ 0 & 1.69 \cdot 10^2 & 0.20 \cdot 10^2 & 0 \\ 0 & 0.20 \cdot 10^2 & 1.69 \cdot 10^2 & 0 \\ 0.20 \cdot 10^2 & 0 & 0 & 1.80 \cdot 10^2 \end{pmatrix}, \begin{pmatrix} 3.87 \cdot 10^2 & 0 & 0 & 0.22 \cdot 10^2 \\ 0 & 3.07 \cdot 10^2 & 0.22 \cdot 10^2 & 0 \\ 0 & 0.22 \cdot 10^2 & 3.07 \cdot 10^2 & 0 \\ 0.22 \cdot 10^2 & 0 & 0 & 2.97 \cdot 10^2 \end{pmatrix}$$

Figure 1.7: Geometry and homogenized tensor for $x = 0.8$, $y = 0.5$ and $x = 0.8$, $y = 0.8$.
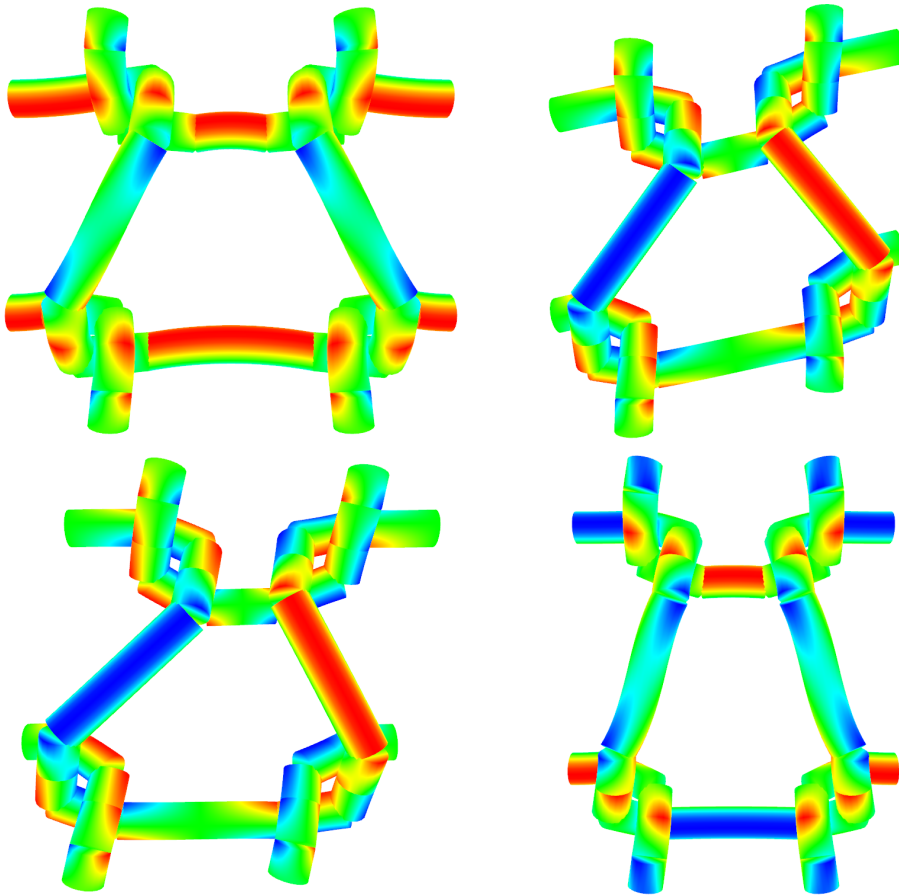
Figure 1.8: Cell problems for geometry parameters $x = 0.5$, $y = 0.5$ (for the boundary conditions multiplied by 0.2, cell problems correspond to 1).

A_{1111}^{inp}

A_{1122}^{inp}

A_{1212}^{inp}

A_{2222}^{inp}
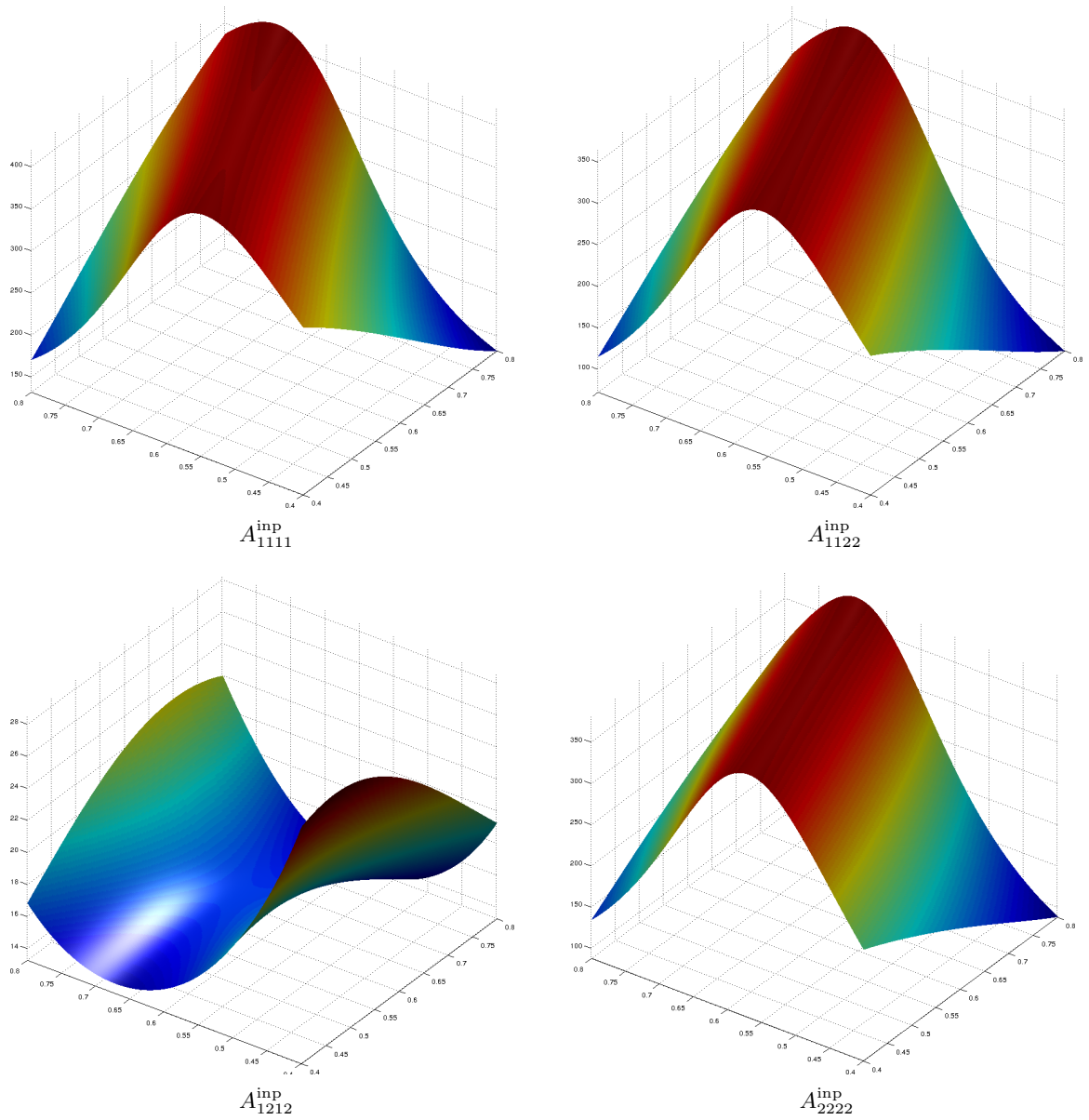
Figure 1.9: Components of the homogenized in-plane tensor as functions of the geometrical parameters.

1.8.1   Poisson's ratio optimization.
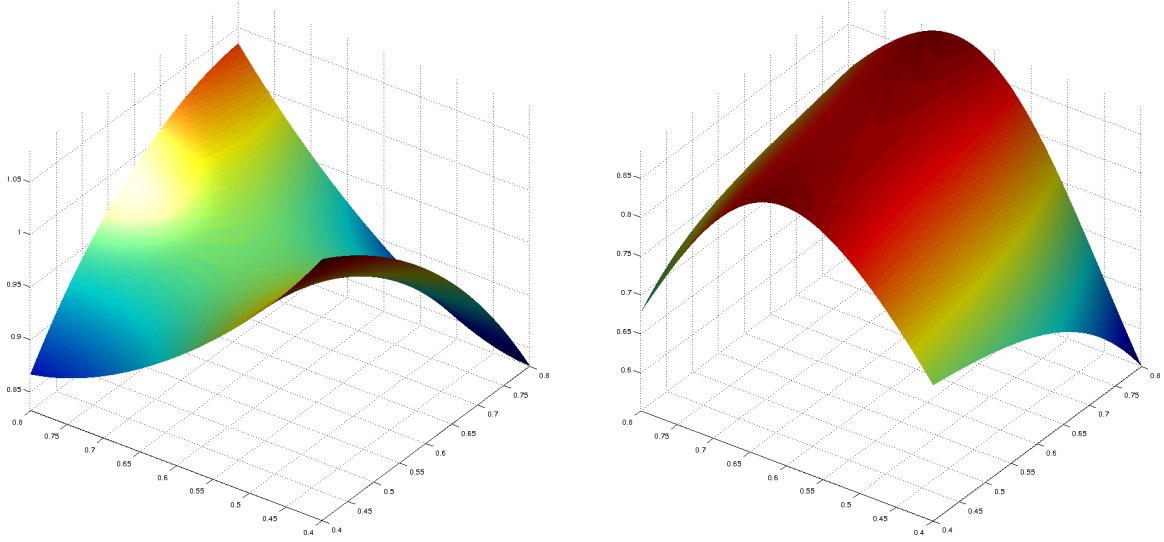
Figure 1.10: Poisson's ratios for horizontal shrinking during vertical stretching (on the left) and vertical shrinking during horizontal stretching (on the right).

Due to the simplicity of the Poisson's ratio optimization problem, we do not provide the details on numerics. Because it is controlled just by two geometrical parameters, Poisson's ratio can be conveniently plotted. This is done in Figure 1.10.

The extremal values and geometries are:

$$\begin{aligned}
\nu_{12}^{\min} &= 0.832, & \boldsymbol{g}_{12\,\min} &= (0.4, 0.8), \\
\nu_{12}^{\max} &= 1.081, & \boldsymbol{g}_{12\,\max} &= (0.4, 0.4), \\
\nu_{21}^{\min} &= 0.552, & \boldsymbol{g}_{21\,\min} &= (0.4, 0.8), \\
\nu_{21}^{\max} &= 0.887, & \boldsymbol{g}_{21\,\max} &= (0.657, 0.8).
\end{aligned}$$

1.8.2   Stress profile optimization

Consider the following optimization problem: find such periodic structure of type described in Section 1.2 that the functional 1.47 is minimized, whereby in the matrix $\boldsymbol{N}$ a single component is one and the others are small, i.e. $N_{1111} = 1$, $N_{ijkl} = 10^{-10}$ for $(i, j, k, l) \neq (1, 1, 1, 1)$. This way we express that only xx-component of the effective stress is important, which is the case in the compression stocking application.
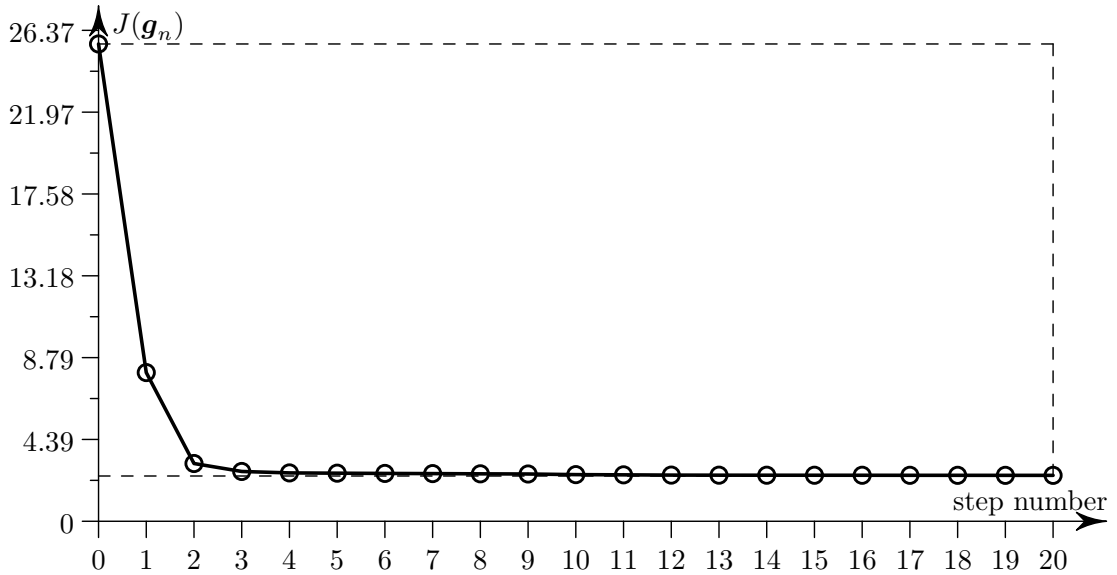
Figure 1.11: The decay of the objective functional.

The macroscopic geometry Ω in this example is a rectangle of width 0.2m and height 0.8 meter. Its top and bottom sides are load-free, and at the lateral sides Dirichlet conditions are applied: $u_1 = -0.05$m at the left side, $u_1 = 0.05$m at the right side and at both sides $u_2 = 0$, i.e. the specimen is stretched in the horizontal direction, and our goal is to reach the xx-stress profile as close to the desired one as possible.

We use 40-points grid in the vertical direction to define piecewise-affine functions g, which are assumed to be constant along the horizontal direction, i.e. we deal with 80-dimensional non-convex optimization problem. We compose, solve and differentiate the cell problems with help of Symbolic Toolbox of MATLAB® according to the algorithms described in Section 1.6.6. In our case the global stiffness matrix has dimensions 320×320, and the linear system for the cell problems is slightly smaller. After we compute the homogenized coefficients, the direct and adjoint 2D elasticity problems have to be solved. We solve them with the help of FreeFem++, see [21].

We use standard projected gradient algorithm as an optimization method (see Section 2.2.2 in [22] or Section 1.5 in [7] and the bibliography therein). If our design variables get outside of the box $[0.4; 0.8] \times [0.4; 0.8]$, we return them using trivial projection routine. For the stepsize rule, we use the following one-dimentional inexact optimization routine: we first compute the functional at 20-points grid on the segment $[0; 2]$, find the minima
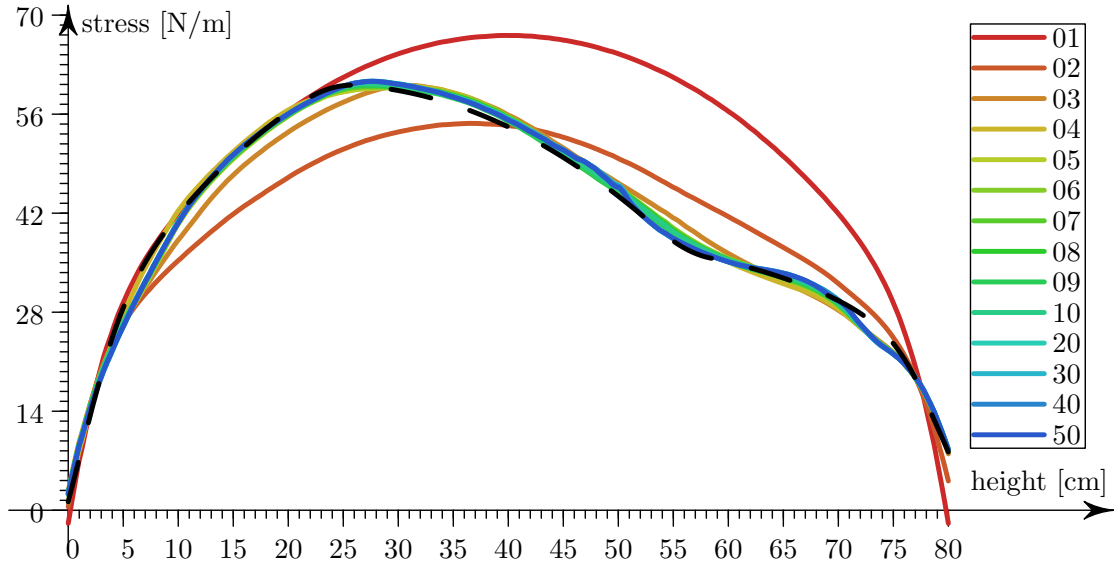
Figure 1.12: Evolution of the stress profile along the center line of the textile. The dashed curve represents the target profile. The legend indicates the optimization algorithm's step number, for which the profile is shown.

and then improve it recursively. Note that though each evaluation requires a solution of a 2-dimensional PDE, this step can be easily parallelized. In any case, we can expect at most linear convergence rate of the algorithm. We stop the algorithm either when the decay of the functional is small or when the change in the design variables is small.

The evolution of the pressure profile is shown in Figure 1.12. The major change is visible at the initial steps, and, as clearly visible form Figure 1.12, the functional decay greatly slows down from a certain step and is even non-monotone. There are two sources for this inefficiency: the first one comes from the error of the numerical scheme for solution of PDEs, and the second is the non-convexity of the functional. In any case, we see that the stress profile approaches the desired one and that the design, shown in Figure 1.13, meets the expectation that it should approach to the more stiff designs where the higher stress is required. One should also keep in mind that the xx stress profile of the textile is not uniform with respect to x, and the closeness of the profile curves to the desired one at the right and left edges of the textile may require a design different from the design we would expect in the middle, this is especially true in the vicinity of the Dirichlet boundary.

(a) the initial approxima- (b) after the 3rd step   (c) after the 10th step   (d) the final design
tion
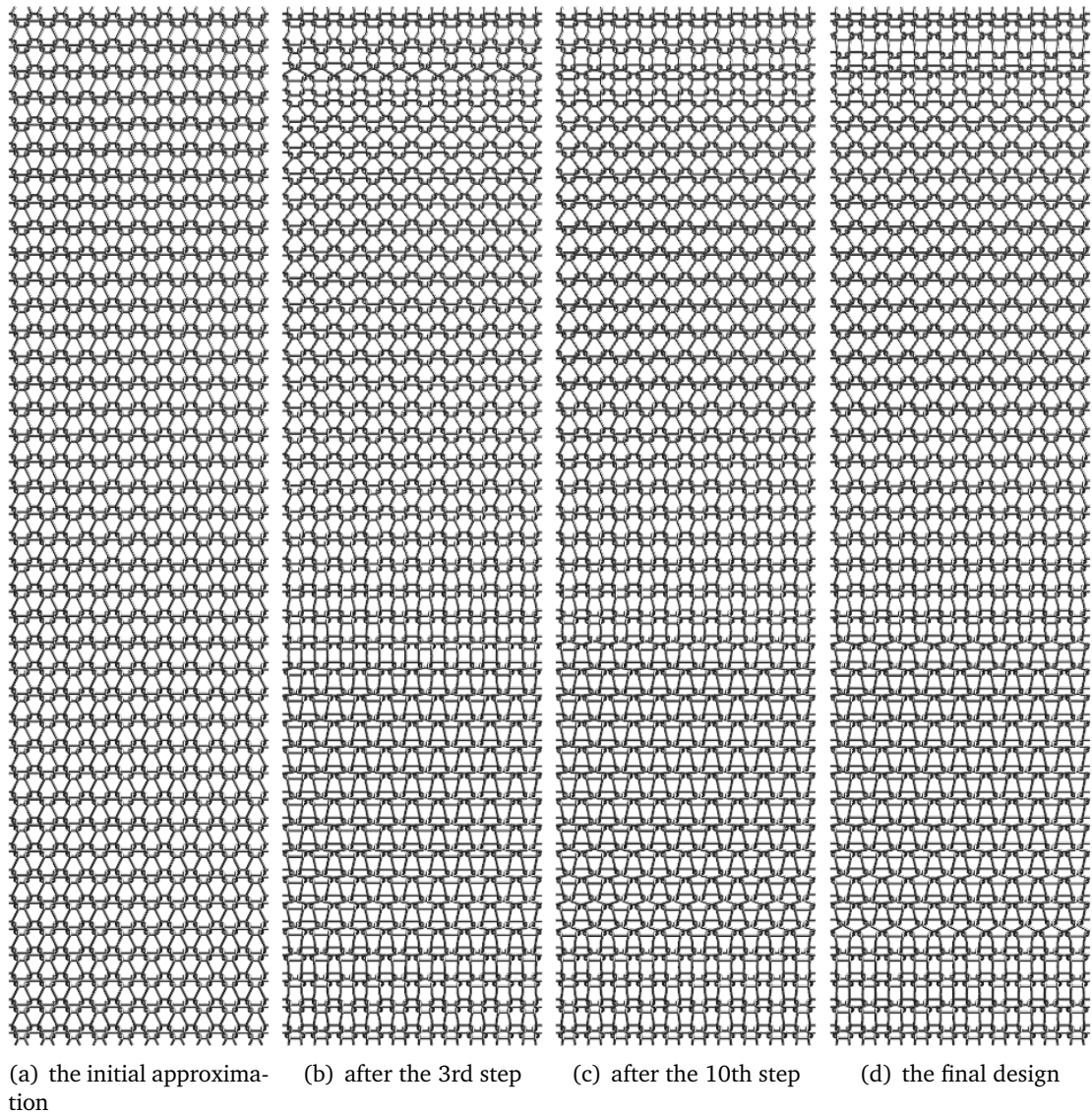
Figure 1.13: Evolution of the design of the textile.

Chapter 2

One-dimensional computational model for hyperelastic string structures with Coulomb friction

2.1 Introduction

Due to the difference in size between thickness of yarns, dimensions of knitting patterns, and macroscopic size of textile products, textiles are generally multi-scale structures. This scale difference causes numerical difficulties for a direct numerical treatment. Therefore, various techniques are required to handle such problems.

The description of major state of the art techniques in mechanical modeling of textiles is provided in [45]. These techniques usually combine two approaches: a direct computation of geometries resolving individual yarns and modeling of textiles as deformable homogeneous shells.

The major difficulties of the approach with modeling of individual yarns are strong non-linearities and the algorithmic complexity associated with modeling of contact phenomenon in large deformation setting. There is vast mechanical literature available on this topic, see, e.g. [49, 47, 26]. State of the art works in simulations of textiles at the level of single threads with massive contact are papers [17, 16].

Modeling of textiles as continua implies development of various hyperelastic models, since large deformations and complicated non-linear constitutive laws must be considered.

Advancement in this direction can be found, among others, in [9].

A common mathematical model for problems with friction is variational inequality with a non-smooth term. Examples of state-of-the-art works in the direction of numerical methods with superlinear convergence rates for non-smooth problems are [46, 41].

Our aim in this chapter is to develop a model and a fast numerical approach, which can be used for design of textiles, i.e. for simulation of the behaviour of textiles on the basis of their knitting pattern and yarn's properties in real time. In this chapter we are concerned with knitted textiles with large stretching deformations, for which bending behavior is not important. Since we have textile design assistance in mind, the model must meet the following requirements:

- arbitrary physically reasonable force-stretch curves of the constituent fibers should be supported;

- large strains, large displacements, and Coulomb friction should be handled adequately;

- various knitting patterns should be supported without construction of complicated meshes;

- an implementation capable to run in time of several minutes for meshes modeling textiles of size of several centimeters on modern desktop machines should be possible.

To meet the last three requirements, a simplified geometrical model is considered: we represent textiles by graphs, where chains of edges represent fibers and some of the nodes represent contact spots. The detailed description of the geometrical model opens Section 2.2. The crucial point here is that we assume that contact interfaces are single points that do not disappear, but can move with respect to the initial configuration of the system. This brings a huge gain in performance in comparison with conventional approaches to contact problems, where complicated geometrical algorithms associated with large displacement contact problems have to be used.

Further in Section 2.2 we describe the 1D hyperelasticity model. It is similar to the model described in [1, 43]. We use its reformulation for the arbitrary force-stretch curves, which are more relevant for fibers. This way we deal with the requirement about arbitrary physically reasonable force-stretch curves. Under "physically reasonable" force-stretch curves we understand piecewise continuously differentiable and monotone continuous curves. Since this is usually observed in measurements, the measured curves can be

interpolated by splines and then plugged directly in our model with no additional model fitting.

After the description of the hyperelasticity model we explain our friction model. We extend the Capstan equation, also known as Euler-Eytelwein formula, to the case of extensible fibers. This way, we obtain conditions in contact points between fibers from Coulomb friction model. The Capstan equation is widely used for measurements of frictional properties of fibers, see [20].

Section 2.2 is concluded with the mathematical problem statement for the whole model. We use the nonlinear evolution equations formulation and later prove its equivalence to the energetic solutions concept. This mathematical model is used for various models with rate-independent dissipation, see [30, 31]. Application of Capstan equation with the reformulated 1D hyperelastic model to simulation of textiles is novel.

In Section 2.3 we prove that our elastic energy is convex and the dissipation potential is convex and also positively homogeneous of degree one. We show that the model yields degenerate Jacobian matrices and consider a regularized model along with the original one. Later in this section we elaborate on the continuity of the solutions. It is observed that the continuity of the solutions to evolution equations is tightly bound to the relation between the strict convexity constant of the elastic energy and the Lipschitz constant of the dissipation potential, see [29]. We conclude Section 2.3 with time-discrete problems suitable for numerical treatment.

The numerical algorithm is described in Section 2.4. We apply classic regularization technique for the non-smooth frictional term and solve the resulting smooth problems with Newton-Raphson method. An analysis of convergence of our numerical scheme is not provided. and due to the regularization, the algorithm is likely to be suboptimal in comparison to the state-of-the art techniques for non-smooth problems described, e.g. in [46, 41]. However, application of these techniques requires non-trivial derivation of the tangent operators. Since our algorithm performs well enough for our examples, we do not seek for the optimal convergence rate, but believe that it can be improved.

The part concludes with section 2.5, where numerical results and a comparison with an experimental measurement are presented.

2.2 Problem Statement

2.2.1 Description of geometrical model

Fabrics are approximated by weighted graphs of geometries similar to the one in Figure 2.1. Denote such a graph by Γ. Fibers are represented by chains of straight one-dimensional segments (elements), which are edges of Γ. The contact points between fibers form a subset of nodes set of Γ.

Introduce rigorous notation. The textile consists of fibers F_i. Each fiber F_i consists of elements e_i^j. Fibers are disjoint sets. Each element e_i^j is defined by two nodes $n_{i,j}^l$ and $n_{i,j}^r$, an undeformed length parameter L_i^j, an undeformed initial length parameter $\mathcal{L}_i^j$, a current length $l_i^j = |\boldsymbol{x}\left(n_{i,j}^r\right) - \boldsymbol{x}\left(n_{i,j}^l\right)|$ (the symbol $\boldsymbol{x}$ is introduced below), and material properties described in Section 2.2.2. The set of all nodes of Γ is denoted by N. For each node $n \in N$, $\boldsymbol{X}(n) \in \mathbb{R}^3$ is the reference position of n. Denote the vector of all undeformed lengths L_i^j by $\mathbf{L}$. Let E be the union of all elements e_i^j. The set of common points between two different fibers F_i and F_j is denoted $N_c^{i,j}$. It represents contact points between F_i and F_j. It is required that $N_c^{i,j} \subseteq N$ for all i and j. We call a node contact if it corresponds to a contact point between some two fibers. Denote the union of all contact nodes by $S_C = \cup_{i,j} N_c^{i,j}$. The set of contact nodes of a single fiber F_i is denoted by N_i^c.

For each node n define the displacement field $\mathbf{u}(n) = \boldsymbol{x}(n) - \boldsymbol{X}(n)$, where $\boldsymbol{x}(n)$ is the position of the node in the current configuration. For each point of element e_i^j, the displacement field is interpolated by an affine function between the corresponding nodes $n_{i,j}^l$ and $n_{i,j}^r$.
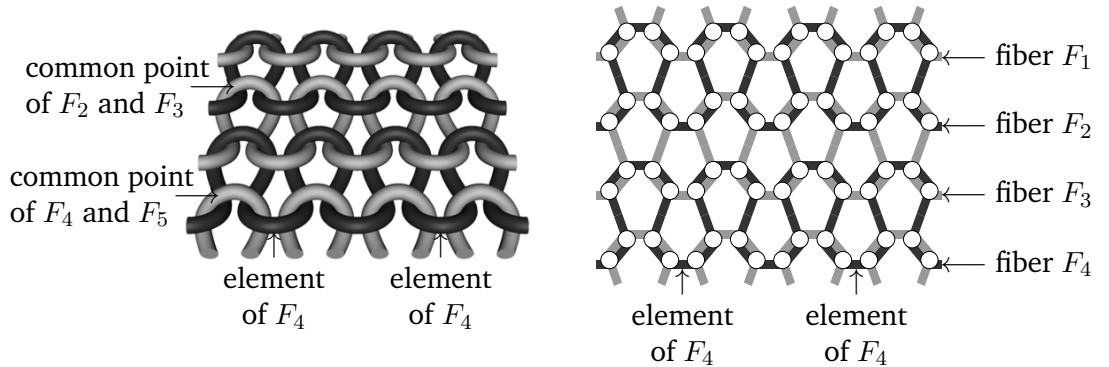
Figure 2.1: Knitted fabric and its 1D graph model

2.2.2   Description of elasticity model

For the modeling of a single element a hyperelastic material is considered, see [10, 48]. In the one-dimensional case the elasticity model is defined by an elastic energy density function $W(\mathbf{u}')$, where $\mathbf{u}'$ is the derivative of the displacement field with respect to the longitudinal coordinate of the element in the reference configuration x_1 (i.e. convective longitudinal coordinate),

$$W(\mathbf{u}') = \frac{1}{A} \int_0^\varepsilon \tilde{f}(\bar{\varepsilon})\, d\bar{\varepsilon}, \text{ where } \varepsilon = \sqrt{\left[1 + \frac{\partial u_1}{\partial x_1}\right]^2 + \left[\frac{\partial u_2}{\partial x_1}\right]^2 + \left[\frac{\partial u_3}{\partial x_1}\right]^2} - 1$$

is the nonlinear principal longitudinal strain, A is the undeformed cross-sectional area of the element, and $\tilde{f}(\varepsilon)$ is the force-strain curve of the element, which satisfies the following properties:

Assumption 6 (on the force functions for convexity and convergence)**.**

$$\begin{aligned}
&\tilde{f}(x) \text{ is strictly increasing for } x > 0, \\
&\tilde{f}(x) = 0 \text{ for } x \leq 0, \\
&\tilde{f}(x) \text{ is a piecewise continuously differentiable continuous function.}
\end{aligned} \qquad (2.1)$$

The total strain energy $U(\mathbf{u}')$ of an element e is thus given by

$$U(\mathbf{u}') = \int_e W(\mathbf{u}')\, dx_1 = L \int_0^\varepsilon \tilde{f}(\bar{\varepsilon})\, d\bar{\varepsilon} = L \int_1^\lambda f(\bar{\lambda})\, d\bar{\lambda}, \qquad (2.2)$$

where $\lambda(\mathbf{u}') = l(\mathbf{u})/L = 1 + \varepsilon(\mathbf{u}')$ is the principal stretch of the element, $f(\lambda) = \tilde{f}(\varepsilon)$, L is the undeformed length of the element, $l(\mathbf{u})$ is the length of the element in the current configuration, which is a function of the displacement field and the initial position of the element. Note that if an element is compressed, then its elastic energy is zero due to the second force function property. See [1] for the derivation of a similar 1D model from conventional 3D hyperelasticity model.

2.2.3   Description of friction model

A common mathematical model for the equilibrium problem of elasticity with friction is variational inequality. If U is the elastic energy and j is the work of friction forces, then the

problem is stated as follows (see [24, 18]):

$$\text{find } \mathbf{w} \in \mathcal{K}: \quad U(\mathbf{w}) + j(\mathbf{w}) \leq U(\mathbf{v}) + j(\mathbf{v}), \quad \forall \mathbf{v} \in \mathcal{K},$$

where $\mathbf{v}$ is a test field, $\mathcal{K}$ is the set of admissible displacement fields, and j is the work of friction forces. For various friction models the problem statement is preserved, but j changes. For thin fibers, the work of friction forces can be expressed in terms of resultant forces only.

Euler-Eytelwein formula

In case of contact between an inextensible fiber and a rigid cylindrical surface, the friction equilibrium condition is given by the Euler-Eytelwein formula, also known as the Capstan equation or the belt friction equation ([20]). The Euler-Eytelwein formula is presented in Figure 2.2 and has the following form:
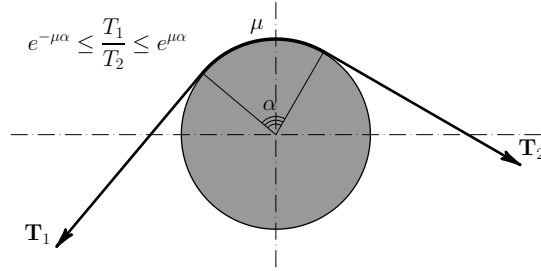
Figure 2.2: The Euler-Eytelwein formula or the Capstan equation

$$
\begin{aligned}
e^{-\mu\alpha} < \frac{T_1}{T_2} < e^{\mu\alpha} &\Rightarrow [\mathbf{w}]_{\mathrm{t}} = 0, \text{ stick phase,} \\
e^{-\mu\alpha} = \frac{T_1}{T_2} \text{ or } \frac{T_1}{T_2} = e^{\mu\alpha} &\Rightarrow \text{ exists } \kappa > 0, \text{ such that } [\mathbf{w}]_{\mathrm{t}} = -\kappa[\mathbf{T}], \text{ slip phase,}
\end{aligned}
\tag{2.3}
$$

where α defines the total angle, swept by the fiber. The total work of friction forces when the fiber slides a small distance $|[\mathbf{w}]_{\mathrm{t}}|$ in the tangential direction at each point of the fiber is given by

$$j_{\text{capstan}}(\mathbf{w}) = \mu \min(T_1, T_2)(e^{\mu\alpha} - 1)\big|[\mathbf{w}]_{\mathrm{t}}\big|. \tag{2.4}$$

We extrapolate this condition to pairs of fibers in contact, where α is computed from the angle between the direction vectors of the elements that are adjacent to the contact node. For the case of an extensible fiber the work of friction forces is given by

$$j_{\text{Fric}} = \mu \big|[\mathbf{w}]_{\text{t}}\big| \min(T_1, T_2) \int_0^\alpha f^{-1}\big(\min(T_1, T_2)e^{\mu\alpha}\big)e^{\mu\alpha}\, d\alpha. \tag{2.5}$$

Slip variables and undeformed lengths

Redistribution of undeformed lengths of the adjacent elements in fibers is characterized by slip variables. Let us consider a sample fiber F in Figure 2.3.
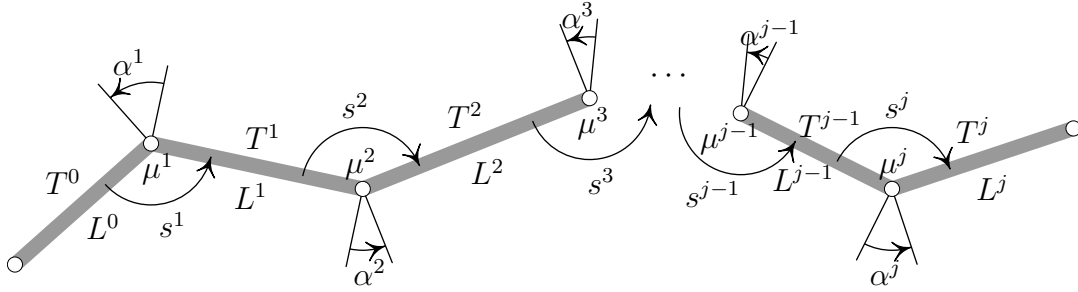
Figure 2.3: Slip variables and undeformed lengths of the sample fiber F

Assume that F consists of $j+1$ elements $e^0, e^1, \ldots, e^j$. Then during the loading process their undeformed lengths $L^0, L^1, \ldots, L^j$ change in such a way that (2.3) is satisfied (note that here the local indexing of elements is used).

Consider two adjacent elements e^k and e^{k+1}. Denote the undeformed fiber length increment by s^{k+1}, i.e. the material redistribution parameter or slip variable, move from element e^k to element e^{k+1}. Then we observe that after this redistribution we have

$$L^k = \mathcal{L}^k - s^{k+1} + s^k.$$

Obviously, the latter relation between L^k and $\mathcal{L}^k$ automatically ensures that the length conservation equation

$$\sum_k L^k = \sum_k \mathcal{L}^k \tag{2.6}$$

holds.

The full system of equations for all the elements of the fiber reads

$$\begin{cases} L^0 = \mathcal{L}^0 - s^1, \\ L^1 = \mathcal{L}^1 - s^2 + s^1, \\ L^2 = \mathcal{L}^2 - s^3 + s^2, \\ \quad \cdots \\ L^{j-1} = \mathcal{L}^{j-1} - s^j + s^{j-1}, \\ L^j = \mathcal{L}^j + s^j. \end{cases}$$

Note that due to (2.6) this system is invertible with respect to s^m. This fact will play an important role later when the existence of the solutions to incremental problems will be discussed.

Assumption 7 (geometric constraint). *During the loading process it must hold that $L^i \geq \varepsilon_{\text{len}}$, where ε_{len} is some small positive constant. This constraint means that undeformed lengths do not turn to be too small. This yields the following constraints for slip variables:*

$$\begin{cases} \varepsilon_{\text{len}} \leq \mathcal{L}^0 - s^1, \\ \varepsilon_{\text{len}} \leq \mathcal{L}^{m-1} - s^m + s^{m-1}, \quad 2 \leq m \leq j, \\ \varepsilon_{\text{len}} \leq \mathcal{L}^j + s^j. \end{cases}$$

Due to invertibility of (2.2.3) with respect to s^m, this system defines a compact convex set S_{adm} (as a system of linear inequalities in a finite-dimensional space, see Chapter 1 in [40]).

Total frictional dissipation for complete fiber

Assume that all nodes of a fiber F are frictional and that friction coefficients in the nodes are defined as in Figure 2.3. Consider time derivatives $\dot{s}^k$ of slip variables s^k. At each frictional node the work of friction forces is given by (2.5). The total work of friction forces along the whole fiber F can be computed as a sum of works in the individual nodes:

$$j_{\text{Fric}}^F = \sum_{k=1}^{j} \mu^i \left| \dot{s}^k \right| T_{\text{min}}^k \int_0^{\alpha^k} f^{-1} \left(T_{\text{min}}^k e^{\mu^k \alpha} \right) e^{\mu^k \alpha} \, d\alpha. \tag{2.7}$$

Remark 15. Non-frictional nodes can be considered as a special case of frictional nodes
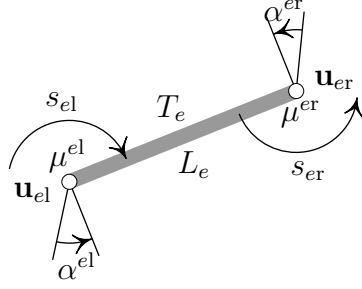
Figure 2.4: A single element

with friction coefficient 0. This means that no work is done by friction forces at such nodes and that the tensional forces in the elements incident to the same non-frictional node are identical. Further we will not specifically distinguish this case from generic frictional nodes.

2.2.4 Description of aggregate model, statement of the evolution problem

In this section we combine the elasticity and friction models for the whole fabric from Figure 2.1. We introduce notation s and $\dot{s}$ for sets of all slip variables s_i^j and their time derivatives. The total elastic energy U_{tot} of the mesh is the sum of the energies of all its elements (2.2):

$$U_{\text{tot}}(\mathbf{u}, s) = \sum_{e \in E} U_e(\mathbf{u}, s), \text{ where} \tag{2.8}$$

$$U_e(\mathbf{u}, s) = (\mathcal{L}_e + s_{\text{el}} - s_{\text{er}}) \int_1^{\lambda_e} f_e(\chi) \, d\chi, \quad \lambda_e = \frac{\|\boldsymbol{X}_{\text{el}} + \mathbf{u}_{\text{el}} - \boldsymbol{X}_{\text{er}} - \mathbf{u}_{\text{er}}\|}{\mathcal{L}_e + s_{\text{el}} - s_{\text{er}}}.$$

U_e is the elastic energy of a single element e, λ_e is its principal stretch, and $\mathcal{L}_e$ is its initial undeformed length. Lower indices l and r are introduced to simplify notations and to denote "left" and "right" quantities of the element e, see Figure 2.4. Namely, the variable s_{el} is the slip variable at the left node of e, $\boldsymbol{X}_{\text{el}}$ is the initial position of the left node of e, and $\mathbf{u}_{\text{el}}$ is the displacement of the left node of e. Note that we used (2.2.3) to represent the element's undeformed length L_e as a function of components of s and $\mathcal{L}$.

Later we will show that the elastic energy presented above yields degenerate Jacobian matrices. For better convergence and continuity properties, strict convexity is required.

Introduce regularization term R and regularized total elastic energy $U_{\mathrm{tot}}^{\mathrm{reg}}$:

$$\mathrm{R}(\mathbf{u}, \boldsymbol{s}) = \varepsilon_r (\langle \mathbf{u}, \mathbf{u} \rangle + \langle \boldsymbol{s}, \boldsymbol{s} \rangle),$$
$$U_{\mathrm{tot}}^{\mathrm{reg}}(\mathbf{u}, \boldsymbol{s}) = \mathrm{R}(\mathbf{u}, \boldsymbol{s}) + U_{\mathrm{tot}}(\mathbf{u}, \boldsymbol{s}), \tag{2.9}$$

where $\varepsilon_r > 0$ and the symbol $\langle \mathbf{u}, \mathbf{v} \rangle$ denotes the standard inner product of finite-dimensional vectors $\mathbf{u}$ and $\mathbf{v}$.

The energy dissipated by friction can be computed as the total energy dissipated on each particular fiber:

$$j_{\mathrm{tot}}(\mathbf{u}, \boldsymbol{s}, \dot{\mathbf{u}}, \dot{\mathbf{s}}) = \sum_{F_i \in E} j_{\mathrm{Fric}}^{F_i}(\mathbf{u}, \boldsymbol{s}, \dot{\mathbf{u}}, \dot{\mathbf{s}}), \text{ where}$$

$$j_{\mathrm{Fric}}^{F_i}(\mathbf{u}, \boldsymbol{s}, \dot{\mathbf{u}}, \dot{\mathbf{s}}) = \sum_{k=1}^{j} \mu^i \left| \dot{s}^k \right| T_{\min}^k(\mathbf{u}, \boldsymbol{s}) \int_0^{\alpha^k(\mathbf{u})} f_{F_i}^{-1} \left(T_{\min}^k(\mathbf{u}, \boldsymbol{s}) e^{\mu^k \alpha} \right) e^{\mu^k \alpha} \, d\alpha$$

is defined according to (2.7). Since a dissipative model is considered, the stretching process is path-dependent, and an additional parametrization is necessary to track the process. We achieve this with a new "time" parameter t and time-dependent boundary conditions.

The governing principle in our model is a doubly nonlinear evolution equation as stated in [29]: find $\mathbf{u} \in W^{1,1}([0; T], V_{\mathbf{u}})$ and $\boldsymbol{s} \in W^{1,1}([0; T], V_s)$, such that

$$0 \in \partial_{\mathbf{u}, \boldsymbol{s}} U_{\mathrm{tot}}(\mathbf{u}, \boldsymbol{s}) + \partial_{\dot{\mathbf{u}}, \dot{\mathbf{s}}} j_{\mathrm{tot}}(\mathbf{u}, \boldsymbol{s}, \dot{\mathbf{u}}, \dot{\mathbf{s}}), \text{ for all time instants } t,$$
$$\mathbf{u}\big|_{\partial \Omega_D} = \mathbf{D}(\mathbf{x}, t), \tag{2.10}$$

where $V_{\mathbf{u}}$ and V_s are the corresponding finite-dimensional spaces, and the notation $\partial_{a,b}$ denotes the subdifferential (see [40]) with respect to variables a and b.

Remark 16. Throughout this part we assume that $\boldsymbol{s}(t) \in S_{\mathrm{adm}}$ for all time instants t. The statement (2.10) can no longer be used in general with this constraint, since it is an optimality condition for some problem. When we add the constraint $\boldsymbol{s}(t) \in S_{\mathrm{adm}}$ to the model, a proper constrained problem's optimality condition has to be considered. However, due to our assumption, any such condition would coincide with (2.10).

In the sequel the following equivalent statement will be used: find $\mathbf{u} \in W^{1,1}([0; T], V_{\mathbf{u}}^D)$

and $s \in W^{1,1}\left([0;T], V_s\right)$ such that

$$0 \in \partial_{\mathbf{u},s}\, U_{\text{tot}}^{\text{D}}(t, \mathbf{u}, s) + \partial_{\dot{\mathbf{u}},\dot{s}}\, j_{\text{tot}}^{\text{D}}(t, \mathbf{u}, s, \dot{\mathbf{u}}, \dot{s}), \ \text{ for all time instants } t, \qquad (2.11)$$

where $U_{\text{tot}}^{\text{D}}$ and $j_{\text{tot}}^{\text{D}}$ are U_{tot} and j_{tot} with the Dirichlet conditions plugged in, and $V_{\mathbf{u}}^{D}$ is the reduced finite-dimensional space of displacement fields with some components fixed due to the Dirichlet conditions. We will also consider the regularized problem: find $\mathbf{u} \in W^{1,1}\left([0;T], V_{\mathbf{u}}^{D}\right)$ and $s \in W^{1,1}\left([0;T], V_s\right)$, such that

$$0 \in \partial_{\mathbf{u},s}\, U_{\text{tot}}^{\text{Dreg}}(t, \mathbf{u}, s) + \partial_{\dot{\mathbf{u}},\dot{s}}\, j_{\text{tot}}^{\text{D}}(t, \mathbf{u}, s, \dot{\mathbf{u}}, \dot{s}), \ \text{ for all time instants } t, \qquad (2.12)$$

where $U_{\text{tot}}^{\text{Dreg}}$ is $U_{\text{tot}}^{\text{reg}}$ with the Dirichlet conditions plugged in.

Remark 17. For the problem statement above to be well defined, one has to show that the functions under the subdifferential operators are convex. The convexity of $U_{\text{tot}}(\mathbf{u}, s)$, $U_{\text{tot}}^{\text{D}}(t, \mathbf{u}, s)$, and $U_{\text{tot}}^{\text{Dreg}}(t, \mathbf{u}, s)$ with respect to $\mathbf{u}$ and s for any $t \in [0;T]$ is shown in Section 2.3. The convexity of $j_{\text{tot}}(\mathbf{u}, s, \dot{\mathbf{u}}, \dot{s})$ and $j_{\text{tot}}^{\text{D}}(t, \mathbf{u}, s, \dot{\mathbf{u}}, \dot{s})$ with respect to variables $(\dot{\mathbf{u}}, \dot{s})$ for any $t \in [0;T]$ follows from the explicit form of j_{tot} and (2.1).

It is assumed that $\mathbf{D}(\mathbf{x}, 0)$ and all tensional forces of elements in the initial state are such that the system is in equilibrium at the initial time instant. The simplest case of an initial state equilibrium is that all tensional forces and Dirichlet conditions are equal to zero.

2.2.5   A model example
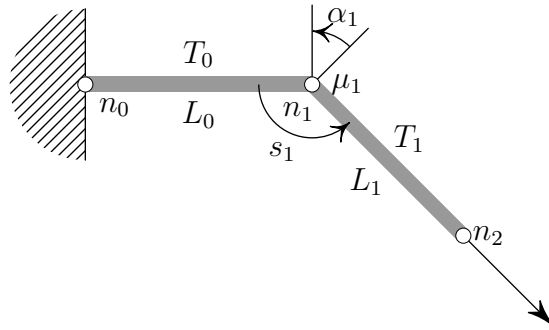
Consider a system in Figure 2.5.

Figure 2.5: Example system

It contains only one fiber with two elements. Out of three nodes, two (n_0, n_1) are fixed

and one is moving due to the prescribed Dirichlet conditions (n_2). The only unknown in this system is s_1 (and its derivative $\dot{s}_1$). Angle α_1 does not change due to the alignment of the prescribed Dirichlet displacement and the element pulled.

Let us check that the governing principle (2.10) for this system yields Euler-Eytelwein condition (2.3) for the tensional forces and the slip variable.

Assume that for this system the force-stretch function f is affine, namely,

$$f(\lambda) = \lambda - 1.$$

The inverse is $f^{-1}(T) = T + 1$. It follows that

$$T_0 = \frac{l_0}{L_0 - s_1} - 1, \quad T_1 = \frac{l_1}{L_1 + s_1} - 1.$$

Assume that $T_1 > T_0 > 0$, $T_1 \leq e^{\alpha_1\mu_1}T_0$, and $T_1 > T_0$. It is easy to see that under such conditions $s_1 \geq 0$. The elastic energy and the total work of friction forces can be written down explicitly:

$$U_{e_0} = \frac{1}{2}\frac{(l_0 - L_0 + s_1)^2}{L_0 - s_1} = \frac{1}{2}(L_0 - s_1)(T_0)^2,$$

$$U_{e_1} = \frac{1}{2}\frac{(l_1 - L_1 - s_1)^2}{L_1 + s_1} = \frac{1}{2}(L_1 + s_1)(T_1)^2,$$

$$j_{\text{tot}} = |\dot{s}_1|\left(\frac{(T_0 e^{\alpha_1\mu_1})^2}{2} - \frac{(T_0)^2}{2} + T_0 e^{\alpha_1\mu_1} - T_0\right).$$

From the governing principle (2.10) we obtain that $\dot{s}_1$ is the solution of the following problem:

$$0 \in \partial_{\mathbf{u},s}U_{e_0} + \partial_{\mathbf{u},s}U_{e_1} + \partial_{\dot{\mathbf{u}},\dot{s}}j_{\text{tot}}.$$

Observe that for s_1 such that $s_1 \leq L_0 - \varepsilon_{\text{len}}$, U_{e_0}, U_{e_1}, j_{tot} are convex with respect to. s_1 and the application of subdifferential operators is legal. Functions U_{e_0} and U_{e_1} are differentiable and j_{tot} is a multiple of the absolute value function. After differentiation with respect to $\dot{s}_1$ and algebraic simplifications we arrive at

$$0 \in -\left(\frac{(T_1)^2}{2} - \frac{(T_0)^2}{2} + T_1 - T_0\right) + \text{Sign}(\dot{s}_1)\left(\frac{(T_0 e^{\alpha_1\mu_1})^2}{2} - \frac{(T_0)^2}{2} + T_0 e^{\alpha_1\mu_1} - T_0\right).$$

Note that since $\dot{s}_1 \geq 0$, the latter condition is equivalent to the following disjunction:

$$
\left[
\begin{array}{l}
T_1 = T_0 e^{\alpha_1 \mu_1} \text{ and } \dot{s}_1 \geq 0, \\
T_1 < T_0 e^{\alpha_1 \mu_1} \text{ and } \dot{s}_1 = 0.
\end{array}
\right.
$$

This condition is similar to (2.3). The slip variable changes only if the tensional forces are in critical state. Otherwise, no slip takes place.

2.3   Analysis of the model properties

For each fixed time instant the problem (2.10) is a finite-dimensional problem with respect to $\dot{\mathbf{u}}$ and $\dot{\boldsymbol{s}}$. We first prove that it possesses the desired convexity properties and then discuss equivalent formulations, existence and properties of time-dependent solutions and possible approaches to a numerical solution.

2.3.1   Convexity properties of elastic and frictional terms

Lemma 8. *The elastic energy term $U_{\mathrm{tot}}(\mathbf{u}, \boldsymbol{s})$ has a positively-semidefinite Hessian matrix with respect to $\mathbf{u}$ and $\boldsymbol{s}$ on the admissible set $\{\boldsymbol{s} \colon \boldsymbol{s} \in S_{\mathrm{adm}}\}$.*

Proof. Due to (2.8) it is enough to prove the statement for a single element. Elastic energy of each element is defined by the independent quantities in its two nodes, see Figure 2.4 (in this proof we omit lower index e to simplify the notations):

1. spatial coordinates of the left and right nodes of the element: $\mathbf{u}_{\mathrm{l}}$ and $\mathbf{u}_{\mathrm{r}}$,

2. left and right slip variables $\dot{s}_{\mathrm{l}}$ and $\dot{s}_{\mathrm{r}}$.

Therefore, the elastic energy U_e of a single element e is a function of these eight variables: $U_e(u_{\mathrm{l}1}, u_{\mathrm{l}2}, u_{\mathrm{l}3}, s_{\mathrm{l}}, u_{\mathrm{r}1}, u_{\mathrm{r}2}, u_{\mathrm{r}3}, s_{\mathrm{r}})$. We write this function explicitly, compute its Hessian matrix, and show that it is always positively-semidefinite.

All of the six spatial nodal element coordinates are represented by a vector

$$
\mathbf{u} = \left[\mathbf{u}_{\mathrm{l}}^T, \mathbf{u}_{\mathrm{r}}^T \right]^T.
$$

Let $\mathbf{c}_e$ be the orientation unit vector of e $\mathbf{c}_e = (\mathbf{u}_{\mathrm{l}} - \mathbf{u}_{\mathrm{r}})l^{-1}$, where l denotes the deformed length of e. Further we will treat $\mathbf{c}_e$ as a column-vector.

The longitudinal principal stretch of the element can be represented as a function of eight variables u_{lj}, u_{rj}, s_l, and s_r:

$$\lambda = \frac{l}{L} = \frac{\sqrt{[u_{l1} - u_{r1}]^2 + [u_{l2} - u_{r2}]^2 + [u_{l3} - u_{r3}]^2}}{\mathcal{L} + (s_l - s_r)}.$$

Here we used (2.2.3) to express L in terms of $\mathcal{L}$ and s. By straightforward differentiation we obtain

$$\frac{\partial \lambda}{\partial u_{lj}} = \frac{c_{ej}}{L}, \quad \frac{\partial \lambda}{\partial s_l} = -\frac{1}{L}\lambda, \quad \frac{\partial \lambda}{\partial u_{rj}} = -\frac{c_{ej}}{L}, \quad \frac{\partial \lambda}{\partial s_r} = \frac{1}{L}\lambda.$$

Let us differentiate (2.2) using (2.2.3) to obtain the derivatives of U_e:

$$\frac{\partial U_e}{\partial u_{lj}} = Lf(\lambda)\frac{\partial \lambda}{\partial u_{lj}} = f(\lambda)c_{ej}, \quad \frac{\partial U_e}{\partial s_l} = \int_1^\lambda f(\bar{\lambda})\,d\bar{\lambda} - Lf(\lambda)\frac{\partial \lambda}{\partial s_{lj}} = \int_1^\lambda f(\bar{\lambda})\,d\bar{\lambda} - \lambda f(\lambda),$$

$$\frac{\partial U_e}{\partial u_{rj}} = Lf(\lambda)\frac{\partial \lambda}{\partial u_{rj}} = -f(\lambda)c_{ej}, \quad \frac{\partial U_e}{\partial s_r} = -\int_1^\lambda f(\bar{\lambda})\,d\bar{\lambda} + \lambda f(\lambda).$$

We also need the following second derivatives:

$$\frac{\partial^2 U_e}{\partial u_{li}^2} = \frac{1}{l} - \frac{(u_{li} - u_{ri})^2}{l^3}, \quad \frac{\partial^2 U_e}{\partial u_{li}\partial u_{lj}} = -\frac{(u_{li} - u_{ri})(u_{lj} - u_{lj})}{l^3}, \; i \neq j,$$

$$\frac{\partial^2 U_e}{\partial u_{li}\partial u_{ri}} = -\frac{\partial^2 U_e}{\partial u_{li}\partial u_{li}}, \quad \frac{\partial^2 U_e}{\partial u_{li}\partial u_{rj}} = -\frac{\partial^2 U_e}{\partial u_{li}\partial u_{lj}}, \; i \neq j,$$

$$\frac{\partial^2 U_e}{\partial u_{li}^2} = \frac{f'(\lambda)}{L}c_{ei}c_{ej} + \frac{f(\lambda)}{l}\left(1 - c_{ei}^2\right), \quad \frac{\partial^2 U_e}{\partial u_{li}\partial u_{lj}} = \frac{f'(\lambda)}{L}c_{ei}c_{ej} + \frac{f(\lambda)}{l}(-c_{ei}c_{ej}), \; i \neq j,$$

$$\frac{\partial^2 U_e}{\partial u_{li}\partial u_{ri}} = -\frac{\partial^2 U_e}{\partial u_{li}\partial u_{li}}, \forall\, i,j,$$

$$\frac{\partial^2 U_e}{\partial s_l^2} = \frac{\lambda^2 f'(\lambda)}{L}, \quad \frac{\partial^2 U_e}{\partial s_l\partial s_r} = -\frac{\lambda^2 f'(\lambda)}{L}, \quad \frac{\partial^2 U_e}{\partial s_l\partial u_{li}} = -c_{ei}\frac{\lambda f'(\lambda)}{L}, \quad \frac{\partial^2 U_e}{\partial s_r\partial u_{li}} = -\frac{\partial^2 U_e}{\partial s_l\partial u_{li}}.$$

Let us introduce matrices

$$\mathbf{Z}_u = \frac{f'(\lambda)}{L}\mathbf{c}_e\mathbf{c}_e^T + \frac{f(\lambda)}{l}\left(\mathbf{I}_3 - \mathbf{c}_e\mathbf{c}_e^T\right), \quad \mathbf{Z}_s = -\frac{\lambda f'(\lambda)}{L}\mathbf{c}_e,$$

where $\mathbf{I}_k$ is a k-by-k identity matrix. Then $\partial^2 U_e$ can be rewritten in the following block

form:

$$\partial^2 U_e = \begin{pmatrix} \mathbf{I}_4 \\ -\mathbf{I}_4 \end{pmatrix} \mathbf{B} \begin{pmatrix} \mathbf{I}_4 & -\mathbf{I}_4 \end{pmatrix}, \quad \mathbf{B} = \begin{pmatrix} \mathbf{Z}_u & \mathbf{Z}_s \\ \mathbf{Z}_s^T & \lambda^2 f' L^{-1} \end{pmatrix}. \tag{2.13}$$

Assume that $\mathbf{c}_e^1$ and $\mathbf{c}_e^2$ are such vectors that $(\mathbf{c}_e, \mathbf{c}_e^1, \mathbf{c}_e^2)$ is a right orthonormal triple. Introduce notation

$$\mathbf{C}_4 = \begin{pmatrix} \mathbf{C} & \mathbf{0}_{1\times 3} \\ \mathbf{0}_{3\times 1} & 1 \end{pmatrix}, \quad \mathbf{B}_{\mathrm{loc}} = \begin{pmatrix} f' L^{-1} & 0 & 0 & -\lambda f' L^{-1} \\ 0 & f l^{-1} & 0 & 0 \\ 0 & 0 & f l^{-1} & 0 \\ -\lambda f' L^{-1} & 0 & 0 & \lambda^2 f' L^{-1} \end{pmatrix}, \tag{2.14}$$

where $\mathbf{C} = \begin{pmatrix} \mathbf{c}_e & \mathbf{c}_e^1 & \mathbf{c}_e^2 \end{pmatrix}$, and $\mathbf{0}_{m\times n}$ is the m-by-n matrix of zeros. It is easy to check that

$$\mathbf{B} = \begin{pmatrix} \mathbf{Z}_u & \mathbf{Z}_s \\ \mathbf{Z}_s^T & \lambda^2 f' L^{-1} \end{pmatrix} = \mathbf{C}_4 \mathbf{B}_{\mathrm{loc}} \mathbf{C}_4^T. \tag{2.15}$$

From (2.13), (2.14), and (2.15) it is easy to deduce that the following equality is true:

$$\mathbf{Q}^T \partial^2 U_e \mathbf{Q} = (\mathbf{Q}_{\mathrm{l}} - \mathbf{Q}_{\mathrm{r}})^T \mathbf{C}_4 \mathbf{B}_{\mathrm{loc}} \mathbf{C}_4^T (\mathbf{Q}_{\mathrm{l}} - \mathbf{Q}_{\mathrm{r}}), \quad \text{where} \tag{2.16}$$

$$\mathbf{Q}_{\mathrm{l}} = \begin{pmatrix} u_{\mathrm{l}1} & u_{\mathrm{l}2} & u_{\mathrm{l}3} & s_{\mathrm{l}} \end{pmatrix}^T, \quad \mathbf{Q}_{\mathrm{r}} = \begin{pmatrix} u_{\mathrm{r}1} & u_{\mathrm{r}2} & u_{\mathrm{r}3} & s_{\mathrm{r}} \end{pmatrix}^T, \quad \mathbf{Q} = \begin{pmatrix} \mathbf{Q}_{\mathrm{l}} & \mathbf{Q}_{\mathrm{r}} \end{pmatrix}^T.$$

By Sylvester's criterion, equality (2.16), and due to the orthogonality of $\mathbf{C}_4$, the quadratic form $\mathbf{Q}^T \partial^2 U_e \mathbf{Q}$ is positively-semidefinite if and only if all principal minors of $\mathbf{B}_{\mathrm{loc}}$ are non-negative. Indeed, due to the properties of force-principal stretch functions (2.1) we observe that

$$\Delta_1(\mathbf{B}_{\mathrm{loc}}) = f' L^{-1} \geq 0, \quad \Delta_2(\mathbf{B}_{\mathrm{loc}}) = f' f l^{-1} L^{-1} \geq 0, \quad \Delta_3(\mathbf{B}_{\mathrm{loc}}) = f' f^2 l^{-2} L^{-1} \geq 0,$$

$$\Delta_4(\mathbf{B}_{\mathrm{loc}}) = \lambda^2 (f')^2 f^2 l^{-2} L^{-2} - \lambda^2 (f')^2 f^2 l^{-2} L^{-2} = 0.$$

These four inequalities conclude the proof. $\square$

Remark 18. Matrix $\mathbf{B}_{\mathrm{loc}}$ is always degenerate, but its rank is 3 even when f and f' are positive. This persistent zero subspace corresponds to the situation, where the slip variables

compensate the change of the deformed length by the change of the undeformed length in such a way that the principal stretch of the element is preserved. However, in the aggregate model (2.10) this zero subspace is penalized by the frictional term, and the whole model is not necessarily degenerate.

Corollary 8. *Functions $U_{\text{tot}}^{\text{D}}(t, \mathbf{u}, \boldsymbol{s})$ and $U_{\text{tot}}^{\text{Dreg}}(t, \mathbf{u}, \boldsymbol{s})$ are convex with respect to $(\mathbf{u}, \boldsymbol{s})$ on the admissible set $\{\boldsymbol{s}\colon \boldsymbol{s} \in S_{\text{adm}}\}$ for all $t \in [0; T]$.*

Lemma 9. *The regularized elastic energy functions $U_{\text{tot}}^{\text{reg}}(\mathbf{u}, \boldsymbol{s})$ and $U_{\text{tot}}^{\text{Dreg}}(t, \mathbf{u}, \boldsymbol{s})$ are strictly convex with respect to variables $(\mathbf{u}, \boldsymbol{s})$ for all $t \in [0; T]$ on the admissible set $\{\boldsymbol{s}\colon \boldsymbol{s} \in S_{\text{adm}}\}$. The strict convexity is uniform with respect to time with coefficient ε_r.*

Proof. The Hessian matrix of $U_{\text{tot}}^{\text{reg}}$ is positively definite due to the relation

$$U_{\text{tot}}^{\text{reg}}(\mathbf{u}, \boldsymbol{s}) = \mathrm{R}(\mathbf{u}, \boldsymbol{s}) + U_{\text{tot}}(\mathbf{u}, \boldsymbol{s}),$$

the positive semidefiniteness of the Hessian of $U_{\text{tot}}(\mathbf{u}, \boldsymbol{s})$, and the positive definiteness of the Hessian of $\mathrm{R}(\mathbf{u}, \boldsymbol{s})$. Since

$$\mathrm{R}(\mathbf{u}, \boldsymbol{s}) = \varepsilon_r(\langle \mathbf{u}, \mathbf{u} \rangle + \langle \boldsymbol{s}, \boldsymbol{s} \rangle),$$

the minimal eigenvalue of the Hessian of $U_{\text{tot}}^{\text{reg}}$ is not less than ε_r. This concludes the proof.
□

Corollary 9. *Function $U_{\text{tot}}^{\text{Dreg}}(t, \mathbf{u}, \boldsymbol{s})$ is uniformly convex on the admissible set $\{\boldsymbol{s}\colon \boldsymbol{s} \in S_{\text{adm}}\}$ for all $t \in [0; T]$ with strict convexity coefficient ε_r.*

Lemma 10. *The frictional energy term $j_{\text{tot}}(\mathbf{u}, \boldsymbol{s}, \dot{\mathbf{u}}, \dot{\boldsymbol{s}})$ is convex with respect to variables $(\dot{\mathbf{u}}, \dot{\boldsymbol{s}})$ for all admissible $(\mathbf{u}, \boldsymbol{s})$.*

Proof. The lemma follows directly from the explicit form of individual terms of j_{tot} given by (2.5), convexity of the absolute value function, and the conditions on force-stretch functions (2.1).
□

Corollary 10. *Function $j_{\text{tot}}^{\text{D}}(t, \mathbf{u}, \boldsymbol{s}, \dot{\mathbf{u}}, \dot{\boldsymbol{s}})$ is convex with respect to variables $(\dot{\mathbf{u}}, \dot{\boldsymbol{s}})$ for all $t \in [0; T]$ and all admissible $(\mathbf{u}, \boldsymbol{s})$.*

2.3.2   A system with discontinuous solution

In general, dissipative processes may show discontinuous behavior even if the input data is Lipschitz-continuous. Let us provide such an example in our setting. In fact, discontinuities may be observed already in the system in Figure 2.5.

Assume that the friction coefficient μ_1 depends on s_1 and that the current and initial length parameters at the initial time instant $t = 0$, are defined as follows:

$$l_0 = 2, \quad L_0 = 1, \quad l_1 = e^{\alpha_1 \mu_1(0)} + 1, \quad L_1 = 1.$$

Assume that the force function is linear. It is easy to check that at the initial time instant the friction equilibrium condition is satisfied:

$$T_0 = 1, \quad T_1 = e^{\alpha_1 \mu_1(0)}, \quad T_1 = T_0 e^{\alpha_1 \mu_1(0)}.$$

As in the previous example, we assume that the Dirichlet conditions are such that the angle α_1 is constant. Here we also assume that the Dirichlet conditions are such that $l_1(t) = e^{\alpha_1 \mu_1(0)} + 1 + t$, i.e. element e_1 is stretched in its longitudinal direction.

Let us analyse $s_1(t)$ as a function of time. It is obvious that it is a non-decreasing non-negative function, and due to the constraint that undeformed lengths are positive, $s_1(t) < 1$. The friction equilibrium condition is

$$\frac{e^{\alpha_1 \mu_1(0)} + t + 1}{1 + s_1(t)} - 1 = e^{\alpha_1 \mu_1(s)} \left(\frac{2}{1 - s_1(t)} - 1 \right).$$

We write the equation for the critical case because the system is in the critical state at the beginning of the process and element e_1, which initially had higher strain, is being stretched further on. The latter equation can be rewritten in the following form:

$$e^{\alpha_1 \mu_1(s_1)} = \mathfrak{f}(s_1, t), \text{ where } \mathfrak{f}(s_1, t) = 1 + t\frac{1 - s_1}{1 + s_1^2} + \frac{e^{\alpha_1 \mu_1(0)} - 1 - s_1 \left(e^{\alpha_1 \mu_1(s_1)+1} \right)}{1 + s_1^2}.$$

Observe that $\mathfrak{f}(s_1, t) > \mathfrak{f}(s_1, 0)$ for all $t > 0$, $s \in [0; 1]$. Consider the following friction coefficient function:

$$\mu_{\text{crit}}(s_1) = \max \left(\frac{1}{\alpha_1} \ln \left(1 + \frac{e^{\alpha_1 \mu_1(0)} - 1 - s_1(e^{\alpha_1 \mu_1(s_1)} + 1)}{1 + s_1^2} \right), \mu_{\min} \right).$$

For some sufficiently small $\mu_{\min} > 0$, the first component of the $\max$ above is greater than the second if

$$s_1 < s^* = -\frac{1}{2} \frac{e^{\alpha_1 \mu_1(0)} + 1}{e^{\alpha_1 \mu_{\min}} - 1} + \frac{1}{2} \frac{\sqrt{(e^{\alpha_1 \mu_1(0)} + 1)^2 + 4(e^{\alpha_1 \mu_{\min}} - 1)(e^{\alpha_1 \mu_1(0)} - e^{\alpha_1 \mu_{\min}})}}{e^{\alpha_1 \mu_{\min}} - 1}.$$

Observe that the friction equilibrium equation for $t = 0$ holds for all s between 0 and s^*. Due to the initial conditions we put $s_1(0) = 0$. However, for $t > 0$ it holds $s_1(t) \geq s^* > 0$. Therefore $s_1(t)$ is discontinuous with respect to time despite the Lipschitz-continuity of the Dirichlet conditions and all the other problem parameters, see Figure 2.6.
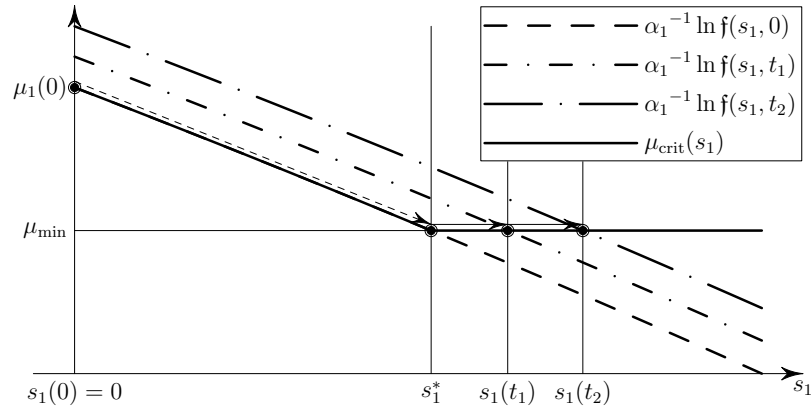
Figure 2.6: $s_1(0)$ instantly jumps to $s_1(t) > s^*$ right as $t > 0$ (the dashed arrow) and then develops continuously with respect to time (the solid arrows)

In the next section we consider conditions, which guarantee Lipschitz-continuity of the solution. Later we will refer to the Lipschitz-continuity of the solutions as to "stability of the model".

2.3.3 Lipschitz properties of the frictional term

The Lipschitz constant of the frictional term plays an important role in the stability of the model. We estimate the constant in this section.

Due to (2.7) it is enough to prove that all the terms are Lipschitz-continuous and have the same Lipschitz constant.

For a single term we re-denote the spatial nodal position by x and the slip variable by s, see Figure 2.7.

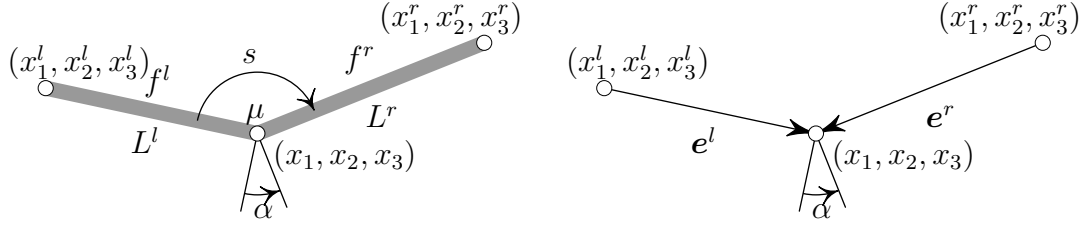In the sequel we will use the following notation: for a scalar function $f(x)$, $\mathrm{grad}_x f$ is its

Figure 2.7: A single frictional node and the direction vectors of the elements

gradient in the form of a row-vector, and for a vector function $\boldsymbol{g}(\boldsymbol{x})$, $\operatorname{grad}_{\boldsymbol{x}} g$ is its Jacobian matrix, where i-th row is the gradient of the i-th component of $\boldsymbol{g}$.

Lemma 11. *Consider three points $\boldsymbol{x}^l$, $\boldsymbol{x}^r$, and $\boldsymbol{x}$ in $\mathbb{R}^3$. Let $\alpha(\boldsymbol{x}) = \pi - \arccos(\langle \boldsymbol{e}^l, \boldsymbol{e}^r \rangle)$, where*

$$\boldsymbol{e}^l = \frac{\boldsymbol{x} - \boldsymbol{x}^l}{\|\boldsymbol{x} - \boldsymbol{x}^l\|}, \; \boldsymbol{e}^r = \frac{\boldsymbol{x} - \boldsymbol{x}^r}{\|\boldsymbol{x} - \boldsymbol{x}^r\|}.$$

The function $\alpha(\boldsymbol{x})$ is Lipschitz-continuous with respect to $\boldsymbol{x}$ on the set
$\{\boldsymbol{x} \colon \|\boldsymbol{x} - \boldsymbol{x}^l\| \geq d\} \cap \{\boldsymbol{x} \colon \|\boldsymbol{x} - \boldsymbol{x}^r\| \geq d\}$ for some $d > 0$ with the Lipschitz constant $3d^{-1}$.

Proof. We prove the lemma by coordinate transformation and direct differentiation.

Observe that $\boldsymbol{e}^l$ and $\boldsymbol{e}^r$ are Lipschitz-continuous with respect to $\boldsymbol{x}$ with constant $3d^{-1}$. This is easy to obtain by the direct differentiation and estimation of the derivatives' norms:

$$\|\operatorname{grad}_{\boldsymbol{x}} \boldsymbol{e}^r\| = \frac{1}{\|\boldsymbol{x} - \boldsymbol{x}^r\|^3} \times$$

$$\times \left\| \begin{pmatrix} (x_2^r - x_2)^2 + (x_3^r - x_3)^2 & -(x_1^r - x_1)(x_2^r - x_2) & -(x_1^r - x_1)(x_3^r - x_3) \\ -(x_2^r - x_2)(x_1^r - x_1) & (x_1^r - x_1)^2 + (x_3^r - x_3)^2 & -(x_2^r - x_2)(x_3^r - x_3) \\ -(x_3^r - x_3)(x_1^r - x_1) & -(x_2^r - x_2)(x_3^r - x_3) & (x_1^r - x_1)^2 + (x_2^r - x_2)^2 \end{pmatrix} \right\| \leq$$

$$\leq \frac{3}{\|\boldsymbol{x} - \boldsymbol{x}^r\|} \leq \frac{3}{d}.$$

Here we have also used that $\|\boldsymbol{e}^r\| = 1$.

Next, it is possible to find such an orthonormal basis, that the coordinate transformation into coordinate system of this basis transforms $\boldsymbol{e}^r$ into $(1, 0, 0)$ and $\boldsymbol{e}^l$ into $\boldsymbol{w} = (w_1, w_2, w_3)$. The coordinate transformation matrix $\boldsymbol{Q}$ is orthogonal. We completely ignore translations because they do not affect the value of $\alpha(\boldsymbol{x})$.

In the new coordinate system we have:

$$\alpha(\boldsymbol{x}) = \pi - \arccos\left(\left\langle \boldsymbol{e}^l, \boldsymbol{e}^r \right\rangle\right) = \pi - \arccos\left(\frac{w_1}{\sqrt{w_1^2 + w_2^2 + w_3^2}}\right) = \tilde{\alpha}(\boldsymbol{w}).$$

Using the condition $w_1^2 + w_2^2 + w_3^2 = 1$ (due to $\left\|\boldsymbol{e}^l\right\| = 1$), by direct differentiation with respect to $\boldsymbol{w}$ we obtain

$$\operatorname{grad}_{\boldsymbol{w}} \tilde{\alpha}(\boldsymbol{w}) = \frac{1}{\sqrt{w_2^2 + w_3^2}} \begin{pmatrix} -w_2^2 - w_3^2 \\ w_1 w_2 \\ w_1 w_3 \end{pmatrix}^T = \begin{pmatrix} -r^2 \\ \operatorname{sign}(w_1) r \sqrt{1 - r^2} \cos(\beta) \\ \operatorname{sign}(w_1) r \sqrt{1 - r^2} \sin(\beta) \end{pmatrix}^T,$$

$$r = \sqrt{w_2^2 + w_3^2} \le 1, \; \beta = \arctan\left(\frac{w_3}{w_2}\right).$$

It is easy to see that $\|\operatorname{grad}_{\boldsymbol{w}} \alpha\| \le 1$.

Finally, due to the relation

$$\begin{pmatrix} w_1 \\ w_2 \\ w_3 \end{pmatrix} = \boldsymbol{Q}(\boldsymbol{x}) \begin{pmatrix} e_1^l(\boldsymbol{x}) \\ e_2^l(\boldsymbol{x}) \\ e_3^l(\boldsymbol{x}) \end{pmatrix}$$

and by the chain rule and the properties of $\boldsymbol{Q}$ we arrive at

$$\|\operatorname{grad}_{\boldsymbol{x}} \alpha(\boldsymbol{x})\| = \left\|\operatorname{grad}_{\boldsymbol{w}} \tilde{\alpha}(\boldsymbol{w}) \operatorname{grad}_{\boldsymbol{e}} \boldsymbol{w} \operatorname{grad}_{\boldsymbol{w}} \boldsymbol{e}^l\right\| =$$

$$= \left\|\operatorname{grad}_{\boldsymbol{w}} \tilde{\alpha}(\boldsymbol{w}) \boldsymbol{Q} \operatorname{grad}_{\boldsymbol{x}} \boldsymbol{e}^l\right\| \le \|\operatorname{grad}_{\boldsymbol{w}} \tilde{\alpha}(\boldsymbol{w})\| \, \|\boldsymbol{Q}\| \left\|\operatorname{grad}_{\boldsymbol{x}} \boldsymbol{e}^l\right\| \le \frac{3}{d}.$$

This inequality concludes the proof. $\qquad\square$

Theorem 12. *Suppose the following conditions hold:*

1. *generalized derivatives of force-principal strain functions are elements of L^∞ and are almost everywhere bounded both from below and from above:*

$$0 < c_{\text{force}} < \left|f'(x)\right| < C_{\text{force}}, \; \forall x > 0,$$

2. *there exist uniform bounds for swept angles: $\alpha(n) \le C_\alpha, \; \forall n \in N,$*

3. *there exists a uniform upper bound for the principal stretches of the elements $\lambda_e \leq C_\lambda$,*
   $\forall\, e \in E$.

4. *there exists a uniform positive lower bound for the undeformed lengths of the elements:*
   $L_e \geq c_{\text{len}} > 0,\ \forall\, e \in E$,

5. *there exists a uniform upper bound for the friction coefficients:* $\mu^k \leq C_\mu$.

Then the work of friction forces in any single node is Lipschitz-continuous:

$$j_{\text{Fric}}(\boldsymbol{q}^1, \boldsymbol{s}^1, \dot{\mathbf{u}}, \dot{\mathbf{s}}) - j_{\text{Fric}}(\boldsymbol{q}^2, \boldsymbol{s}^2, \dot{\mathbf{u}}, \dot{\mathbf{s}}) \leq C_{\text{Lip}}^{\text{loc}} \left\| (\dot{\mathbf{u}}, \dot{\mathbf{s}}) \right\| \left\| (\boldsymbol{q}^1, \boldsymbol{s}^1) - (\boldsymbol{q}^2, \boldsymbol{s}^2) \right\| \qquad (2.17)$$

for all admissible $(\boldsymbol{q}^1, \boldsymbol{s}^1)$ and $(\boldsymbol{q}^2, \boldsymbol{s}^2)$,

$$C_{\text{Lip}}^{\text{loc}} \leq C_\mu e^{2C_\alpha C_\mu} C_{\text{force}}^2 c_{\text{force}}^{-1} c_{\text{len}}^{-1} C_\lambda \max(2C_\lambda C_\alpha, 2C_\alpha + 3C_\lambda).$$

Proof. We find the derivative of the frictional term and show that it is bounded.

Note that the only nonsmooth term subject to the differentiation is $\min(f^l, f^r)$. Due to the strict monotonicity of force functions, this term is differentiable almost everywhere and at the points of non-differentiability the superdifferential can be analyzed, see Theorem 3.18 in [8]. To avoid technicalities arising from superdifferentials, we refer to Theorem 25.6 in [40] and work only with directional derivatives.

The following derivatives of the principal strain and the force-principal stretch function will be required for further estimates:

$$\lambda^l(\boldsymbol{x}, s) = \frac{\|\boldsymbol{x} - \boldsymbol{x}^l\|}{\mathcal{L}^l - s + s^l}, \quad \text{grad}_{\boldsymbol{x}}\, \lambda^l(\boldsymbol{x}) = \frac{\boldsymbol{e}^l}{\mathcal{L}^l - s + s^l}, \quad \boldsymbol{e}^l = \frac{\boldsymbol{x} - \boldsymbol{x}_l}{\|\boldsymbol{x} - \boldsymbol{x}^l\|},$$

$$\left(\lambda^l\right)'_s = \frac{\|\boldsymbol{x} - \boldsymbol{x}^l\|}{(\mathcal{L}^l - s + s^l)^2} = \frac{\lambda^l(\boldsymbol{x}, s)}{\mathcal{L}^l - s + s^l},$$

$$\text{grad}_{\boldsymbol{x}}\, f^l = f^{l\prime}_{\lambda^l}\, \text{grad}_{\boldsymbol{x}}\, \lambda^l = f^{l\prime}_{\lambda^l} \frac{\boldsymbol{e}^l}{\mathcal{L}^l - s + s^l}, \quad \left(f^l\right)'_s = \left(f^l\right)'_{\lambda^l} \frac{\lambda^l(\boldsymbol{x}, s)}{\mathcal{L}^l - s + s^l}.$$

Differentiation with respect to s yields:

$$\left| \frac{\partial}{\partial s} \mu \left| \dot{s} \right| \min(f^l, f^r) \int_0^\alpha f^{-1}(\min(f^l, f^r)e^{\mu\alpha})e^{\mu\alpha}\, d\alpha \right| \leq$$

$$\leq \mu \left| \dot{s} \right| \max\left(\left| f^{l\prime}_s \right|, \left| f^{r\prime}_s \right| \right) \int_0^\alpha f^{-1}\left(\min(f^l, f^r)e^{\mu\alpha} \right) e^{\mu\alpha}\, d\alpha +$$

$$+ \mu \left| \dot{s} \right| \min(f^l, f^r) \int_0^\alpha \frac{e^{2\mu\alpha} \max\left(\left| f^{l\prime}_s \right|, \left| f^{r\prime}_s \right| \right)}{f'\left(f^{-1}\left(\min(f^l, f^r)e^{\mu\alpha} \right) \right)}\, d\alpha \leq 2\mu \left| \dot{s} \right| e^{2C_\alpha\mu} C_{\text{force}}^2 c_{\text{force}}^{-1} c_{\text{len}}^{-1} C_\lambda^2 C_\alpha.$$

Differentiation with respect to $\boldsymbol{x}$ yields:

$$\left| \text{grad}_{\boldsymbol{x}}\, \mu \left| \dot{s} \right| \min(f^l, f^r) \int_0^\alpha f^{-1}(\min(f^l, f^r)e^{\mu\alpha})e^{\mu\alpha}\, d\alpha \right| \leq$$

$$\leq \mu \left| \dot{s} \right| \max\left(\left\| \text{grad}_{\boldsymbol{x}}\, f^l \right\|_1, \left\| \text{grad}_{\boldsymbol{x}}\, f^r \right\|_1 \right) \int_0^\alpha f^{-1}\left(\min(f^l, f^r)e^{\mu\alpha} \right) e^{\mu\alpha}\, d\alpha +$$

$$+ \mu \left| \dot{s} \right| \min(f^l, f^r) \left\| \text{grad}_{\boldsymbol{x}}\, \alpha \right\|_1 f^{-1}\left(\min(f^l, f^r)e^{\mu C_\alpha} \right) e^{\mu C_\alpha} +$$

$$+ \mu \left| \dot{s} \right| \min(f^l, f^r) \int_0^\alpha \frac{e^{2\mu\alpha} \max\left(\left\| \text{grad}_{\boldsymbol{x}}\, f^l \right\|_1, \left\| \text{grad}_{\boldsymbol{x}}\, f^r \right\|_1 \right)}{f'\left(f^{-1}\left(\min(f^l, f^r)e^{\mu\alpha} \right) \right)}\, d\alpha \leq$$

$$\leq \mu \left| \dot{s} \right| e^{2C_\alpha\mu} C_{\text{force}}^2 c_{\text{force}}^{-1} c_{\text{len}}^{-1} C_\lambda \left(2C_\alpha + 3C_\lambda \right).$$

Here the terms without $\text{grad}_{\boldsymbol{x}}\, \alpha$ are estimated in the same way as for the derivative with respect to s. For the estimate of $\left\| \text{grad}_{\boldsymbol{x}}\, \alpha \right\|_1 \leq 3c_{\text{len}}^{-1}$ see Lemma 11. It remains to estimate the friction coefficients and take maximum of the two estimates above. $\qquad \square$

Corollary 11. *Suppose that the conditions of Theorem 12 hold. Then the total work of friction forces is Lipschitz-continuous:*

$$j_{\text{tot}}^{\text{D}}(t, \boldsymbol{q}^1, \boldsymbol{s}^1, \dot{\mathbf{u}}, \dot{\mathbf{s}}) - j_{\text{tot}}^{\text{D}}(t, \boldsymbol{q}^2, \boldsymbol{s}^2, \dot{\mathbf{u}}, \dot{\mathbf{s}}) \leq C_{\text{Lip}} \left\| (\dot{\mathbf{u}}, \dot{\mathbf{s}}) \right\| \left\| (\boldsymbol{q}^1, \boldsymbol{s}^1) - (\boldsymbol{q}^2, \boldsymbol{s}^2) \right\| \qquad (2.18)$$

for all admissible $(\boldsymbol{q}_1, \boldsymbol{s}_1)$, $(\boldsymbol{q}_2, \boldsymbol{s}_2)$, *for all* $t \in [0; T]$,

$$(2.19)$$

$$C_{\text{Lip}} \leq \left| S_C \right| C_{\text{Lip}}^{\text{loc}},$$

where $C_{\text{Lip}}^{\text{loc}}$ *is defined in Theorem 12.*

Remark 19. Condition 1 is physically reasonable, but rules out discontinuous force curves.

Condition 2 may be false for some special meshes, but it is quite reasonable for textile modeling. Condition 3 can be derived from the energy conservation law and does not impose any non-physical restrictions. Condition 4 can be a problem, since it is natural to put c_{len} to be very small. However, it enters the denominator of the estimate for the Lipschitz constant and, as we will see further, it is desirable that this constant is small.

2.3.4 Energetic formulation and time-discrete problems

Following [29] and [32], consider the energetic formulation of the problem: find $\mathbf{u} \in W^{1,1}\left([0;T], V_{\mathbf{u}}^D\right)$ and $\boldsymbol{s} \in W^{1,1}\left([0;T], V_s\right)$, such that

$$U_{\text{tot}}^{\text{D}}(t, \mathbf{u}, \boldsymbol{s}) \leq U_{\text{tot}}^{\text{D}}(t, \hat{\mathbf{u}}, \hat{\boldsymbol{s}}) + j_{\text{tot}}^{\text{D}}(t, \mathbf{u}, \boldsymbol{s}, \hat{\mathbf{u}} - \mathbf{u}, \hat{\boldsymbol{s}} - \boldsymbol{s}) \quad \text{for all admissible } (\hat{\mathbf{u}}, \hat{\boldsymbol{s}}), \ t \in [0, \mathrm{T}],$$

$$\text{(S)}$$

$$U_{\text{tot}}^{\text{D}}(t, \mathbf{u}(t), \boldsymbol{s}(t)) + \int_0^t j_{\text{tot}}^{\text{D}}\big(\tau, \mathbf{u}(\tau), \boldsymbol{s}(\tau), \dot{\mathbf{u}}(\tau), \dot{\boldsymbol{s}}(\tau)\big) \, d\tau =$$

$$\text{(E)}$$

$$= U_{\text{tot}}^{\text{D}}(0, \mathbf{u}(0), \boldsymbol{s}(0)) + \int_0^t \mathrm{P}_{\text{ext}}(\tau, \mathbf{u}(\tau), \boldsymbol{s}(\tau)) \, d\tau,$$

where the last integral term represents the work of external forces (caused by the boundary conditions).

Theorem 13. *Assume the conditions of Theorem 12 are satisfied. Then the problems* (S)–(E) *and* (2.10) *are equivalent.*

Proof. The theorem is a direct corollary of Proposition 2.7 from [29]. To use this proposition, we must ensure that the following conditions hold:

1. $U_{\text{tot}}^{\text{D}}(t, \mathbf{u}, \boldsymbol{s})$ is convex w.r.t. $(\mathbf{u}, \boldsymbol{s})$ for all $t \in [0;T]$.

2. $j_{\text{tot}}^{\text{D}}(t, \mathbf{u}, \boldsymbol{s}, \dot{\mathbf{u}}, \dot{\boldsymbol{s}})$ is convex and positively homogeneous of degree 1 with respect to $(\dot{\mathbf{u}}, \dot{\boldsymbol{s}})$ for all admissible $(\mathbf{u}, \boldsymbol{s})$ and all $t \in [0;T]$,

3. $\exists \, C_{\text{Fric}} > 0 : \forall (\mathbf{u}, \boldsymbol{s}, \dot{\mathbf{u}}, \dot{\boldsymbol{s}}) \quad j_{\text{tot}}^{\text{D}}(t, \mathbf{u}, \boldsymbol{s}, \dot{\mathbf{u}}, \dot{\boldsymbol{s}}) \leq C_{\text{Fric}} \, \|(\dot{\mathbf{u}}, \dot{\boldsymbol{s}})\|$ for all $t \in [0;T]$.

Condition 1 follows from Lemma 8, condition 2 is true by definition of $j_{\text{tot}}^{\text{D}}$, and the last condition is a corollary of Theorem 12. Hence Proposition 2.7 of [29] is applicable and the proof is complete. $\qquad\square$

Consider a partition

$$P_\tau = \left\{ t_\tau^0 = 0 < t_\tau^1 < \ldots < t_\tau^N = T \right\}, \quad \tau = \max_{j=1,\ldots,N} \left\{ t_\tau^j - t_\tau^{j-1} \right\}$$

and the following problem:

Problem 1. Given $(\mathbf{u}_\tau^0, \boldsymbol{s}_\tau^0) = (\mathbf{u}_0, \boldsymbol{s}_0)$, find $(\mathbf{u}_\tau^k, \boldsymbol{s}_\tau^k)$, $k = 1, \ldots, N$ such that

$$(\mathbf{u}_\tau^k, \boldsymbol{s}_\tau^k) \in \operatorname{argmin}_{\mathbf{u} \in V_{\mathbf{u}}^D, \boldsymbol{s} \in V_s \cap S_{\mathrm{adm}}} \left(U_{\mathrm{tot}}^{\mathrm{Dreg}}(t_\tau^k, \mathbf{u}, \boldsymbol{s}) + j_{\mathrm{tot}}^{\mathrm{D}}(t_\tau^k, \mathbf{u}_\tau^{k-1}, \boldsymbol{s}_\tau^{k-1}, \mathbf{u} - \mathbf{u}_\tau^{k-1}, \boldsymbol{s} - \boldsymbol{s}_\tau^{k-1}) \right).$$
(2.20)

Due to the strict convexity of $U_{\mathrm{tot}}^{\mathrm{Dreg}}$ and convexity of $j_{\mathrm{tot}}^{\mathrm{D}}$, problems 2.20 always have unique solutions. From Lemma 4.4 and Corollary 4.5 of [29] we immediately conclude that these solutions satisfy the condition (S) with $U_{\mathrm{tot}}^{\mathrm{Dreg}}$ instead of $U_{\mathrm{tot}}^{\mathrm{D}}$.

Introduce interpolants

$$(\overline{\mathbf{u}}(t), \overline{\boldsymbol{s}}(t)) = (\mathbf{u}_\tau^k, \boldsymbol{s}_\tau^k) \text{ for } t \in (t_\tau^{k-1}, t_\tau^k], (\underline{\mathbf{u}}(t), \underline{\boldsymbol{s}}(t)) = (\mathbf{u}_\tau^{k-1}, \boldsymbol{s}_\tau^{k-1}) \text{ for } t \in [t_\tau^{k-1}, t_\tau^k),$$

$$(\widehat{\mathbf{u}}(t), \widehat{\boldsymbol{s}}(t)) = \frac{t - t_\tau^{k-1}}{t_\tau^k - t_\tau^{k-1}}(\mathbf{u}_\tau^k, \boldsymbol{s}_\tau^k) + \frac{t_\tau^k - t}{t_\tau^k - t_\tau^{k-1}}(\mathbf{u}_\tau^{k-1}, \boldsymbol{s}_\tau^{k-1}), \ t \in [t_\tau^{k-1}, t_\tau^k].$$

The following analog of Theorem 4.6 from [29] provides an approach to numerical solution of (2.10).

Theorem 14. *Assume that conditions of Theorem 12 are satisfied and $2\varepsilon_r > C_{\mathrm{Lip}}$, see (2.9), (2.19)). Then problem (2.12) with initial state satisfying (S) admits a solution. Moreover, if P_{τ_i} is a sequence of uniform time-step partitions of $[0, T]$ with fineness $\tau_i \to 0$ as $i \to \infty$, then there exist a subsequence τ_{i_n} and a solution $\mathbf{u} \in W^{1,\infty}\left([0; T], V_{\mathbf{u}}^D\right)$, $\boldsymbol{s} \in W^{1,\infty}\left([0; T], V_s\right)$ such that the following convergences hold as $n \to \infty$:*

1. $\forall t \in [0; T]$

$$(\overline{\mathbf{u}}(t), \overline{\boldsymbol{s}}(t)) \to (\mathbf{u}(t), \boldsymbol{s}(t)), \quad (t, \underline{\mathbf{u}}(t), \underline{\boldsymbol{s}}(t)) \to (\mathbf{u}(t), \boldsymbol{s}(t)), \quad (\widehat{\mathbf{u}}(t), \widehat{\boldsymbol{s}}(t)) \to (\mathbf{u}(t), \boldsymbol{s}(t)),$$

2. $(\widehat{\mathbf{u}}, \widehat{\boldsymbol{s}}) \overset{*}{\rightharpoonup} (\mathbf{u}, \boldsymbol{s})$ *in* $W^{1,\infty}([0; T], V_{\mathbf{u}}^D \times V_s)$,

3. $\forall t \in [0; T] \quad U_{\mathrm{tot}}^{\mathrm{Dreg}}(t, \underline{\mathbf{u}}(t), \underline{\boldsymbol{s}}(t)) \to U_{\mathrm{tot}}^{\mathrm{Dreg}}(t, \mathbf{u}(t), \boldsymbol{s}(t))$,

4. $\forall\, t \in [0; T]$

$$\int_0^t j_{\text{tot}}^{\text{D}}(\xi, (\underline{\mathbf{u}}(\xi), \underline{\boldsymbol{s}}(\xi)), (\widehat{\mathbf{u}}'(\xi), \widehat{\boldsymbol{s}}'(\xi)))\, d\xi \to \int_0^t j_{\text{tot}}^{\text{D}}(\xi, (\mathbf{u}(\xi), \boldsymbol{s}(\xi)), (\dot{\mathbf{u}}(\xi), \dot{\boldsymbol{s}}(\xi)))\, d\xi.$$

Proof. To apply Theorem 4.6 the following conditions must be satisfied:

1. there exists $\kappa > 0$ such that $\forall\, (\mathbf{u}_0, \boldsymbol{s}_0),\ (\mathbf{u}_1, \boldsymbol{s}_1) \in \mathbf{U}_{\text{adm}},\ \forall\, t \in [0, \mathrm{T}],\ \forall\, \theta \in [0; 1]$

$$U_{\text{tot}}^{\text{D}}(t, \mathbf{u}_\theta, \boldsymbol{s}_\theta) \leq (1 - \theta)U_{\text{tot}}^{\text{D}}(t, \mathbf{u}_0, \boldsymbol{s}_0) + \theta U_{\text{tot}}^{\text{D}}(t, \mathbf{u}_1, \boldsymbol{s}_1) + $$
$$+ \frac{\kappa}{2}\theta(1 - \theta) \left\| (\mathbf{u}_0, \boldsymbol{s}_0) - (\mathbf{u}_1, \boldsymbol{s}_1) \right\|^2,$$

   where $(\mathbf{u}_\theta, \boldsymbol{s}_\theta) = (1 - \theta)(\mathbf{u}_0, \boldsymbol{s}_0) + \theta(\mathbf{u}_1, \boldsymbol{s}_1)$.

2. there exists $\psi^* > 0$ such that for all $t \in [0; T]$,

$$\left| j_{\text{tot}}^{\text{D}}(t, \hat{\mathbf{u}}, \hat{\boldsymbol{s}}, \dot{\mathbf{u}}, \dot{\mathbf{s}}) - j_{\text{tot}}^{\text{D}}(t, \mathbf{u}, \boldsymbol{s}, \dot{\mathbf{u}}, \dot{\mathbf{s}}) \right| \leq \psi^* \left\| r(\hat{\mathbf{u}}, \hat{\boldsymbol{s}}) - (\mathbf{u}, \boldsymbol{s}) \right\| \left\| (\dot{\mathbf{u}}, \dot{\mathbf{s}}) \right\|.$$

3. the following condition holds for Lipschitz constants of $j_{\text{tot}}^{\text{D}}$ and strict convexity of $U_{\text{tot}}^{\text{D}}$: $\psi_* < \kappa$.

Condition 1 is fulfilled for $U_{\text{tot}}^{\text{reg}}$ with $\kappa = 2\varepsilon_r$. Condition 2 holds by Theorem 12 with $\psi^* = C_{\text{Lip}}$. Finally, Condition 3 is satisfied by the condition of the theorem being proved. At this point Theorem 4.6 can be applied, and this concludes the proof. $\qquad\square$

Remark 20. The Lipschitz constant from Theorem 12 may be large and Condition 3 means that ε_r is large. However, ε_r is a regularization constant, and it should be small. At the same time, the model is highly anisotropic and the analysis based on uniform properties, such as Lipschitz constants and strong ellipticity, may be too rough. We believe that it is possible to derive finer conditions for the parameters based on anisotropic Lipschitz and strict ellipticity properties. In our numerical experiments ε_r was small, and we didn't observe any discontinuities of the solutions.

2.4   Numerical algorithm

Observe that Problems (2.20) are finite-dimensional nonsmooth optimization problems. We apply convenient regularization technique for the friction term for numeric calculations

(see [24, 44]). This renders the problems (2.20) finite-dimensional and smooth, and standard numeric optimization techniques are applicable.

The stiffness matrices induced by $U_{\mathrm{tot}}^{\mathrm{Dreg}}$ are similar to those derived in Lemma 8, and for the regularized version of $j_{\mathrm{tot}}^{\mathrm{D}}$ the derivation is standard.

2.4.1 Continuation method

Consecutive solution of problems (S) for increasing sequence of time instants t_k in $[0, \mathrm{T}]$ can be seen as a variation of continuation Newton-Raphson method ([48, 14, 35]). In our implementation we use adaptive time step size selection based on the algorithm's convergence behavior.

1. Set the initial estimate of the solution to $(\mathbf{u}(t_k), \boldsymbol{s}(t_k))$.

2. Update Dirichlet displacements corresponding to t_{k+1}.

3. Set an inner iterations counter to zero.

4. Apply a Newton-Raphson iteration to problem (S) for time instant t_k:

   (a) If the error norm is small enough, go to step 5.

   (b) If the error norm violates the convergence criterion and the inner iterations counter does not exceed the limit, go to step 4(d).

   (c) Otherwise reduce the time step size and go to step 1.

   (d) Increment the inner iterations counter.

   (e) Apply an additional Newton-Raphson iteration to problem (S) for the time instant t_k,

   (f) Go to step 4(a).

5. At this point the problem (S) for the time instant t_k is solved. Proceed to the next step.
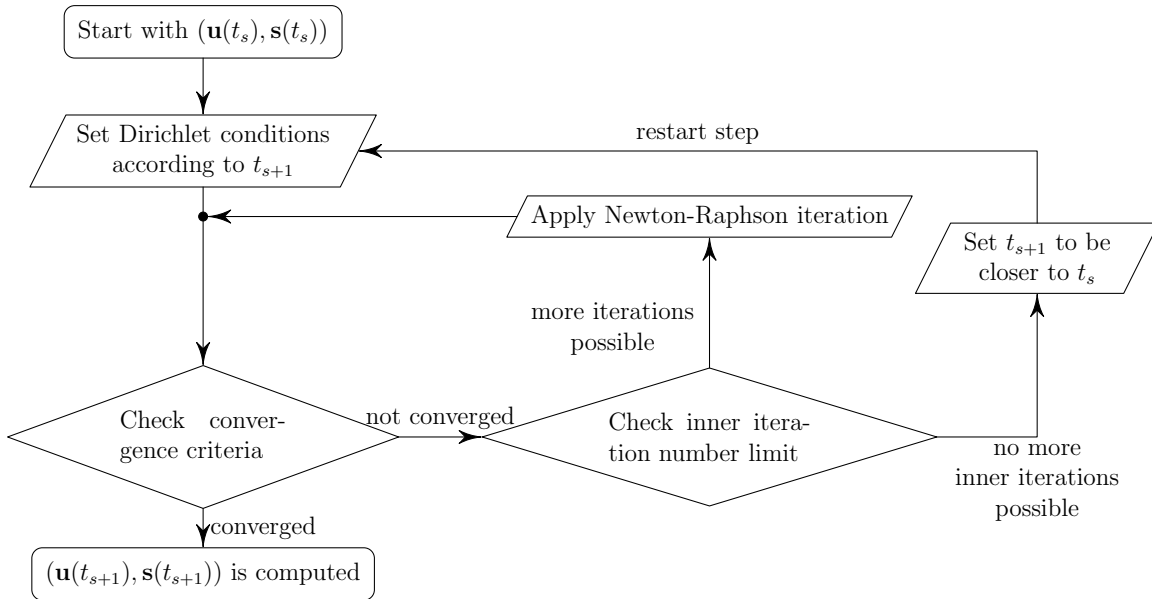
The solution process is presented in Figure 2.8.

Figure 2.8: Single step of the continuation method

2.5   Numerical examples

Let us first study the influence of the friction coefficient on the effective behaviour of textiles. The results of computational experiments are presented in Figure 2.9.

In these experiments, four initially square fabric cutouts are stretched up to 80% deformation. The cutouts have identical geometrical properties, but the friction coefficients differ. Width of the cutouts is fixed only at the top and bottom sides by the boundary conditions. The lateral sides are free.

In the stretching experiments vertically aligned parts of fibers are stressed stronger than the corresponding horizontal parts. Therefore, undeformed length flows from the horizontal parts to the vertical parts. The smaller the friction coefficient, the easier it is for the undeformed length to redistribute. At the same time, this higher redistribution leads to higher shrinkage. This observation agrees with the behaviour observed in Figure 2.9. Note that though the input force curves for individual yarns are monotone, the curves for yarn structures may be non-monotone due to geometrical effects.

We proceed with an investigation of influence of the friction coefficient on the total force applied to the cutouts to reach some fixed deformation.
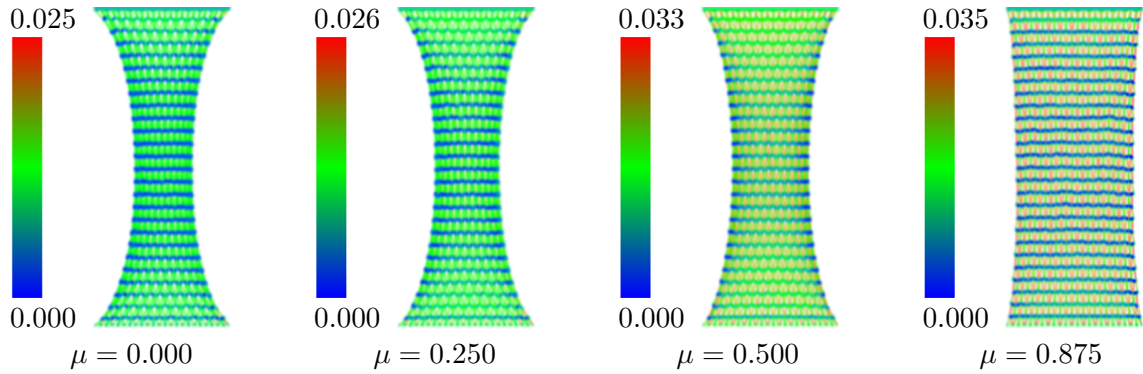
Figure 2.9: Tensional force plot of the cutouts computed for various friction coefficients.
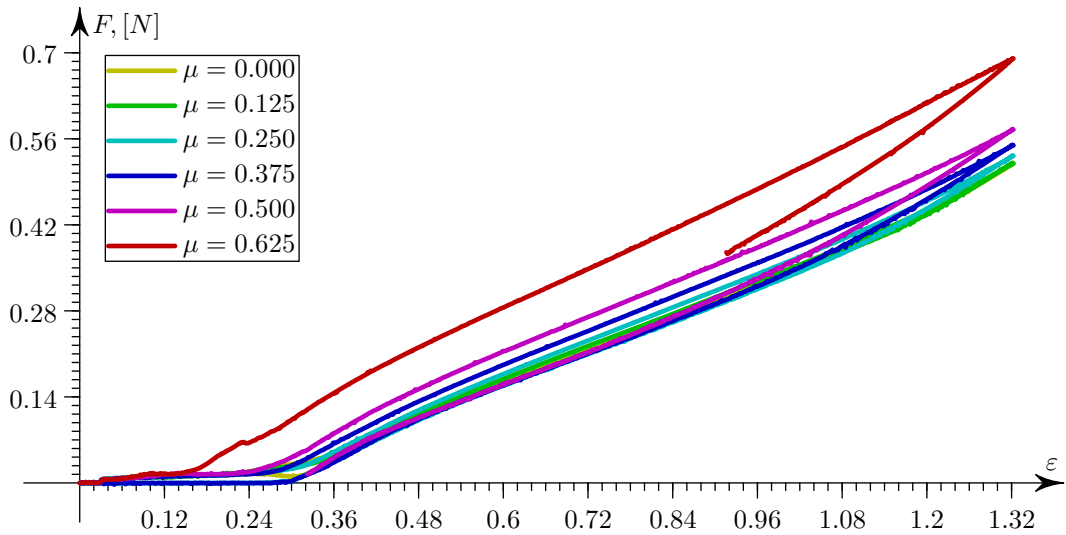

Figure 2.10: Load-unload Hysteresis for various friction coefficients associated with the specimen in Figure 2.9.

We expect lower total force values for smaller friction coefficients, because the fibers are more likely to redistribute than to develop high tension.

The corresponding hysteresis behavior for single load-unload cycle is shown in Figure 2.10. The curve for $\mu = 0$ is almost indistinguishable from the curve for $\mu = 0.125$. Indeed, the higher the friction coefficient, the higher the total applied force for a fixed deformation.

In Figure 2.11 comparison of measured and computed force for a square cutout of a technical textile is presented. The relative error between the curves is high in the beginning but is low for higher strain values. The operating range of the textile is between 50% and

150%. The figure shows that the model gives a good approximation of the force behavior of the textile.
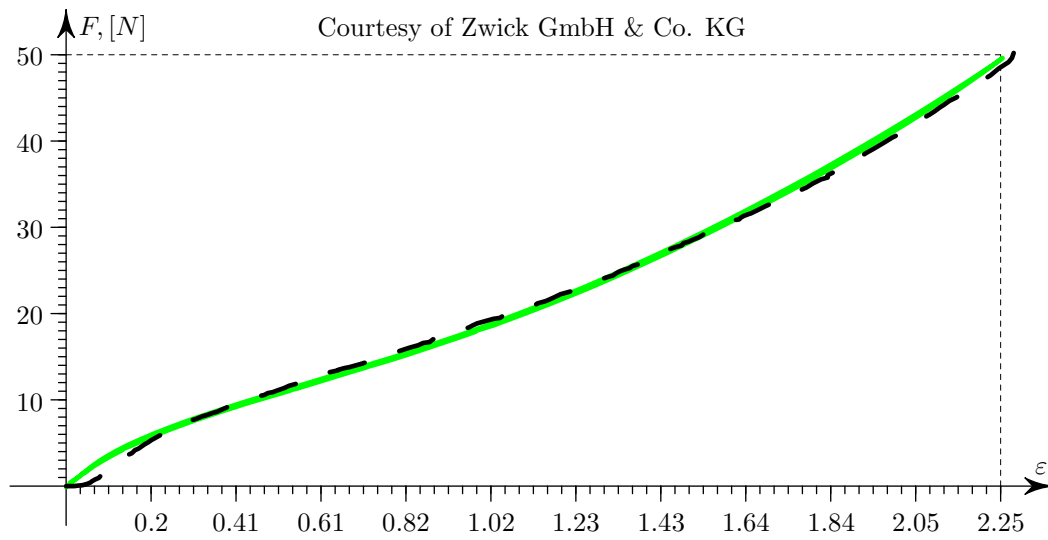

Figure 2.11: Comparison of computed (green) and measured (dashed) forces for a real fabric sample

Chapter 3

Summary

In the first chapter an optimization approach for beam structures with Robin boundary conditions modeling contact is proposed. Homogenization approach can be used not only to reduce the problem dimensionality, but also to formulate new optimization problems, which would be difficult to state for the non-homogenized problem statement. Numerical examples illustrating the approach are provided, both for stress profile and Poisson's ratio optimization problems.

In the second chapter a 1D truss method for the computational modeling of technical textiles is developed. The existing FEM procedure is extended to the contact involving Coulomb friction. The model is analyzed mathematically, numerical aspects are discussed, and a computational algorithm is proposed. Finally, numerical experiments are presented and the model is verified by a comparison with real measurements.

Bibliography

[1] Emilio Acerbi, Giuseppe Buttazzo, and Danilo Percivale. A variational definition of the strain energy for an elastic string. *Journal of Elasticity*, 25:137–148, 1991.

[2] G. Allaire. *Shape Optimization by the Homogenization Method*, volume 146 of *Applied Mathematical Sciences*. Springer, 2001.

[3] Grégoire Allaire. Homogenization and two-scale convergence. *SIAM Journal on Mathematical Analysis*, 23(6):1482–1518, 1992.

[4] Grégoire Allaire, Eric Bonnetier, Gilles Francfort, and François Jouve. Shape optimization by the homogenization method. *Numerische Mathematik*, 76(1):27–68, 1997.

[5] Nikolaï Bakhvalov and G Panasenko. *Homogenisation: Averaging processes in periodic media*. Springer, 1989.

[6] Z. Bare, J. Orlik, and G.P. Panasenko. Asymptotic dimension reduction of a robin-type elasticity boundary value problem in thin beams. *Applicable Analysis*, 2012.

[7] D.P. Bertsekas. *Constrained optimization and Lagrange multiplier methods*. Optimization and neural computation series. Athena Scientific, 1996.

[8] J.M. Borwein and A.S. Lewis. *Convex Analysis and Nonlinear Optimization: Theory and Examples*. CMS Books in Mathematics. Springer, 2006.

[9] A. Charmetant, J.G. Orliac, E. Vidal-Sallé, and P. Boisse. Hyperelastic model for large deformation analyses of 3d interlock composite preforms. *Composites Science and Technology*, 72(12):1352 – 1360, 2012.

[10] P.G. Ciarlet. *Mathematical Elasticity: Three-Dimensional Elasticity*. Studies in Mathematics and Its Applications. North-Holland, 1993.

[11] D. Cioranescu, A. Damlamian, and J. Orlik. Homogenization via unfolding in periodic elasticity with contact on closed and open cracks. *Asymptotic Analysis*, 2012.

[12] Doina Cioranescu, Alain Damlamian, and Julia Orlik. Homogenization via unfolding in periodic elasticity with contact on closed and open cracks. *Asymptotic Analysis*, 82(3):201–232, 2013.

[13] C. Delfour and J.P. Zolésio. *Shapes and Geometries: Metrics, Analysis, Differential Calculus, and Optimization, Second Edition*. Advances in Design and Control. Society for Industrial and Applied Mathematics (SIAM, 3600 Market Street, Floor 6, Philadelphia, PA 19104), 2011.

[14] P. Deuflhard. *Newton Methods for Nonlinear Problems: Affine Invariance and Adaptive Algorithms*. Springer Series in Computational Mathematics. Springer, 2011.

[15] AR Diaz and MPe Bendsøe. Shape optimization of structures for multiple loading conditions using a homogenization method. *Structural Optimization*, 4(1):17–22, 1992.

[16] Damien Durville. Simulation of the mechanical behaviour of woven fabrics at the scale of fibers. *International Journal of Material Forming*, 3:1241–1251, 2010.

[17] Damien Durville. Contact-friction modeling within elastic beam assemblies: an application to knot tightening. *Computational Mechanics*, 49(6):687–707, 2012.

[18] C. Eck and J. Jarušek. *Existence Results for the Static Contact Problem with Coulomb Friction*. Bericht // Universität Stuttgart, Sonderforschungsbereich 404, Mehrfeldprobleme in der Kontinuumsmechanik. SFB 404, Geschäftsstelle, 1997.

[19] Gaetano Fichera. Existence theorems in elasticity. In C. Truesdell, editor, *Linear Theories of Elasticity and Thermoelasticity*, pages 347–389. Springer Berlin Heidelberg, 1973.

[20] Nils Gralén and Bertil Olofsson. Measurement of friction between single fibers. *Textile Research Journal*, 17(9):488–496, 1947.

[21] F. Hecht. New development in freefem++. *J. Numer. Math.*, 20(3-4):251–265, 2012.

[22] M. Hinze, R. Pinnau, M. Ulbrich, and S. Ulbrich. *Optimization with PDE Constraints*. Mathematical Modelling: Theory and Applications. Springer, 2010.

[23] Hans-Karl Hummel. Homogenization for heat transfer in polycrystals with interfacial resistances. *Applicable Analysis*, 75(3-4):403–424, 2000.

[24] N. Kikuchi and J.T. Oden. *Contact Problems in Elasticity: A Study of Variational Inequalities and Finite Element Methods*. SIAM studies in applied mathematics. Society for Industrial and Applied Mathematics, 1987.

[25] Peter I Kogut and Günter Leugering. Homogenization of constrained optimal control problems for one-dimensional elliptic equations on periodic graphs. *ESAIM: Control, Optimisation and Calculus of Variations*, 15(02):471–498, 2009.

[26] Alexander Konyukhov and Karl Schweizerhof. Geometrically exact covariant approach for contact between curves. *Computer Methods in Applied Mechanics and Engineering*, 199(37):2510–2531, 2010.

[27] Jacques Louis Lions and Sanjoy K Mitter. *Optimal control of systems governed by partial differential equations*, volume 1200. Springer Berlin, 1971.

[28] J.E. Mark, B. Erman, and M. Roland. *The Science and Technology of Rubber*. Elsevier Science, 2013.

[29] Alexander Mielke and Riccarda Rossi. Existence and uniqueness results for general rate-independent hysteresis problems. 2005.

[30] Alexander Mielke and Tomáš Roubíček. A rate-independent model for inelastic behavior of shape-memory alloys. *Multiscale Modeling & Simulation*, 1(4):571–597, 2003.

[31] Alexander Mielke and Tomáš Roubíček. Rate-independent damage processes in nonlinear elasticity. *Mathematical Models and Methods in Applied Sciences*, 16(02):177–209, 2006.

[32] Alexander Mielke and Florian Theil. On rate-independent hysteresis models. *NoDEA, Nonlinear Differ. Equ. Appl.*, 11(2):151–189, 2004.

[33] Maria Neuss-Radu and Willi Jäger. Effective transmission conditions for reaction-diffusion processes in domains separated by an interface. *SIAM Journal on Mathematical Analysis*, 39(3):687–720, 2007.

[34] O.A. Oleinik, A.S. Shamaev, and G.A. Yosifian. *Mathematical Problems in Elasticity and Homogenization*. Studies in Mathematics and Its Applications. Elsevier Science, 1992.

[35] Ortega, J.M.A. and Rheinboldt, W.C.A. *Iterative Solution of Non Linear Equations in Several Variables*. Computer science and applied mathematics. Society for Industrial and Applied Mathematics (SIAM, 3600 Market Street, Floor 6, Philadelphia, PA 19104), 1970.

[36] G Panasenko. *Multi-scale modelling for structures and composites*. Springer, 2005.

[37] G.P. Panasenko. Asymptotic solutions of the elasticity theory system of equations for lattice and skeletal structures. *Russian Academy of Sciences. Sbornik Mathematics*, 183(1):89–113, 1992.

[38] G.P. Panasenko. Asymptotic solutions of the system of elasticity theory for rod and frame structures. *Russian Academy of Sciences. Sbornik Mathematics*, 75(1):85–110, 1993.

[39] S. Pastukhova. Homogenization of problems of elasticity theory on periodic box and rod frames of critical thickness. *Journal of Mathematical Sciences*, 130:4954–5004, 2005. 10.1007/s10958-005-0392-8.

[40] R.T. Rockafellar. *Convex Analysis*. Convex Analysis. Princeton University Press, 1997.

[41] Martin Sauter and Christian Wieners. On the superlinear convergence in computational elasto-plasticity. *Computer Methods in Applied Mechanics and Engineering*, 200(49):3646–3658, 2011.

[42] Katsuyuki Suzuki and Noboru Kikuchi. A homogenization method for shape and topology optimization. *Computer methods in applied mechanics and engineering*, 93(3):291–318, 1991.

[43] L. Trabucho and J.M. Viaño. *Mathematical Modelling of Rods. Handbook of Numerical Analysis*, volume 4, pages 487–974. Elsevier Science, 1996.

[44] R. Trémolières, J.L. Lions, and R. Glowinski. *Numerical Analysis of Variational Inequalities*. Studies in Mathematics and Its Applications. Elsevier Science, 1981.

[45] Vassiliadis, Savvas, Kallivretaki, Argyro, Domvoglou, Dimitra, and Provatidis, Christofer. *Mechanical Analysis of Woven Fabrics:The State of the Art*. InTech, 2011.

[46] Christian Wieners. Nonlinear solution methods for infinitesimal perfect plasticity. *ZAMM-Journal of Applied Mathematics and Mechanics/Zeitschrift für Angewandte Mathematik und Mechanik*, 87(8-9):643–660, 2007.

[47] P. Wriggers. *Computational Contact Mechanics*. Springer, 2006.

[48] P. Wriggers. *Nonlinear Finite Element Methods*. Springer, 2008.

[49] Zavarise, G. and Wriggers, P. Contact with friction between beams in 3-d space. *International Journal for Numerical Methods in Engineering*, 49:977—1006, 2000.

[50] V. V. Zhikov. Homogenization of elasticity problems on singular structures. *Izvestiya: Mathematics*, 66(2):299, 2002.

[51] V. V. Zhikov and S. E. Pastukhova. Homogenization for elasticity problems on periodic networks of critical thickness. *Sbornik: Mathematics*, 194(5):697, 2003.

Curriculum vitae

01.09.2005–30.06.2010	Study of mathematics and computer science, Lomonosov Moscow State University, Moscow, Russia.
01.09.2009–30.06.2010	Diploma thesis "Elaboration of the ellipsoidal method of reachability sets estimation of linear systems with disturbances". Lomonosov Moscow State University, Moscow, Russia.
01.07.2010–30.06.2011	Research assistant at Lomonosov Moscow State University, Moscow, Russia.
01.07.2011–31.01.2012	Project Studies in Advanced Technologies, Technical University of Kaiserslautern and Fraunhofer Institute for Industrial and Financial Mathematics, Kaiserslautern, Germany.
01.02.2012–30.11.2014	PhD studies at TU Kaiserslautern and Fraunhofer ITWM, Kaiserslautern, Germany.

Lebenslauf

01.09.2005–30.06.2010 Studium der Mathematik und Informatik, Staatliche M.-W.-Lomonossow-Universität Moskau, Moskau, Russland.

01.09.2009–30.06.2010 Diplomarbeit "Entwicklung der Ellipsoid-methoden zur Approximation erreichbarer Mengen bei linearen Systemen mit Störungen". Staatliche M.-W.-Lomonossow-Universität Moskau, Moskau, Russland.

01.07.2010–30.06.2011 Wissenschaftliche Hilfskraft bei der Staatlichen M.-W.-Lomonossow-Universität Moskau, Moskau, Russland.

01.07.2011–31.01.2012 Project Studies in Advanced Technologies, Technische Universität Kaiserslautern und Fraunhofer Institut für Techno- und Wirtschaftsmathematik, Kaiserslautern, Deutschland.

01.02.2012–30.11.2014 Doktorand bei der TU Kaiserslautern und Fraunhofer ITWM, Kaiserslautern, Deutschland.